

ANNUAL SUMMARY

Atlantic Hurricane Season of 2005

JOHN L. BEVEN II, LIXION A. AVILA, ERIC S. BLAKE, DANIEL P. BROWN, JAMES L. FRANKLIN,
RICHARD D. KNABB, RICHARD J. PASCH, JAMIE R. RHOME, AND STACY R. STEWART

Tropical Prediction Center, NOAA/NWS/National Hurricane Center, Miami, Florida

(Manuscript received 2 November 2006, in final form 30 April 2007)

ABSTRACT

The 2005 Atlantic hurricane season was the most active of record. Twenty-eight storms occurred, including 27 tropical storms and one subtropical storm. Fifteen of the storms became hurricanes, and seven of these became major hurricanes. Additionally, there were two tropical depressions and one subtropical depression. Numerous records for single-season activity were set, including most storms, most hurricanes, and highest accumulated cyclone energy index. Five hurricanes and two tropical storms made landfall in the United States, including four major hurricanes. Eight other cyclones made landfall elsewhere in the basin, and five systems that did not make landfall nonetheless impacted land areas. The 2005 storms directly caused nearly 1700 deaths. This includes approximately 1500 in the United States from Hurricane Katrina—the deadliest U.S. hurricane since 1928. The storms also caused well over \$100 billion in damages in the United States alone, making 2005 the costliest hurricane season of record.

1. Introduction

By almost all standards of measure, the 2005 Atlantic hurricane season was the most active of record. Twenty-eight storms—27 tropical and one subtropical—formed during the year (Table 1; Fig. 1), breaking the record of 21 set in 1933. Fifteen of the storms became hurricanes, breaking the record of 12 set in 1969. Seven hurricanes became major hurricanes [maximum 1-min winds of at least 96 kt ($1 \text{ kt} = 0.5144 \text{ m s}^{-1}$)] corresponding to category 3 or higher on the Saffir–Simpson hurricane scale (Simpson 1974). This was just short of the record of eight set in 1950 (Norton 1951). Four hurricanes reached category 5 strength (maximum 1-min winds greater than 135 kt), which was the first time this had been observed in one season. There were also two tropical and one subtropical depressions that did not reach storm strength.

In terms of accumulated cyclone energy (ACE; the sum of the squares of the maximum wind speed at 6-h

intervals for all tropical and subtropical cyclones with intensities of 34 kt or greater; Bell et al. 2000), the 2005 season had a record value of about 256% of the long-term (1944–2003) mean. The previous record was about 249% of the long-term mean set in 1950. A record seven named storms formed before the end of July (two in June, five in July), including Hurricane Emily, the earliest category 5 hurricane of record in the basin. The season also ran late, as Tropical Storm Zeta was the second-latest developing storm of record and lasted into January 2006.

Three of the category 5 hurricanes featured very low minimum central pressures. The central pressure of Hurricane Wilma was estimated from aircraft data to be 882 mb. This is the lowest known central pressure in an Atlantic hurricane, eclipsing the pressure of 888 mb observed in Hurricane Gilbert in 1988 (Lawrence and Gross 1989). Additionally, Hurricane Rita had an estimated minimum central pressure of 895 mb (the fourth lowest of record in the Atlantic basin), while Hurricane Katrina had a minimum central pressure of 902 mb (the sixth lowest of record). As might be expected, these storms underwent periods of rapid to explosive deepening as defined by Holliday and Thompson (1979) for

Corresponding author address: Dr. John L. Beven II, National Hurricane Center, 11691 SW 17th St., Miami, FL 33165-2149.
E-mail: john.l.beven@noaa.gov

TABLE 1. Atlantic hurricanes, tropical storms, and subtropical storms of 2005.

Name	Class ^a	Dates ^b	Max 1-min wind (kt)	Min sea level pressure (mb)	Direct deaths	U.S. damages (\$ million)
Arlene	T	8–13 Jun	60	989	1	Minor ^c
Bret	T	28–30 Jun	35	1002	1	
Cindy	H	3–7 Jul	65	991	1	320
Dennis	H	4–13 Jul	130	930	42	2230
Emily	H	11–21 Jul	140	929	6	Minor ^c
Franklin	T	21–29 Jul	60	997		
Gert	T	23–25 Jul	40	1005		
Harvey	T	2–8 Aug	55	994		
Irene	H	4–18 Aug	90	970		
Jose	T	22–23 Aug	50	998	6	
Katrina	H	23–30 Aug	150	902	1500	81 000
Lee	T	28 Aug–2 Sep	35	1006		
Maria	H	1–10 Sep	100	962		
Nate	H	5–10 Sep	80	979		
Ophelia	H	6–17 Sep	75	976	1	70
Philippe	H	17–24 Sep	70	985		
Rita	H	18–26 Sep	155	895	7	11 300
Stan	H	1–5 Oct	70	977	80	
Unnamed	ST	4–5 Oct	45	997		
Tammy	T	5–6 Oct	45	1001		Minor ^c
Vince	H	8–11 Oct	65	988		
Wilma	H	15–25 Oct	160	882	23	20 600
Alpha	T	22–24 Oct	45	998	26	
Beta	H	26–31 Oct	100	962		
Gamma	T	14–21 Nov	45	1002	37	
Delta	T	22–28 Nov	60	980		
Epsilon	H	29 Nov–8 Dec	75	981		
Zeta	T	30 Dec–6 Jan	55	994		

^a T = tropical storm and ST = subtropical storm, wind speed 34–63 kt (17–32 m s⁻¹); H = hurricane, wind speed 64 kt (33 m s⁻¹) or higher.

^b Dates begin at 0000 UTC and include tropical and subtropical depression stages but exclude extratropical stage.

^c Only minor damage was reported, but the extent of the damage was not quantified.

western Pacific typhoons. The aircraft-measured central pressure of Wilma fell 88 mb in about 12 h, shattering records for deepening rates of Atlantic tropical cyclones. The central pressure of Rita fell 70 mb in about 24 h, while the central pressure of Katrina fell 46 mb in about 24 h.

The 2005 hurricane season was the deadliest in the Atlantic basin since 1998. Katrina is believed to be directly responsible for about 1500 deaths, while heavy rains caused by a large area of disturbed weather during Hurricane Stan produced floods that caused 1000–2000 deaths. The season caused over \$100 billion in property damage in the United States alone, making it the costliest season of record.

While a full explanation of the record level of activity will require considerable research, there were several likely contributing factors. One was the warmth of the Caribbean Sea and tropical Atlantic Ocean, as sea surface temperatures (SSTs) during the hurricane season were the warmest ever observed there. Figure 2 shows

the SST anomalies over the North Atlantic basin for July–October 2005. The tropical Atlantic had above-normal SSTs, with anomalies of greater than 1°C in the western part of that area. Above-normal anomalies were also present throughout the Caribbean Sea and the Gulf of Mexico. It should be noted that the warm anomalies in the eastern Gulf of Mexico were tempered due to cooling caused by repeated hurricane passages.

A striking contrast between the 2004 and 2005 hurricane seasons was the level of activity in the tropical Atlantic between the Lesser Antilles and the coast of Africa. In 2004 (Franklin et al. 2006), three long-track major hurricanes (Frances, Ivan, and Karl) and several less intense systems formed in this area. Despite the great activity during 2005, only two hurricanes (Emily and Philippe—both category 1) occurred in this region. This was not due to lack of opportunities, as five named storms and two depressions formed in the region, and two other named storms began over the eastern Caribbean Sea.

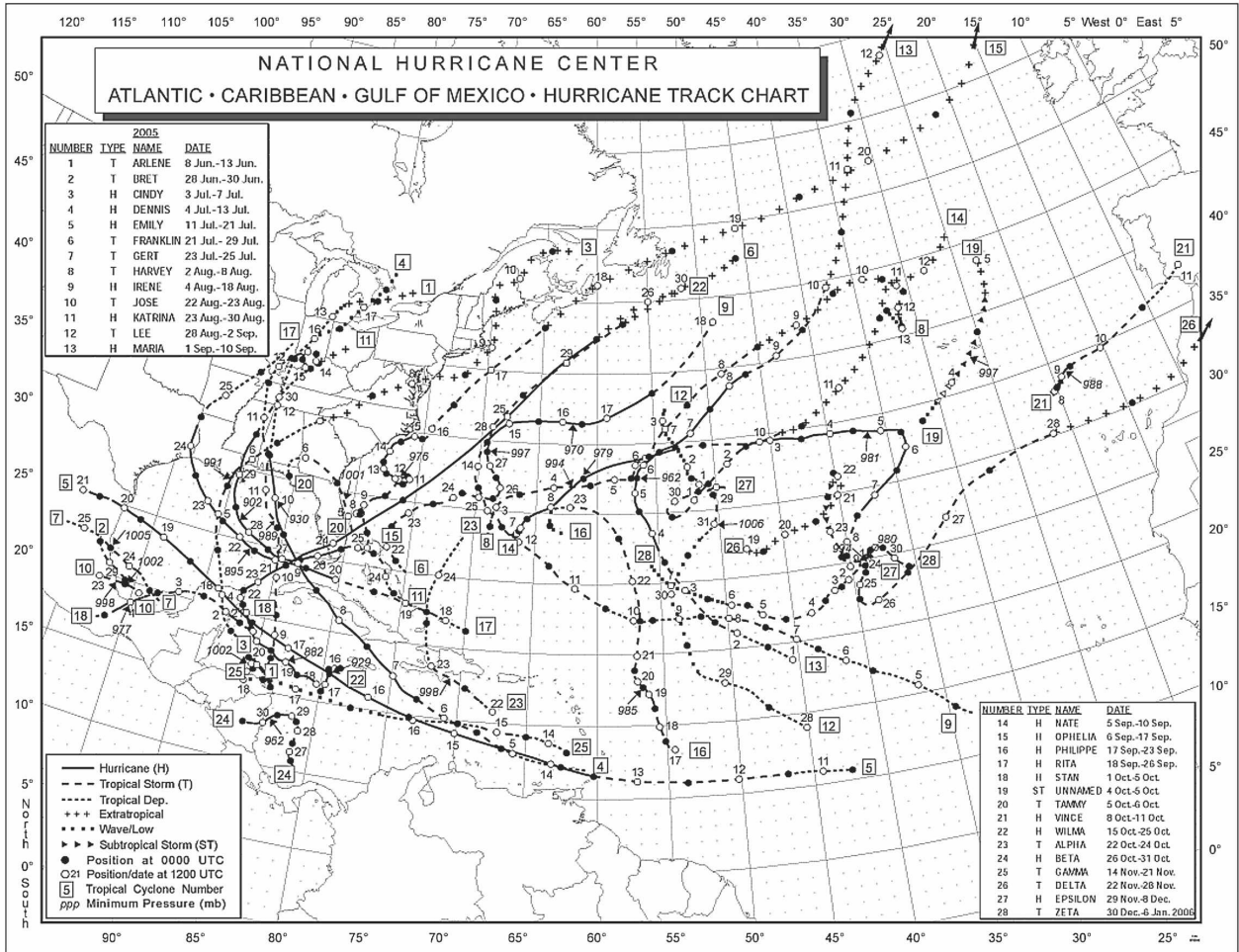


FIG. 1. Atlantic hurricanes, tropical storms, and subtropical storms of 2005.

A possible factor in the large number of landfalling cyclones during 2005—particularly the record four major hurricanes to hit the United States—was anomalous ridging in the middle troposphere that persisted over the eastern United States in a fashion somewhat similar to that seen in 2004 (Fig. 3). This ridge was a little farther south and west in 2005 than in 2004 and likely helped steer hurricanes farther west and south into the Gulf of Mexico during 2005.

There were several cases during the 2005 season where a portion of a tropical wave contributed to tropical cyclogenesis, and two cases where the same wave contributed to the development of two cyclones. Riehl (1979) discusses the structural aspects of Atlantic tropical waves, which include a meridional extent of several hundred nautical miles (1 n mi = 1.852 km). This structure can lead to portions of the tropical wave being in different environmental wind flows, which can lead to the wave “splitting” into two parts. It also means that

tropical cyclogenesis in one portion of the wave may leave other portions of the wave relatively unaffected.

2. Individual storm summaries

The following individual cyclone summaries are based on the National Hurricane Center’s (NHC) post-storm meteorological analyses of the variety of (often contradictory) data described below. These analyses result in the creation of a “best track” database for each storm, consisting of 6-hourly representative estimates of the cyclone’s center location, maximum sustained (1-min average) surface (10 m) wind (the cyclone’s “intensity”), minimum sea level pressure, and maximum extent of 34-, 50-, and 64-kt winds in each of four quadrants around the center (“wind radii”). The life cycle of each cyclone (corresponding to the dates given in Table 1) is defined to include the tropical or subtropical depression stage, but it does not include remnant low or

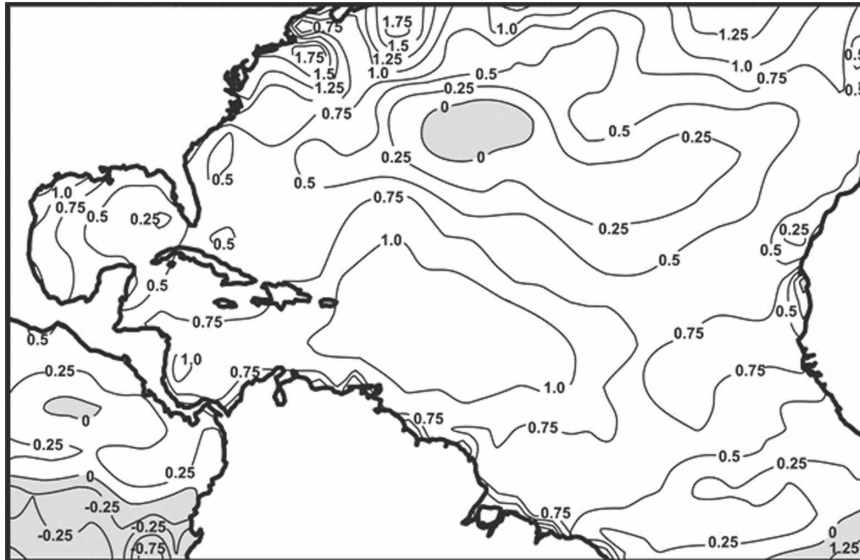


FIG. 2. Atlantic sea surface temperature anomalies ($^{\circ}\text{C}$) during July–October 2005. Contour interval is 0.25°C . Shading indicates areas that are cooler than normal.

extratropical stages. The tracks for the season's tropical storms, subtropical storms, and hurricanes are shown in Fig. 1.¹

For storms east of 55°W longitude, or those not threatening land, the primary (and often sole) source of information is geostationary and polar-orbiting weather satellite imagery, interpreted using the Dvorak (1984) and Hebert and Potat (1975) intensity estimation techniques. These estimates ("classifications") are provided by the Tropical Analysis and Forecast Branch (TAFB) of the National Oceanographic and Atmospheric Administration/National Weather Service's (NOAA/NWS) Tropical Prediction Center (TPC), the NOAA/Satellite Analysis Branch in Washington, D.C., and the Air Force Weather Agency in Omaha, Nebraska.

For systems threatening land, in situ observations are generally available from aircraft reconnaissance flights conducted by the 53rd Weather Reconnaissance Squadron (WRS; "Hurricane Hunters") of the Air Force Reserve Command (AFRC) and by the NOAA/Aircraft Operations Center (AOC). During these flights, minimum sea level pressures are either measured by dropsondes released at the circulation center or are extrapolated hydrostatically from flight level. Surface (or very

near-surface) winds in the eyewall or maximum wind band can be measured directly using global positioning system (GPS) dropwindsondes (Hock and Franklin 1999), but more frequently are estimated from flight-level winds using empirical relationships derived from a 3-yr sample of GPS dropwindsonde data (Franklin et al. 2003). During NOAA reconnaissance missions, surface winds can be estimated remotely using the Stepped-Frequency Microwave Radiometer (SFMR) instrument (Uhlhorn and Black 2003). Satellite and reconnaissance data are supplemented by available land-based surface and upper-air observations, ship and buoy reports, and weather radars, including the NWS network of Doppler radars. In key forecast situations, the kinematic and thermodynamic structure of the storm environment is obtained from dropwindsondes released during operational "synoptic surveillance" flights of NOAA's Gulfstream IV jet aircraft (Aberson and Franklin 1999).

Several remote sensors on low earth orbit satellites play an important role in the analysis of tropical weather systems. Foremost among these are multichannel passive microwave instruments [e.g., the Tropical Rainfall Measuring Mission (TRMM) Microwave Imager], which over the past decade have provided radar-like depictions of systems' convective structure (Hawkins et al. 2001) and are of great help in assessing system location and organization. The SeaWinds scatterometer on board the National Aeronautics and Space Administration (NASA) Quick Scatterometer (QuikSCAT) satellite (Tsai et al. 2000) provides surface winds over

¹ Tabulations of the 6-hourly best-track positions and intensities can be found in the NHC Tropical Cyclone Reports, available online at <http://www.nhc.noaa.gov/pastall.shtml>. These reports contain storm information omitted here because of space limitations, including additional surface observations and a forecast and warning critique.

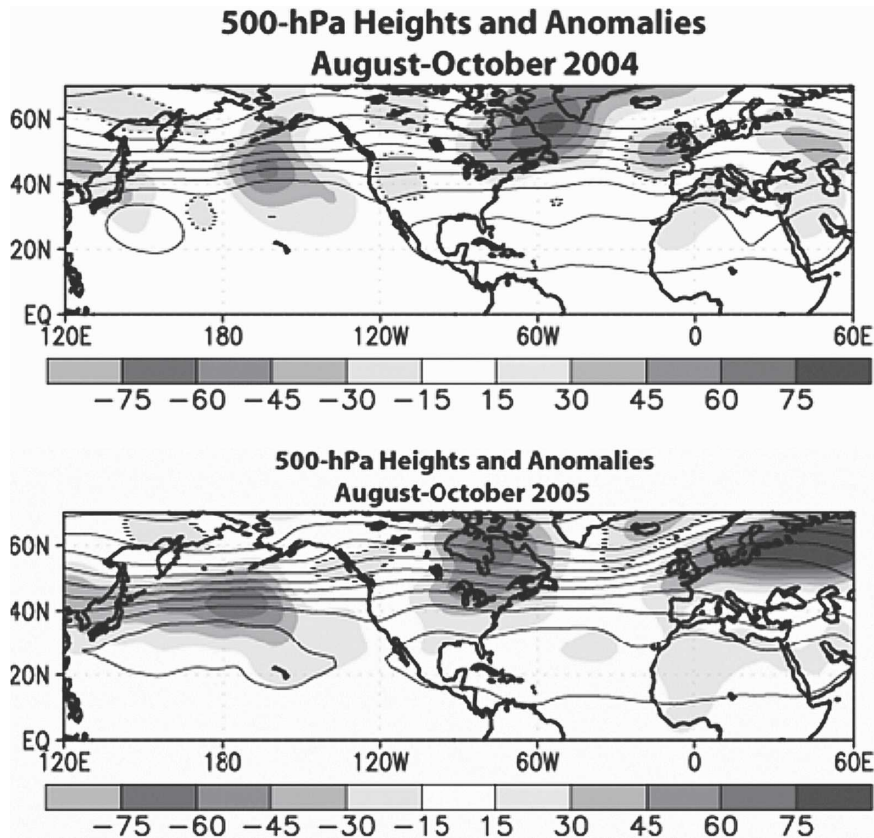


FIG. 3. 500-hPa mean geopotential heights and anomalies for (top) August–October 2004 and (bottom) August–October 2005. Negative height anomalies are enclosed in the dotted areas. Contour interval is 60 m and shading interval is 15 m.

large oceanic swaths. While the QuikSCAT suffers from contamination by rain and generally does not have the horizontal resolution to determine a hurricane's maximum winds, it can be used to estimate the intensity of weaker systems and to determine the extent of various wind radii. It can also help in determining whether an incipient tropical cyclone has acquired a closed surface circulation. Finally, information on the thermal structure of cyclone cores is provided by the Advanced Microwave Sounder Unit (AMSU; Velden and Brueske 1999). Intensity estimates derived from such data are comparable in accuracy to Dvorak classifications (Herndon and Velden 2004).

A number of organizations have developed Web sites that aid tropical cyclone forecasting and postanalysis. These include the Naval Research Laboratory (NRL) Monterey Marine Meteorology Division Tropical Cyclone Page (http://www.nrlmry.navy.mil/tc_pages/tc_home.html), with its comprehensive suite of microwave satellite products. The cyclone phase diagnostics page of The Florida State University (<http://moe.met.fsu.edu/cyclonephase/>) is frequently consulted to help

categorize systems as tropical, subtropical, or nontropical. Also, the tropical cyclone page of the University of Wisconsin/Cooperative Institute for Meteorological Satellite Studies (<http://cimss.ssec.wisc.edu/tropic/tropic.html>) contains a variety of useful satellite-based synoptic analyses.

In the cyclone summaries below, U.S. damage estimates have been generally estimated by doubling the insured losses reported by the Property Claim Services (PCS) of the Insurance Services Office for events exceeding their minimum reporting threshold (\$25 million). However, the uncertainty in estimating meteorological parameters for tropical cyclones remains notably less than the uncertainty in determining the cost of the damage they cause. Descriptions of the type and scope of damage are taken from a variety of sources, including local government officials, media reports, and local NWS Weather Forecast Offices (WFOs) in the affected areas. Tornado counts are based on reports provided by the WFOs and the NWS Storm Prediction Center. Hard copies of these various reports are archived at the NHC.

TABLE 2. List of acronyms used in the surface observation tables, along with associated wind-averaging periods where applicable.

Acronym	Meaning	Wind-averaging period
AFB	Air Force Base	2 min
AOML	Atlantic Oceanographic and Marine Laboratories	—
ARB	Air Reserve Base	2 min
ASOS	Automated Surface Observing System	2 min
AWS	AWS Convergence Technologies	—
C-MAN	Coastal Marine Automated Network	2 min unless otherwise noted
CARO-COOPS	Carolinas Coastal Ocean Observing and Prediction System	—
CoE	U.S. Army Corps of Engineers	—
COMPS	University of South Florida Coastal Ocean Monitoring and Prediction System	—
COOP	NWS Cooperative Station	—
CORMP	North Carolina Coastal Ocean Research and Monitoring Program	—
FAWN	Florida Automated Weather Network	—
FCMP	Florida Coastal Monitoring Program	1 min
GOMOOS	Gulf of Maine Ocean Observing System	—
LUMCON	Louisiana Universities Marine Consortium	—
LLWAS	Low-level Wind Shear Alert System	—
NAS	Naval Air Station	2 min
NASA	National Aeronautics and Space Administration	1 min
NOAA	National Oceanic and Atmospheric Administration	8 min unless otherwise noted
NOS	National Ocean Service	6 min
NWR	National Wildlife Refuge	—
NWS	National Weather Service	—
RAWS	Remote Automated Weather Stations	—
RSMAS	Rosenstiel School of Marine and Atmospheric Sciences	—
SFWMD	South Florida Water Management District	15 min
TABS	Texas Automated Buoy System	—
TCOON	Texas Coastal Ocean Observing Network	6 min
TTU	Texas Tech University	1 min
ULM	University of Louisiana at Monroe	—
USCG	U.S. Coast Guard	—
USM	University of Southern Mississippi	—
WFO	NWS Weather Forecast Office	2 min
WAVECIS	Louisiana State University Wave-Current-Surge Information System	—

Although specific dates and times in these summaries are given in coordinated universal time (UTC), local time is implied whenever general expressions such as “afternoon,” “midday,” etc. are used. Table 2 lists the various acronyms used in the surface data tables in the storm summaries, along with any applicable wind-averaging periods.

a. Tropical Storm Arlene

Arlene appears to have formed from the interaction of the intertropical convergence zone (ITCZ) and a tropical wave. The ITCZ was centered over Central America during early June and showed increased convection when a tropical wave moved westward across Central America on 5–6 June. A second and slightly more vigorous tropical wave moved across the western Caribbean Sea on 7–8 June, resulting in pressure falls and increased cloudiness and thunderstorms over the

region. Vertical wind shear decreased as an upper-level ridge developed over the large area of disturbed weather. The disturbance became better organized and it is estimated that a tropical depression formed at 1800 UTC 8 June just north of the northeastern coast of Honduras (Fig. 1). Deep convection developed in cyclonically curved bands north and east of the center, and the depression became a tropical storm at 0600 UTC 9 June about 150 n mi west-southwest of Grand Cayman Island.

Arlene moved slowly northward with steady intensification, and its center crossed western Cuba near Cabo Corrientes early on 10 June with maximum winds near 45 kt. Once in the Gulf of Mexico, Arlene moved generally north-northwestward and continued to strengthen. It reached a peak intensity of 60 kt with a minimum pressure of 989 mb at 0100 UTC 11 June. Thereafter, deep convection diminished considerably

due to dry air entrainment, resulting in gradual weakening. Arlene made landfall as a tropical storm with 50-kt winds just west of Pensacola, Florida, about 1900 UTC 11 June. It moved northward and then northeastward over the eastern United States, became extratropical at 1800 UTC 13 June just northeast of Flint, Michigan, and was absorbed by a front at 1200 UTC 14 June.

The highest 1-min average wind reported by a land station was 41 kt at Punta del Este, on the Isle of Youth, Cuba (Table 3), while the highest gust was 52 kt at a fire station in Navarre, Florida. A ship with the call sign 3FPS9 reported 58-kt winds at 1800 UTC 10 June. After landfall, Arlene spread 75–175 mm of rain over the central and eastern United States with a maximum reported total of 249.9 mm at Lake Toxaway, North Carolina.

A Russian exchange student died in a rip current triggered by Arlene on 10 June at Miami Beach. The storm caused minimal property damage.

b. Tropical Storm Bret

Bret formed from a tropical wave accompanied by a weak area of surface low pressure that crossed Central America and eastern Mexico during 24–27 June. An associated area of disturbed weather moved westward into the Bay of Campeche early on 28 June. The system began to organize soon thereafter, with curved banding features and a small circulation forming. Flight-level winds (300-m elevation) from an AFRC aircraft suggest a tropical depression formed around 1800 UTC 28 June about 55 n mi northeast of Veracruz, Mexico (Fig. 1). The cyclone quickly strengthened into a small tropical storm. In response to a midlevel ridge to its north, Bret moved generally northwestward until making landfall just south-southeast of Tuxpan, Mexico, around 1200 UTC 29 June. Based on Dvorak classifications, it is estimated that Bret's intensity remained near 35 kt until landfall. However, TRMM data near the time of landfall showed increasing organization and possible intensification. After landfall, the cyclone turned north-northwestward and dissipated over Mexico just after 0000 UTC 30 June.

Bret caused heavy rains in eastern Mexico, with a total of 265.9 mm reported at El Raudal. There was significant flooding in the state of Veracruz, where one person drowned in the town of Cerro Azul.

c. Hurricane Cindy

A poststorm analysis indicates Cindy was a category 1 hurricane near the time of landfall along the southeastern coast of Louisiana. The hurricane produced heavy rainfall across coastal areas of southeastern Loui-

siana, Mississippi, and Alabama, and it caused minor wind damage in the New Orleans metropolitan area.

1) SYNOPTIC HISTORY

The tropical wave that eventually developed into Cindy moved westward across the coast of Africa on 24 June. The wave moved quickly westward for the next three days with little convection. By 28 June, deep convection developed along the northern portion of the wave axis just east of the Lesser Antilles. While the southern portion of the wave broke away and continued westward, the active northern portion moved west-northwestward across the northern Caribbean Sea. On 3 July, thunderstorm activity became more concentrated over the northwestern Caribbean Sea. Surface observations showed the development of a broad low pressure area, and reports from an AFRC aircraft indicated a tropical depression formed at 1800 UTC that day about 70 n mi east of Chetumal, Mexico (Fig. 1).

The depression moved slowly west-northwestward along the southern periphery of a deep-layer subtropical ridge, with the center crossing the east coast of the Yucatan peninsula about 55 n mi north-northeast of Chetumal early on 4 July. The cyclone then turned northwestward and reached the north coast of the Yucatan just east of Merida, Mexico at around 1500 UTC 4 July. A midlevel trough over the central United States dropped southward into the southern plains and the northwestern Gulf of Mexico, causing the depression to accelerate. Although the cyclone was in an environment of moderate southerly shear, it became a tropical storm over the central Gulf of Mexico at 0600 UTC 5 July. Cindy turned northward with some decrease in forward speed. Decreasing shear resulted in steady strengthening, and Cindy became a hurricane at 0000 UTC 6 July about 40 n mi south-southwest of Grand Isle, Louisiana. It maintained hurricane status until it made landfall just southwest of Grand Isle 3 h later.

Cindy turned northeastward and weakened to a tropical storm over extreme southeastern Louisiana. It again made landfall at 0900 UTC 6 July near Ansley, Mississippi, then continued northeastward and weakened to a tropical depression by 1800 UTC that day over southwestern Alabama. Cindy then moved across central Alabama to northern Georgia, where it merged with a frontal system and became an extratropical low. The low moved northeastward along the eastern slopes of the Appalachian Mountains and emerged off the mid-Atlantic coast of United States on 8 July. Over the Gulf Stream, the low turned northeastward and then northward, strengthening to just below gale force near Cape Cod, Massachusetts, on 9 July. It moved inland

TABLE 3. (Continued)

Location	Min sea level pressure		Max surface wind speed			Storm surge (ft) ^c	Storm tide (ft) ^d	Tot rain (mm)
	Date/time (UTC)	Pressure (mb)	Date/time (UTC) ^a	Sustained (kt) ^b	Gust (kt)			
Mississippi								
Aberdeen Lock and Dam								172.0
Pascagoula (KPQL)	11/2036	1000.7						44.2
Georgia								
Choestoe								125.2
Clayton								134.9
Crisp County Power Dam								104.6
Nacoochee								108.5
Pine Mountain								154.9
Sautee								116.6
North Carolina								
Lake Toxaway								249.9
Buoys and C-MAN sites								
Apalachicola, FL, NOS (29.7°N, 85.0°W)	11/1330	1005.5	11/1000		38			
Dauphin Island, AL, C-MAN (30.3°N, 88.1°W)	11/1905	997.8	11/1520	35 ^e	43			
Fowey Rocks, FL, C-MAN (25.6°N, 80.1°W)	11/0100	1010.1	10/2000	34	43			
Long Key, FL, C-MAN (24.8°N, 80.9°W)	11/0000	1008.1	10/0900		36			
Molasses Reef, FL, C-MAN (25.0°N, 80.4°W)	11/0100	1008.8	10/0200	32	40			
Panama City Beach, FL, NOS (30.1°N, 85.9°W)	11/1512	1002.7	11/1512	33	41			
Sand Key, FL, C-MAN (24.5°N, 81.9°W)	10/2200	1005.5	10/0010	32 ^e	38			
Sombrero Key, FL, C-MAN (24.6°N, 81.1°W)	10/2200	1008.3	11/0110	34 ^e	39			
Tyndall AFB Tower, FL, C-MAN (29.4°N, 89.9°W)	11/0800	1004.2	11/0900		46			
Buoy 42007, NOAA (30.1°N, 88.8°W)	11/1810	1000.7	11/1748		37			
Buoy 42036, NOAA (28.5°N, 84.5°W)	11/1050	997.7	11/0650		41			
Buoy 42039, NOAA (28.8°N, 86.0°W)	11/0650	1002.5	11/0350		45			
Buoy 42040 NOAA (29.2°N 88.2°W)	11/1350	998.6	11/1350	34 ^e	43			
Buoy 42056, NOAA (19.9°N, 85.1°W)	09/2217	1001.7	09/0450		35			

^a Date/time is for sustained wind when both sustained and gust are listed.

^b Except as noted, sustained wind-averaging periods for land-based ASOS reports are 2 min.

^c Storm surge is water height above normal astronomical tide level.

^d Storm tide is water height above National Geodetic Vertical Datum (1929 mean sea level).

^e 10-min average.

along the southwestern coast of Maine later that day, then it weakened and moved northeastward across northern Maine and New Brunswick, Canada, on 10 July. The system dissipated over the Gulf of St. Lawrence on 11 July.

2) METEOROLOGICAL STATISTICS

An automated station operated by Louisiana State University at South Timbalier Block 52 (40.4-m elevation) reported sustained winds of 67 kt at 0100 UTC 6 July, along with a peak gust of 75 kt (Table 4). The moveable semisubmersible oil rig Deepwater Horizon (call sign V7HC9; likely 45–90-m elevation) located 37 n mi east of the center reported a southeast wind of 60

kt at 1700 UTC 5 July. In addition, fixed oil platform South Timbalier (ST-308; 45-m elevation) reported a northwesterly wind gust of 87 kt at around 1800 UTC 5 July. Tropical-storm-force winds were reported at New Orleans Lakefront Airport from 0400 to 0930 UTC 6 July, and tropical storm conditions were reported at other stations along the northern Gulf Coast.

Real-time SFMR data obtained from the NOAA WP-3D aircraft on 5 July at 1821 UTC showed 63–66-kt winds about 13 n mi east of the center. However, post-storm analysis and recalibration by the NOAA/Hurricane Research Division (HRD) indicates the maximum SFMR observed winds were actually 59 kt at that time.

TABLE 4. (Continued)

Location	Min sea level pressure		Max surface wind speed			Storm surge (ft) ^c	Storm tide (ft) ^d	Tot rain (mm)
	Date/time (UTC)	Pressure (mb)	Date/time (UTC) ^a	Sustained (kt) ^b	Gust (kt)			
Georgia								
Atlanta-Hartsfield (KATL)								133.1
Jefferson								143.0
Lithonia								162.1
Newman								146.1
Peachtree City								132.1
South Carolina								
Greenville—Reedy River								117.9
Greenville-Spartanburg Airport (KGSP)								117.1
C-MAN stations, shore-based towers, buoys, and fixed oil-drilling platforms								
Calcasieu Pass, LA, NOS (29.8°N, 93.3°W)						2.5		
Cocodrie, LA, LUMCON (29.3°N, 90.7°W)	06/0342	1001.5	06/0223	38	51			
Dauphin Island, AL, C-MAN (30.2°N, 88.1°W)	06/1105	1005.5	06/0905	48	64			
Grand Isle, LA, C-MAN (29.3°N, 90.0°W)	06/0600	997.3	06/0129	42 ^f	60			
Isle Dernieres, LA, WAVECIS (29.0°N, 90.5°W)	06/0100	1000.3	06/0300	53	65			
Marsh Island, LA, WAVECIS (29.4°N, 92.1°W)						2.7		
Ocean Springs, MS, NOS (30.4°N, 88.8°W)	06/1124	996.2	06/1006	34	45	5.03	6.28	
Ship Pass, MS, WAVECIS (30.3°N, 89.0°W)			06/0600	37				
South Timbalier Block 52, LA, WAVECIS (28.9°N, 90.5°W)	06/0100	999.5	06/0100	67	75			
Southwest Pass, LA, C-MAN (29.0°N, 89.5°W)	06/0600	1003.6	06/0400	54	63			
Southwest Pass, LA, NOS (28.9°N, 89.4°W)	06/0636	1003.5	06/0700	49	59	2.0		
Tambour Bay, LA, LUMCON (29.2°N, 90.7°W)	06/0410	1001.2	06/0331	45	59			
Waveland, MS, NOS (30.3°N, 89.4°W)	06/0954	999.9	06/0542	37	44	3.30	4.00	183.9
Buoy 42007, NOAA (30.1°N, 88.8°W)	06/1100	996.2	06/0950	43 ^{e,f}	53			
Buoy 42067, USM (30.0°N, 88.6°W) ^e			06/1030	43	51			
ST-308 (28.2°N, 90.2°W) Oil platform/ 150 ft ASL	05/1800	994.0	05/1800	52	87			
ELXL3 (28.6°N, 89.9°W) Oil platform/ 150 ft ASL	06/0700	1009.0	06/0700	48				

^a Date/time is for sustained wind when both sustained and gust are listed.

^b Except as noted, sustained wind-averaging periods for land-based ASOS reports are 2 min.

^c Storm surge is water height above normal astronomical tide level.

^d Storm tide is water height above National Geodetic Vertical Datum (1929 mean sea level).

^e Incomplete record because of a power failure at 06/0436 UTC.

^f 10-min average.

Cindy was operationally assessed to be a tropical storm with 60-kt winds at its Louisiana landfall on 6 July. No aircraft data were available in the last few hours before landfall. However, poststorm analysis of Doppler velocity data from the NWS Slidell, Louisiana, Weather Surveillance Radar-1988 Doppler (WSR-88D) radar indicated Cindy was briefly a 65-kt hurricane. The data showed a narrow but relatively long swath of spotty velocities of at least 71 kt east of the center between 8 500–11 500 ft. These winds were first detected at 2330 UTC 5 July at a distance of about 120 n

mi south of the radar site and continued to just inland of the southeastern Louisiana coast a few hours later. The velocities imply, when applying the 90% adjustment factor used for 700-mb aircraft winds, a region of surface wind speeds exceeding 64 kt from 0000 UTC to at least 0220 UTC 6 July.

Cindy generated a storm surge of 4–6 ft above normal tide levels along the coasts of southeastern Louisiana and Mississippi, including Lake Borgne and the south shore of Lake Pontchartrain. Storm surge values of 3–4 ft were reported along the Alabama coast, while

a storm surge of 2–3 ft occurred as far west as southwestern Louisiana and as far east as the western Florida panhandle.

Rainfall totals were generally 100–150 mm across southeastern Louisiana, southern Mississippi, and southern Alabama, with a maximum total of 241.3 mm at St. Bernard, Louisiana. Heavy rains triggered flooding across portions of Louisiana, Mississippi, Alabama, and Georgia. Significant rainfall amounts also occurred during the extratropical stage from the Carolinas northward to the mid-Atlantic states. Localized flooding occurred in Virginia, where more than 5 in. of rain fell across a large portion of the Appalachian Mountain region.

In the United States, a total of 33 tornadoes occurred from 5 to 7 July: 8 in North Carolina, 7 each in Alabama and Virginia, 6 in Georgia, 2 in Mississippi, and 1 each in Louisiana, South Carolina, and Maryland. The bulk of the tornadoes formed well after landfall on 6–7 July, which is not uncommon. While the vast majority of the tornadoes were small and short-lived F0s or F1s, a damaging F2 tornado occurred near Hampton, Georgia, on 6 July.

3) CASUALTY AND DAMAGE STATISTICS

Cindy directly caused one fatality. An 18-yr-old male was swept to his death in a flooded drainage ditch in Peachtree City, Georgia, on 6 July. An F0 tornado caused one injury in Elmore, Alabama, on 6 July.

In the New Orleans metropolitan area and much of southeastern Louisiana, wind damage occurred to trees, other foliage, and power lines. An estimated 278 000 customers lost electrical power during the event. Storm surge flooding and overwash caused some beach erosion at Grand Isle. The tornadoes caused considerable damage to roofs, mobile homes, and commercial and industrial buildings, with the Hampton tornado causing more than \$40 million in damage at the Atlanta Motor Speedway. The PCS estimates the insured property losses in the United States at \$160 million. Therefore, total damages in the United States are estimated to be \$320 million.

d. Hurricane Dennis

Dennis was an unusually strong July major hurricane that left a trail of destruction from the Caribbean Sea to the northern coast of the Gulf of Mexico.

1) SYNOPTIC HISTORY

Dennis formed from a tropical wave that moved westward from the coast of Africa on 29 June. A broad

low pressure area with two embedded swirls of low clouds formed on 2 July. Convection increased near both low-level centers on 3 July. The western system moved through the southern Windward Islands on 4 July and lost organization over the southeastern Caribbean. The eastern system continued to develop, becoming a tropical depression over the southern Windward Islands near 1800 UTC 4 July (Fig. 1).

The depression initially moved westward over the eastern Caribbean, then it turned west-northwestward on 5 July as it became a tropical storm. Dennis reached hurricane strength early on 7 July south of Hispaniola. It then rapidly intensified into a category 4 hurricane with winds of 120 kt before landfall near Punta del Ingles in southeastern Cuba near 0245 UTC 8 July. During this intensification, the central pressure fell 31 mb in 24 h.

Dennis weakened to a category 3 hurricane over southeastern Cuba. Once offshore in the Gulf of Guacanayabo, the hurricane moved west-northwestward parallel to the south coast of Cuba and again intensified to category 4 strength. Maximum sustained winds reached a peak of 130 kt at 1200 UTC 8 July, then decreased to 120 kt before Dennis made landfall near Punta Mangles Altos, Cuba, near 1845 UTC that day (Fig. 4). Dennis then traversed a long section of western Cuba before emerging into the Gulf of Mexico just east of Havana around 0900 UTC 9 July. Dennis weakened significantly over Cuba, with the maximum sustained winds decreasing to 75 kt by the time the center left the island.

Dennis slowly intensified for the next 6–12 h over the Gulf of Mexico, then began rapid intensification near 1800 UTC 9 July, accompanied by a turn toward the north-northwest. The central pressure fell 37 mb in 24 h, including 20 mb in 6 h and 11 mb in 1 h 35 min. Maximum sustained winds reached a third peak of 125 kt near 1200 UTC 10 July. Thereafter, weakening occurred, likely due to mid-/upper-level dry air from the western Gulf of Mexico entraining into the hurricane. The maximum sustained winds decreased to 105 kt and the central pressure rose to 946 mb before Dennis made landfall on Santa Rosa Island, Florida, between Navarre Beach and Gulf Breeze, at about 1930 UTC 10 July.

Dennis continued north-northwestward after landfall, with the center moving across the western Florida panhandle into southwestern Alabama before it weakened into a tropical storm. It became a depression as it moved into east-central Mississippi on 11 July. The cyclone turned northward later that day and northeastward on 12 July as it moved into the Ohio Valley. On 13 July, Dennis weakened to a low pressure area that me-

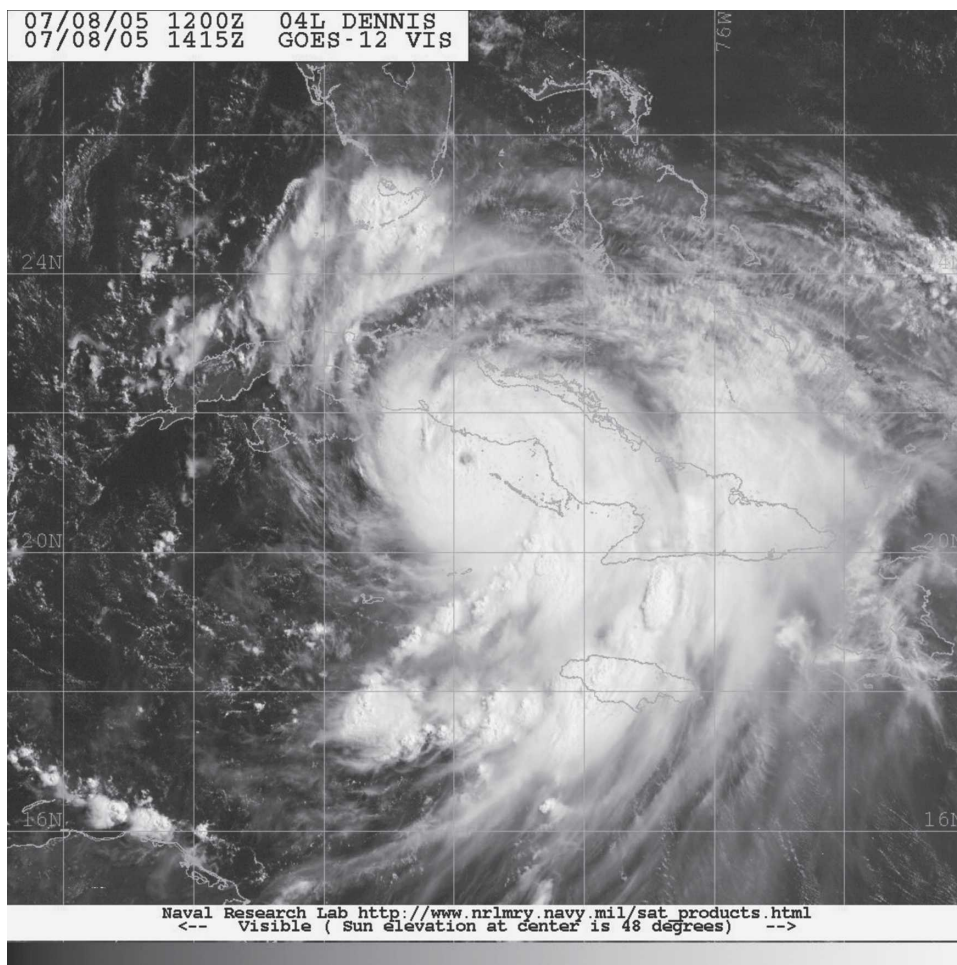


FIG. 4. Geostationary Operational Environmental Satellite-12 (GOES-12) visible image of Hurricane Dennis at 1415 UTC 8 Jul 2005. Image courtesy of the NRL, Monterey, CA.

andered over the Ohio Valley through 15 July. The remnants of Dennis accelerated northeastward on 16 July and were absorbed into a larger low over northwestern Ontario on 18 July.

2) METEOROLOGICAL STATISTICS

The 53rd WRS made 43 center penetrations or “fixes” on Dennis, with NOAA aircraft contributing an additional 10 fixes. The maximum flight-level winds observed at 700 mb were 150 kt at 1325 UTC 8 July. Eyewall dropwindsondes reported 116-kt surface winds at 1515 UTC 10 July and 114 kt at 1705 UTC 8 July. The minimum aircraft-reported central pressure was 930 mb at 1143 UTC 10 July, with a 937-mb pressure measured at 1517 UTC 8 July. The last aircraft-reported pressure near landfall in Florida was 946 mb at 1930 UTC 10 July.

Dennis brought hurricane conditions to portions of southeastern Cuba, and to a swath through central and

western Cuba (Table 5). Cabo Cruz reported 116-kt sustained winds with a gust to 129 kt at 0200 UTC 8 July, with a minimum pressure of 956 mb at 0240 UTC just before the eye passed over the station. The anemometer was destroyed, and it is possible stronger winds occurred. Unión de Reyes reported sustained winds of 96 kt with a gust to 107 kt at 2350 UTC 8 July, and there were numerous other reports of sustained hurricane-force winds.

Dennis also brought hurricane conditions to portions of the western Florida panhandle and southwestern Alabama. An instrumented tower run by the Florida Coastal Monitoring Program (FCMP) at Navarre (5-m elevation) measured 1-min average winds of 86 kt and a gust to 105 kt at 1921 UTC 10 July. This tower was a few nautical miles east of the radius of maximum winds. Another FCMP tower at the Pensacola Airport (10-m elevation) measured 1-min average winds of 71 kt with a gust to 83 kt just west of the eye at 1946 UTC. A

TABLE 5. Selected surface observations for Hurricane Dennis, 4–13 Jul 2005.

Location	Min sea level pressure		Max surface wind speed			Storm surge (ft) ^c	Storm tide (ft) ^d	Tot rain (mm)
	Date/time (UTC)	Pressure (mb)	Date/time (UTC) ^a	Sustained (kt) ^b	Gust (kt)			
Jamaica								
Montego Bay			07/2049	60				
Cuba								
Aguada de Pasajeros	08/2100	977.9	08/2108	96	104			
Bainoa	09/0250	974.5	09/0230	62	67			237.2
Batabanó	09/0455	991.7	09/N/A	38	48			133.6
Bauta	09/0410	988.9	09/N/A	35	43			141.0
Cabo Cruz	08/0240	956.0	08/0200	116 ^c	129 ^c			
Caibarién	08/1800	1000.0	08/1600	31	46			
Camagüey	08/0600	1007.0	08/0500	38	51			
Camilo Cienfuegos	08/1000	1007.1	08/N/A	36	41			
Casa Blanca	09/0445	975.0	09/0610	68	75			92.5
Cayo Coco	08/0900	1008.3	08/N/A	30	49			
Cienfuegos	08/1800	982.1	08/1850	81	85			
Colón	08/2110	988.6	08/2110	58	73			273.3
El Jíbaro	08/1400	1002.0	08/1315	56	63			235.5
Esmeralda	08/0700	1005.9	08/0650	35	47			
Florida	08/0900	1005.2	08/0803	38	51			
Guantánamo	07/N/A	1001.3	07/1850	37	41			
Güines	09/0210	981.1	09/0200	50	57			
Güira de Melena	09/0515	994.2	09/N/A	29	36			107.4
Indio Hautey	08/2200	994.0	08/2000	62	67			
Jovellanos	08/2200	985.2	08/2350	58	73			311.4
Júcaro	08/1200	1004.5	08/N/A	45	57			243.1
Jucarito	08/0200	1006.2	08/0440	35	46			
Las Piedra	08/1550	1000.9	08/1543	64	99			384.3
Las Tunas	08/0200	1008.0	08/0950	35	42			
Manzanillo	08/0215	1003.6	08/0135	38	51			
Melena del Sur	09/0230	990.8	09/N/A	44	56			264.2
Nuevitas	08/0700	1000.8	08/0600	43	51			
Palo Seco	08/0600	1007.5	08/0600	29	39			
Puerto Padre	08/0000	1008.4	07/1910	35	44			
Sagua la Grande	08/2100	1002.1	08/1700	43	59			
Sancti Spiritus	08/1500	1003.3	08/1750	46	60			235.0
Santa Cruz del Sur	08/0645	999.4	08/0600	71	89			
Santiago de las Vegas	09/0540	989.0	09/0610	68	75			140.7
Santo Domingo	08/1750	1000.9	08/1700	56	63			316.5
Tapaste	09/0230	977.0						286.5
Topes de Collantes			08/1555	81	89			702.8
Trinidad	08/1620	988.6	08/1600	94	103			358.4
Unión de Reyes	09/0000	972.5	08/2350	96	107			294.4
Varadero	09/0000	994.2	08/2330	54	67			168.1
Veguitas	08/0200	1002.8	08/0000	28	41			
Venezuela	08/1200	1005.6	08/N/A	45	50			
Yabú	08/1800	1001.3	08/1300	31	51			204.7
Florida								
Big Pine Key			09/1600	34	48			
Brooksville (KBKV)	09/2228	1009.1	10/1652	24	37			46.2
Cache RAWS			09/0716		50			
Carysfort Reef Light			09/1500	51	59			
Chekika RAWS			09/0337		63			103.6
Crestview (KCEW)	10/2009	989.5	10/2024	37	50			
Cross City (KCTY)	10/1754	1008.5	09/2318		39			109.7
Destin (KDTS)			10/1929	49	64			
Destin FCMP tower	10/1858	986.9	10/1921	55	70			
Eglin AFB A-5	10/1844	983.1	10/1544	73				
Eglin AFB A-13B			10/1934	73	90			

TABLE 5. (Continued)

Location	Min sea level pressure		Max surface wind speed			Storm surge (ft) ^c	Storm tide (ft) ^d	Tot rain (mm)
	Date/time (UTC)	Pressure (mb)	Date/time (UTC) ^a	Sustained (kt) ^b	Gust (kt)			
Florida								
Eglin AFB B-71	10/1958	982.1	10/1906	51	82			
Eglin AFB B-75	10/1940	977.7	10/1958	46	77			
Eglin AFB Valparaiso (KVPS)	10/1923	986.1	10/1923	48	72			
Eglin AFB Yellow River	10/1952	968.5						
Everglades City	09/1201	1007.2	09/1601	22	39			
Flamingo	09/0703	1005.5	09/0703	52	59			
Ft. Lauderdale (KFLL)	09/0841	1010.9	09/0857	26	41			
Ft. Lauderdale (KFXE)	09/0921	1011.2	09/1008	29	39			
Ft. Myers (KFMY)	09/2336	1007.8	09/2000	30	40			115.3
Ft. Myers (KRSW)	09/2336	1007.5	09/1929	29	37			
Homestead ARB (KHST)	09/0555	1007.5	09/0102	24	38			
Jay FAWN (unofficial)			10/1845	62				
Key West (KEYW)	09/0853	1001.9	09/1017	53	64			147.6
Marathon (KMTN)	09/0853	1006.5	09/0752	33	47			47.8
Miami Beach	09/0902	1005.8	09/0202	35	60			48.8
Miami Int. (KMIA)	09/0622	1009.7	08/2222	36	44			60.7
Monticello								176.5
Naples (KAPF)	09/2210	1005.8	09/1759	33	47			74.9
Navarre FCMP tower	10/1909	965.2	10/1921	86	105			
New Pass Mote Laboratory COMPS	10/0000	1005.0	09/1630		40			
Oasis Ranger Station RAWS			00/0034		37			
Ochopee RAWS			09/1536		37			83.6
Opa Locka (KOPF)	08/0140	1010.9	09/0315	44	58			62.2
Pace (unofficial)	10/1910	945.0						
Panama City (KPFN)	10/1707	1001.5	10/1757	33	48			87.9
Pembroke Pines (KHWO)	09/0706	1010.5	09/0753	33	50			78.5
Pensacola (KPNS)	10/1952	956.6	10/2002	66	81			104.4
Pensacola FCMP tower	10/1943	956.3	10/1946	71	83			
Pensacola NAS (KNPA)	20/1956	976.6	10/1750	39	50			
Pompano Beach (KPMP)	09/0900	1011.6	09/1025	30	43			25.9
Punta Gorda (KPGD)	09/2359	1008.5	08/2038	35	44			111.5
St. Marks NWR East RAWS			10/2114		37			
St. Marks NWR West RAWS			10/1546		44			95.3
St. Petersburg (KPIE)	09/2353	1007.5	09/1044	38	50			61.0
St. Petersburg (KSPG)	09/2350	1007.1	09/1706	37	45			62.2
Sarasota (KSRQ)	10/0009	1006.1	09/2057	31	38			46.5
Summerland Key			09/0800	36	50			
Tallahassee (KTLH)	10/2027	1005.4	10/1537	33	44			168.7
Tampa Int. (KTPA)	09/2354	1008.5	09/1718	27	37			43.9
Tampa MacDill AFB (KMCF)			10/1155	33	43			41.4
Tampa Sunshine Skyway NOS	09/2252	1004.1	09/2222	39	48			
Tenraw RAWS			09/0723		48			
The Villages (KVVG)			09/2225		41			
Vandenburg (KVDF)			09/1757		35			
West Kendall Tamiami (KTMB)	09/0728	1007.5	09/0112	38	56			91.2
West Palm Beach (KPBI)	09/0709	1012.2	09/1053	27	38			51.8
Winter Haven (KGIF)	09/2226	1009.8	09/2314	26	35			61.0
Alabama								
Camden 10 NW								325.1
Covington County RAWS			10/2220		43			
Dothan (KDHN)	10/2237	999.2	10/1839	33	44			78.0
Mobile Airport (KMOB)	10/2228	990.5	10/1837	32	42			94.2
Tuskegee RAWS			10/2325		36			
Georgia								
Adel RAWS			10/2000		34			
Albany	10/2310	1007.5	10/1853	25	37			116.6
Valdosta	10/2048	1009.8	10/1858	24	34			99.3

TABLE 5. (Continued)

Location	Min sea level pressure		Max surface wind speed			Storm surge (ft) ^c	Storm tide (ft) ^d	Tot rain (mm)
	Date/time (UTC)	Pressure (mb)	Date/time (UTC) ^a	Sustained (kt) ^b	Gust (kt)			
Mississippi								
Bienville RAWS			11/0505		34			
Biloxi–Keesler AFB (KBIX)	06/1050	995.3	06/0959		41			92.7
Biloxi NOS						2.21	3.36	
Greene RAWS			10/2310		34			
Gulfport (KGPT)	10/2254	997.6	10/1952	27	36			10.9
Lauderdale RAWS			10/2310		48			
Neshoba RAWS			11/0310		41			
Pascagoula (KPQL)	10/2325	994.2	10/1931		34			26.9
Wausau RAWS			11/0105		37			
Louisiana								
Lake Pontchartrain NWS—Mid-Lake			10/2210	34	42			
New Orleans Lakefront (KNEW)	11/0030	1003.7	10/2120	31	41			2.0
Buoys/C-MAN								
Apalachicola, FL, NOS (29.7°N, 85.0°W)	10/1700	1001.5	10/1124	41	56	6.94	8.11	
Cedar Key, FL, C-MAN (29.1°N, 83.0°W)	10/1000	1009.7	10/0050	42 ^f	51	4.81	7.79	
Clearwater Beach, FL NOS (28.0°N 82.8°W)	10/1000	1006.4	09/2100	30	42	3.87	5.15	
Dauphin Island, AL, C-MAN (30.2°N, 88.1°W)	10/2100	990.6	10/1740	44 ^f	57	2.76	3.51	
Ft. Myers, FL, NOS (26.7°N, 81.9°W)	09/2300	1008.7	09/2000		36	2.85	3.20	
Fowey Rocks, FL, C-MAN (25.6°N, 80.1°W)	09/0800	1009.7	09/0720	52 ^f	73			
Grand Isle, LA, C-MAN (29.3°N, 90.0°W)	11/0000	1004.7	10/2120	27 ^f	35	1.05	2.01	
Homosassa, FL, COMPS (28.8°N, 82.7°W)	10/0948	1008.8	09/1948	36	52			
Keaton Beach, FL, C-MAN (29.8°N, 83.6°W)	10/1500	1008.1	10/1920	34 ^f	48			
Key West, FL, NOS (24.6°N, 81.8°W)	09/0848	1002.3	09/1524	27	44	1.67	2.97	
Long Key, FL, C-MAN (24.8°N, 80.9°W)	09/0700	1005.7	09/1250	41 ^f	54			
Molasses Reef, FL, C-MAN (25.0°N, 80.4°W)	09/0700	1007.6	09/0000	45	58			
Naples, FL, NOS (26.1°N, 81.8°W)	09/2300	1009.4	09/0800		38	2.99	4.26	
NW Florida Bay COMPS (25.1°N, 81.1°W)	09/0724	1006.1	09/0600	41	54		1.2	
Ocean Springs, MS, NOS (30.4°N, 88.8°W)	10/2242	995.9				2.50	2.97	
Panama City Beach, FL, NOS (30.1°N, 85.9°W)	10/1800	994.1	10/1800	51	63	5.72	6.79	
Pensacola, FL, NOS (30.4°N, 87.2°W)	10/1900	968.7	10/1900	35	51	4.16	5.52	
Port Manatee, FL, NOS (27.6°N, 82.6°W)			09/2242	28	41	2.87	4.09	
St. Petersburg, FL, NOS (27.8°N, 82.6°W)			10/1212	31	42	3.15	4.49	
Sand Key, FL, C-MAN (24.5°N, 81.9°W)	09/0900	999.4	09/0920	54 ^f	68			
Shell Point, FL, COMPS (30.1°N, 84.3°W)	10/1430	1006.0	10/1700	32	41			
Sombrero Key, FL, C-MAN (24.6°N, 81.1°W)	09/0800	1005.5	09/0800	64	76	1.3	2.6	
Southwest Pass, LA, C-MAN (29.0°N, 89.5°W)	10/2300	1003.7	10/0640	33 ^f	39			
Southwest Pass, LA, NOS (28.9°N, 89.4°W)	10/2306	1004.0	10/0636	33	38	1.29	2.54	
Tampa McKay Bay, FL, NOS (27.9°N, 82.4°W)			09/1706	28	47	3.38	4.84	
Tyndall AFB Tower, FL, C-MAN (29.4°N, 89.9°W)	10/1400	1000.4	10/1440	55 ^f	68			
Vaca Key, FL, NOS (24.7°N, 81.1°W)	09/0718	1005.8	09/0600		44		1.2	
Venice, FL (27.1°N, 82.5°W)	10/0000	1006.0	10/1500	36	41			
Waveland, MS, NOS (30.3°N, 89.4°W)	10/2254	1000.0				1.66	2.11	
Buoy 42003, NOAA (26.0°N, 85.9°W)	10/0000	991.5	09/2310	38 ^f	49			
Buoy 42007, NOAA (30.1°N, 88.8°W)	10/2150	995.1	10/1940	34 ^f	45			
Buoy 42013, COMPS (27.2°N, 82.9°W)	09/2210	1004.5	10/0210	45				
Buoy 42036, NOAA (28.5°N, 84.5°W) ^e	10/1150	996.4	10/0640	46 ^f	58			
Buoy 42039, NOAA (28.8°N, 86.0°W) ^e	10/1250	979.0	10/1050	47	58			
Buoy 42058, NOAA (15.0°N, 75.0°W)	07/0750	1006.9	07/1350	27	35			
Buoy 42067, USM (30.0°N, 88.7°W) ^e			10/2140	34	45			

^a Date/time is for sustained wind when both sustained and gust are listed.

^b Except as noted, sustained wind-averaging periods for land-based ASOS reports are 2 min.

^c Storm surge is water height above normal astronomical tide level.

^d Storm tide is water height above National Geodetic Vertical Datum (1929 mean sea level).

^e Incomplete record—more extreme values may have occurred.

^f 10-min average.

Florida Automated Weather Network station at Jay reported sustained winds of 62 kt at 1845 UTC.

While hurricane-force winds associated with Dennis covered only a small area near the eye, it had a large cyclonic envelope with tropical-storm-force winds extending well east of the center over Florida. The Coastal Marine Automated Network Station (C-MAN) at Sombrero Key, Florida (48.5-m elevation), reported 2-min average winds of 64 kt with a gust of 76 kt at 0800 UTC 9 July. A National Ocean Service (NOS) station at Panama City Beach, Florida (6.1-m elevation), reported 6-min average winds of 51 kt with a gust to 63 kt at 1800 UTC 10 July. Tropical storm conditions also occurred over the metropolitan areas of southeastern Florida, elsewhere along the Florida west coast and the Florida Big Bend region, over portions of southwestern Alabama, and across Jamaica. Wind gusts to tropical storm force occurred as far inland as eastern Mississippi and as far west as southeastern Louisiana.

The FCMP tower at the Pensacola Airport measured a pressure of 956.3 mb at 1943 UTC 10 July, while the FCMP tower in Navarre measured a pressure of 965.2 mb at 1909 UTC that day. A storm chaser in Pace, Florida, unofficially measured a pressure of 945 mb at 1910 UTC 10 July as the eye passed over.

Dennis produced a storm surge of 6–7 ft above normal tide levels on Santa Rosa Island near where the center made landfall. This surge washed over Santa Rosa Island near and west of Navarre Beach. A storm surge of 6–9 ft above normal tide levels occurred in Apalachee Bay, Florida (roughly 150 n mi east of the landfall area), which inundated parts of the town of St. Marks and other nearby areas. This surge was higher than known wind reports would support, and roughly 3.5 ft higher than the surge forecast from the Sea, Lake, and Overland Surge from Hurricanes (SLOSH) model. This surge was likely triggered by an oceanic trapped shelf wave that propagated northward along the Florida west coast. Modeling by the Center for Ocean–Atmospheric Prediction Studies at The Florida State University suggest this remotely generated sea level rise added 3–4 ft to the surge in and around Apalachee Bay (Morey et al. 2006). A storm surge of 4–6 ft occurred elsewhere along the Florida panhandle. Storm surges of 3–5 ft above normal tide levels occurred elsewhere along the Florida west coast, in the Florida Keys, and along the coast of Alabama. Storm tides of 2–4 ft above normal were reported along the coasts of Mississippi and southeastern Louisiana. Storm surge data from Cuba are not available.

Dennis produced widespread heavy rainfall over Cuba. Topes de Collantes reported a 24-h total of 702.8 mm, while Las Piedra reported a 24-h total of 384.3

mm. Storm totals for both places were likely higher. Rainfall of 150–300 mm was reported from other Cuban stations. Very heavy rains also occurred in Jamaica, where Mavis Bank reported a storm total of 623.3 mm and Shirley Castle reported a total of 591.1 mm. In the United States, Dennis produced widespread heavy rainfall along the track from the western Florida panhandle to the Ohio Valley, and east of the track in Georgia and the remainder of Florida. A station 8 n mi northwest of Camden, Alabama, reported a storm-total rainfall of 325.1 mm, while Monticello, Florida, reported 176.5 mm.

Dennis caused nine tornadoes in Florida and one in Georgia. All were rated F0 except for an F1 near Bradenton, Florida. Additionally, numerous strong squalls occurred in the outer bands of Dennis over southern Florida. These squalls produced a gust of 73 kt at the Fowey Rocks C-MAN station and a gust of 63 kt at Chekika in southern Miami-Dade County.

3) CASUALTY AND DAMAGE STATISTICS

Reports from the Meteorological Service of Jamaica and the media indicate that Dennis was directly responsible for 42 deaths—22 in Haiti, 16 in Cuba, 3 in the United States, and 1 in Jamaica. The fatalities in the United States included a drowning on a sunken boat in the Florida Keys, a drowning in rough surf at Dania Beach, Florida, and a man crushed by a falling tree near Atlanta, Georgia. Dennis was also indirectly responsible for 12 deaths in Florida—2 from electrocution, 2 from carbon monoxide poisoning, 4 from automobile accidents, 2 accidental falls during cleanup, and 2 cases of natural causes exacerbated by storm stress.

The PCS estimates the insured property damage in the United States at \$1.115 billion. Therefore, the total U.S. damage estimate for Dennis is \$2.23 billion. The Meteorological Service of Jamaica estimates the damage from Dennis at \$1.9 billion Jamaican (approximately \$31.7 million U.S.).

e. Hurricane Emily

Emily was briefly a category 5 hurricane in the Caribbean Sea that, at lesser intensities, struck Grenada, resort communities on Cozumel and the Yucatan peninsula, and northeastern Mexico just south of the Texas border. Emily is the earliest-forming category 5 hurricane of record in the Atlantic basin and the only known hurricane of that strength to occur during the month of July.

1) SYNOPTIC HISTORY

Emily developed from a tropical wave that moved across the west coast of Africa on 6 July. The wave was

associated with a large area of cyclonic vorticity and disturbed weather while it crossed the eastern tropical Atlantic. Shower activity became more concentrated on 10 July, and by 0000 UTC 11 July the system had become a tropical depression about 1075 n mi east of the southern Windward Islands (Fig. 1).

The depression moved westward to the south of a narrow ridge. Initial development was slow because of modest easterly shear and a relatively dry environment. Although the circulation remained broad and somewhat ill defined, the system became a tropical storm at 0000 UTC 12 July about 800 n mi east of the southern Windward Islands. Emily accelerated westward on 12 July due to a low-level easterly surge. This surge enhanced the dry environment and produced some westerly shear that appeared to prevent further convective organization. On 13 July, however, with the core convection still disorganized, the central pressure hovering near 1003 mb, and flight-level winds showing little change, visual estimates of the sea state suggested increasing surface winds. Aircraft center fixes at 2331 UTC 13 July and 0112 UTC 14 July suggested that the center of circulation reformed northeast of its previous position within the convection. It is estimated that Emily became a hurricane at about this time when centered about 85 n mi east-southeast of Grenada. The convective pattern became much more symmetric and organized over the next several hours, and Emily's maximum winds increased to near 75 kt by the time the center passed over Grenada near 0700 UTC 14 July.

Emily entered the Caribbean Sea and turned west-northwestward, maintaining this heading for the next week as midlevel high pressure built westward to the north of the hurricane. It continued to strengthen, with its peak winds reaching 115 kt (category 4) and its minimum pressure falling to 952 mb early on 15 July. Near 1200 UTC an AFRC aircraft reported concentric eyewalls of 8 and 25 n mi diameter, and by 1800 UTC Emily had weakened to category 2 strength. A second strengthening phase began almost immediately, however, and continued on 16 July while Emily passed about 90 n mi south of Jamaica. Emily became a category 5 hurricane, with winds of 140 kt and a minimum pressure of 929 mb, at 0000 UTC 17 July about 100 n mi southwest of Jamaica (Fig. 5).

Emily began to slowly weaken on 17 July in the western Caribbean Sea, this time in the absence of concentric eyewalls but also without any obvious external synoptic forcing. It was still a category 4 hurricane, with winds of 115 kt, when the eyewall passed over Cozumel and when the center made landfall on the Yucatan peninsula near Tulum at 0630 UTC 18 July. Emily quickly cut across the Yucatan, emerging into the Gulf of

Mexico near 1200 UTC that day while just maintaining hurricane strength.

Once over water, Emily began its third and final intensification phase as it continued west-northwestward. Because of the broad overall circulation, Emily strengthened slowly for the first 24 h or so over the Gulf, its winds increasing to 80 kt by 1200 UTC 19 July. Over the next 12 h, however, a sharp inner wind maximum developed, the minimum pressure fell 29 mb, and maximum winds increased to near 110 kt. Early on 20 July as Emily neared the coast, data from land-based radars and reconnaissance aircraft showed a well-defined concentric eyewall structure, with the strongest flight-level winds associated with the outer feature. Intensification stopped and Emily made landfall near San Fernando, Mexico at 1200 UTC 20 July as a category 3 hurricane with winds of near 110 kt. After landfall, Emily turned westward and weakened rapidly, dissipating on 21 July over the Sierra Madre Oriental of Mexico.

2) METEOROLOGICAL STATISTICS

Emily's peak intensity is estimated to be 140 kt, based on 700-mb flight-level winds of 153 kt observed at 0324 UTC 17 July. Application of the standard 90% adjustment gives a surface estimate of 138 kt—just above the category 5 threshold. Two surface-adjusted flight-level observations of 136 kt during the preceding several hours also met the category 5 threshold. An eyewall dropwindsonde reported an instantaneous surface wind of 136 kt at 0536 UTC 17 July, although surface estimates inferred from layer averages of the dropwindsonde profile were near 115 kt. The lowest aircraft-reported central pressure reported was 929 mb, at 2341 UTC 16 July.

Emily's intensity on 13–14 July was particularly difficult to assess. Flight-level winds near 1200 UTC 13 July implied an intensity near 45 kt, while visual sea-state observations by the AFRC aircrew suggested surface winds near 55 kt. Later, near 0100 UTC 14 July, an AFRC aircraft reported an 850-mb flight-level wind of 79 kt, which corresponds to 63 kt at the surface using typical adjustment factors. Concurrent with this latter observation was a dropwindsonde that suggested surface winds were near 80 kt. It is possible that during this intensification phase the surface winds were leading the winds aloft.

Emily passed directly over Grenada. Point Salines International Airport, just south of the path of the center, reported a peak gust of 58 kt (Table 6). The northeastern tip of Grenada, as well as the smaller islands of Carriacou and Petite Martinique to the northeast, bore

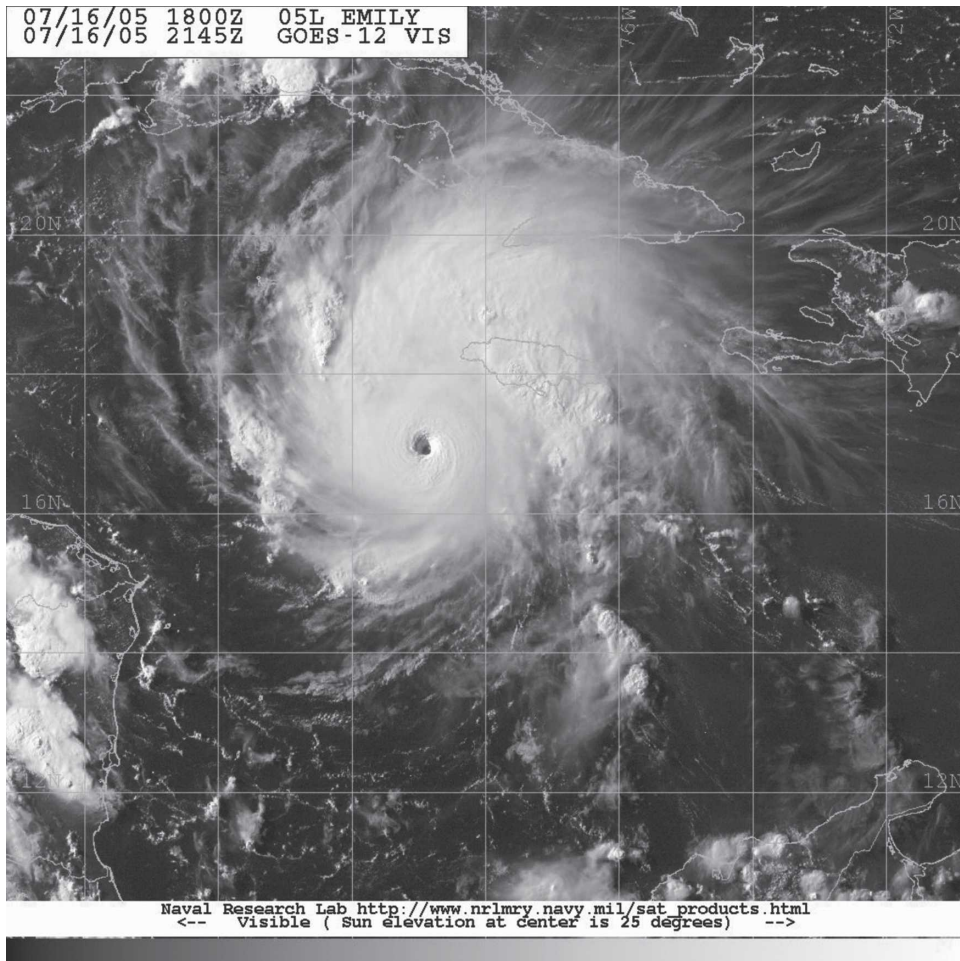


FIG. 5. GOES-12 visible image of Hurricane Emily at 2145 UTC 16 Jul 2005. Image courtesy of the NRL, Monterey, CA.

the brunt of the hurricane, but no wind measurements from these areas are available.

Heavy rains from Emily affected Jamaica, with the heaviest accumulations occurring in St. Elizabeth Parish on the southwestern part of the island. Potsdam reported 391.9 mm of rainfall, with other reports in excess of 250 mm.

At 0509 UTC 18 July, as the eyewall passed over Cozumel, an AFRC aircraft a few nautical miles offshore measured a 700-mb flight-level wind of 124 kt. A flight-level wind of 141 kt was reported 2 h earlier. These are the basis for the 115-kt intensity for the Yucatan landfall. No wind observations are available from the landfall area. An unofficial report received via amateur radio estimated a 15-ft storm surge in San Miguel on Cozumel. Official rainfall totals on the Yucatan were generally close to 25 mm, although there was an unofficial report from Cozumel of 124.4 mm.

No surface data are available at the coast for Emily's

final landfall. An automated station at San Fernando, located about 30 n mi inland from the landfall location, reported a 10-min sustained wind of 55 kt, a gust to 84 kt, and a minimum pressure of 965 mb. There were several reports from northeastern Mexico of rainfall in excess of 250 mm, with 350.0 mm reported at Cerralvo. No estimates of storm surge at the final landfall were received.

In Texas, there were a few reports of sustained tropical-storm-force winds, with the highest sustained wind reported at Harlingen. Minor coastal flooding occurred in south Texas, with estimated storm tides in the 4–5-ft range. Moderate beach erosion was reported in Cameron County. Eleven tornadoes were reported in southeastern Texas.

3) CASUALTY AND DAMAGE STATISTICS

The Caribbean Disaster Emergency Response Agency reports that in Grenada damage was concen-

TABLE 6. Selected surface observations for Hurricane Emily, 11–21 Jul 2005.

Location	Min sea level pressure		Max surface wind speed			Storm surge (ft) ^c	Storm tide (ft) ^d	Tot rain (mm)
	Date/time (UTC)	Pressure (mb)	Date/time (UTC) ^a	Sustained (kt) ^b	Gust (kt)			
	Grenada							
Point Salines Int. Airport	14/0700	991.5	14/0840	35	58			83.3
	Barbados							
Grantly Adams			13/1900	37				
	Jamaica							
Fullerwood								290.1
Holland								228.6
Mountainside								329.9
Non-Pariel								296.9
Potsdam								391.9
	Mexico							
Matamoros			20/1440	35	59			
Monterrey Airport			20/1440	35	59			
San Fernando	20/1550	965	20/1510	55 ^e	84			
Cabazones								212.9
Cadereyta								164.6
Cerralvo								350.0
Cienega de Flores								166.1
El Canada								188.0
Las Enramadas								182.1
Higuera								180.1
Iturbide								158.0
Madero								329.7
Monterrey								247.9
Presa Cerro Prieto								285.5
Presa El Cuchillo								230.1
Presa La Boca								235.0
Reynosa								204.7
Rio Bravo								204.7
Sabinas Hidalgo								272.5
Vallehermoso								251.5
	Texas							
Alice			20/1310	34	40			
Bayview (KPIL)			21/0536		34			
Brownsville (KBRO)	20/0807	1002.4	20/1204	42	55			65.8
Edinburg	20/1000	1007.1	20/1824	26	34			
Harlingen (KHRL)	20/0833	1004.7	20/1107	44	51			76.2
McAllen (KMFJ)	20/1032	1005.7	20/0833	33	41			108.2
Weslaco			20/1420	33	42			
	Buoys							
Buoy 42002, NOAA (25.2°N, 94.4°W)	19/2150	1002.6	19/1610	46 ^e	66			
Buoy 42020, NOAA (26.9°N, 96.7°W)	20/0850	1006.4	19/1840	34 ^e	45			
Buoy 42055, NOAA (22.0°N, 94.1°W)	19/0959	1003.6	19/0959	36 ^f	39			
Buoy 42056, NOAA (19.9°N, 85.1°W)	17/2151	996.7	17/2151	63 ^f	74			
Buoy 42057, NOAA (15.0°N, 80.0°W)			16/2208	34 ^f	39			
Buoy 42058, NOAA (15.0°N, 75.0°W)	16/0455	999.0	16/0455	40 ^f	51			

^a Date/time is for sustained wind when both sustained and gust are listed.

^b Except as noted, sustained wind-averaging periods for land-based ASOS reports are 2 min.

^c Storm surge is water height above normal astronomical tide level.

^d Storm tide is water height above National Geodetic Vertical Datum (1929 mean sea level).

^e 10-min average.

^f 1-min average.

trated in the northern parishes of St. Patrick's and St. Andrew's, where many homes lost their roofs, and on the outlying islands of Petite Martinique and Carriacou, where the island's only hospital suffered roof damage, forcing the evacuation of patients to another portion of the building. There were also scattered reports of flooding, and media reports mention the destruction of crops. There was some roof damage in St. Vincent, the Grenadines, and Tobago.

Playa del Carmen, Tulum, and the island of Cozumel were hardest hit during Emily's first landfall in Mexico, although the reported damage was unexpectedly light, suggesting that Emily's strongest winds were extremely limited in extent. The winds, however, were strong enough to snap concrete utility poles between Playa del Carmen and Cancun. Water was knee-deep in some streets. At Emily's second landfall in northern Mexico, officials reported that 80%–90% of the homes in the fishing community of Laguna Madre were destroyed. Elsewhere near the landfall site, the storm drove 90 000 people from their homes, and thousands of buildings were reported destroyed.

In Texas, damage was minor; there were reports of tree damage in the Brownsville area and scattered minor roof damage on South Padre Island.

Six deaths were directly attributed to Emily. One fatality occurred in a Grenada mudslide. In southwestern Jamaica, four people in a car were driving through a flooded roadway when a surge of water pushed them over a cliff. One person assisting the motorists also perished. Amazingly, there were no deaths directly attributable to Emily's two landfalls in Mexico, although a helicopter crash before the storm claimed two lives. Massive evacuations, which by some estimates involved nearly 100 000 people, mostly tourists, undoubtedly contributed to the lack of casualties.

f. Tropical Storm Franklin

The tropical wave that led to the formation of Tropical Storm Franklin emerged from the west coast of Africa on 10 July. The wave reached the Lesser Antilles on 18 July essentially void of deep convection, apparently due to vertical shear east of an upper-level trough over the Caribbean Sea. The southern portion of the wave passed through the Caribbean Sea and eventually spawned Tropical Storm Gert over the southwestern Gulf of Mexico. Meanwhile, the upper-level trough weakened and moved northwestward, allowing anticyclonic upper-level flow to develop over the northern portion of the wave on 19 July. Deep convection became concentrated north of Hispaniola the next day. Convective bands formed as the system proceeded northwestward just east of the Bahamas on 21 July. A

midlevel circulation was evident by about 1600 UTC, and AFRC aircraft reports at around 2030 UTC indicated a closed low-level circulation. It is estimated that a tropical depression formed by 1800 UTC 21 July, centered about 60 n mi east of Eleuthera in the northwestern Bahamas (Fig. 1).

The depression became a tropical storm with winds of 40 kt by 0000 UTC 22 July while centered about 70 n mi east-southeast of Great Abaco. However, most of the winds and rains of Franklin were east of both its center and the Bahamas. After initially moving northwestward, the cyclone turned northward on 22 July, with strengthening limited by westerly shear. The shear abated early on 23 July, which allowed Franklin to reach its peak intensity of 60 kt at 2100 UTC that day. The storm turned northeastward that day because of an upper-level trough moving eastward from the east coast of the United States. The trough bypassed the storm, leaving strong northwesterly shear over a weakening Franklin on 24–25 July. Franklin's track during those two days was generally eastward but quite erratic. The storm turned northward on 26 July, passing about 175 n mi west of Bermuda, as a deep layer ridge built to its east.

Franklin continued slowly northward between Bermuda and North Carolina during 27–28 July. The shear gradually relaxed during this period, and Franklin slowly reintensified. Franklin turned northeastward on 28 July in advance of another midlatitude trough and associated cold front over the northeastern United States. The tropical storm steadily accelerated on 29 July and its center passed about 250 n mi south of Nova Scotia. Franklin transformed into an extratropical cyclone by 0000 UTC 30 July and passed just south of Cape Race, Newfoundland, later that day. It was absorbed by a larger extratropical system the next day.

Two ships reported tropical-storm-force winds from Franklin while it was a tropical cyclone. The *Alkin Kalkavan* (call sign V7GY3) reported 50-kt winds at 2100 UTC 29 August as Franklin was becoming extratropical, while the *Liberty Sun* (call sign WCOB) reported 37-kt winds at 0900 UTC 25 August. There were no reports of casualties or damages from Franklin.

g. Tropical Storm Gert

Gert formed from the southern portion of the tropical wave that spawned Tropical Storm Franklin. This system continued westward over the central and western Caribbean Sea where thunderstorm activity increased on 20 July. A low pressure area formed in the Gulf of Honduras just east of Chetumal on 22 July, which moved inland over Yucatan with no additional development. The low emerged into the Bay of

Campeche early the next day with a broad circulation lacking deep convection. Convective bands developed around the broad inner circulation and it is estimated that a tropical depression formed at 1800 UTC 23 July about 255 n mi east-southeast of Tuxpan (Fig. 1). Convection developed near the center and it is estimated that the depression became a tropical storm at 0600 UTC 24 July. The cyclone reached its maximum intensity of 40 kt, with a minimum pressure of 1005 mb, at landfall around 0000 UTC 25 July, just north of Cabo Rojo, Mexico. Gert continued west-northwestward and then westward, dissipating over high terrain by 0000 UTC 26 July. There were no reports of casualties or damages from Gert.

h. Tropical Storm Harvey

The tropical wave that eventually generated Harvey crossed the west coast of Africa on 22 July. The wave moved westward for the next several days without significant development. A surface low associated with the northern portion of the wave crossed Puerto Rico and then moved generally northward away from that island during 30 July–1 August. The system was poorly organized because of southerly wind shear associated with an upper-level low to its west.

Convection increased on 2 August north and east of the surface low. It is estimated that a tropical depression formed by 1800 UTC that day about 320 n mi southwest of Bermuda (Fig. 1). The circulation center was poorly defined at the time and the cyclone had a subtropical appearance in satellite imagery. However, the depression is designated tropical rather than subtropical since: 1) deep convection was within about 60 n mi of the center, and 2) the nearby upper-level low was primarily shearing the depression and not directly involved in its circulation.

The upper-level low helped steer the tropical cyclone northward during the first 24 h or so after genesis. The cyclone became a tropical storm by 0600 UTC 3 August while centered about 250 n mi southwest of Bermuda. Steered by a mid- to upper-level trough to its north, Harvey turned east-northeastward and strengthened. The center passed about 40 n mi south of Bermuda shortly after 0600 UTC 4 August. Harvey reached its peak intensity of 55 kt at 1800 UTC that day, and then increasing shear caused weakening during the next 24 h. The storm moved generally eastward on 4–5 August, but on 6 August it drifted northward as the trough departed to the northeast. On 7 August another short-wave mid- to upper-level trough moving eastward from the United States forced Harvey northeastward, with gradual acceleration during the next couple of days. Harvey is estimated to have become extratropical by

0000 UTC 9 August when centered about 490 n mi southeast of Cape Race. The system continued north-eastward until 10 August, when it decelerated and turned southward. After meandering northwest of the Azores, the cyclone dissipated on 13 August.

Bermuda International Airport reported sustained winds of 32 kt with a gust to 44 kt at 0824 UTC 4 August, along with a storm-total rainfall of 127.5 mm. One ship reported tropical-storm-force winds from Harvey—the *Fortune Pioneer I* (call sign H3VT), which reported 35-kt winds while located about 125 n mi south-southeast of the center at 1200 UTC 3 August. There were no reports of casualties or damages due to Harvey.

i. Hurricane Irene

A vigorous tropical wave, accompanied by a broad surface low, crossed the coast of Africa on 1 August. Convection weakened significantly as the system moved over relatively cool waters southeast of the Cape Verde Islands. The wave moved westward over warmer waters during the next two days with convection redeveloping. QuikSCAT data at 1940 UTC 3 August indicated the surface circulation had become better defined. Convection became organized near the low center, and it is estimated that a tropical depression formed at 1800 UTC 4 August about 600 n mi southwest of the Cape Verde Islands (Fig. 1).

The depression moved northwestward, passing beneath stronger upper-level northwesterly winds, over cooler waters, and into more stable trade wind flow. These unfavorable environmental conditions caused a decrease in the organization and amount of convection. Despite this, QuikSCAT data indicated the cyclone slowly strengthened. By 1200 UTC 7 August, deep convection increased again and the cyclone became a tropical storm about 1080 n mi east of the northern Leeward Islands. Irene remained a tropical storm for 24 h as it moved west-northwestward. Then, strong northwesterly shear and a dry, stable environment eroded the convection and caused Irene to weaken back to a depression by 1200 UTC 8 August.

The cyclone's vertical depth decreased on 9 August, which caused it to turn westward in low-level easterly flow on the south side of a large subtropical ridge. By 0000 UTC 11 August, the shear decreased enough to allow persistent convection near the center. This allowed Irene to once again become a tropical storm about 300 n mi northeast of the Leeward Islands.

Irene turned northwestward early on 11 August in southeasterly steering flow associated with the subtropical ridge situated east-to-west across Bermuda. Decreasing shear and an increasingly unstable environ-

ment allowed gradual strengthening. As the cyclone moved into a weakness in the subtropical ridge between Bermuda and North Carolina, it became a hurricane at 0000 UTC 15 August. Irene then turned sharply toward the east-northeast and east as it moved north of the ridge axis. Strengthening continued, and Irene reached its peak intensity of 90 kt at 1800 UTC 16 August about 300 n mi northeast of Bermuda.

Shortly thereafter, west to southwesterly shear increased ahead of a large deep-layer midlatitude trough approaching from the west. This caused Irene to weaken to a tropical storm by 0000 UTC 18 August. After turning northeastward, the tropical cyclone was absorbed by the larger extratropical low around 1800 UTC that day about 250 n mi east-southeast of Cape Race. There were no reports of casualties or damages from Irene.

j. Tropical Storm Jose

Jose developed from a tropical wave that left the coast of Africa on 8 August, which was likely the same wave that spawned Tropical Depression 10 on 13 August. An area of convection developed in the central Caribbean Sea on 17 August, which persisted and moved west-northwestward toward the Yucatan peninsula over the next few days. Satellite imagery showed the system had a well-defined midlevel circulation in the northwestern Caribbean Sea, and some thin banding features were briefly evident over the Yucatan. Little convection accompanied the system when it entered the Bay of Campeche late on 21 August. However, early on 22 August convection increased rapidly in both coverage and organization under divergent upper-level anticyclonic flow. Surface observations and QuikSCAT data indicate that a tropical depression formed around 1200 UTC about 95 n mi east of Veracruz (Fig. 1).

The depression moved westward with increasing convective organization, and it became a tropical storm near 1800 UTC 22 August. Aircraft data showed the strongest winds were southwest of the center, where the flow may have been orographically enhanced on the east side of the Sierra Madre. Imagery from the Mexican radar at Alvarado indicates that an eyewall was developing as the center made landfall at 0330 UTC 23 August, about 30 n mi north of Veracruz. At the time of landfall the peak winds are estimated to have been 50 kt. Jose weakened rapidly after moving inland, becoming a depression by 1200 UTC 23 August. The cyclone dissipated over the mountains of eastern Mexico shortly thereafter.

Misantla, Mexico, reported a storm-total rainfall of 255.0 mm, with other stations in eastern Mexico report-

ing amounts of 100–225 mm. These rains spawned mudslides that killed six people in Mexico and caused the evacuations of thousands.

k. Hurricane Katrina

Katrina was an extraordinarily powerful hurricane that carved a wide swath of catastrophic damage and inflicted large loss of life, particularly in Louisiana and Mississippi. It was the costliest and one of the five deadliest hurricanes to strike the United States. Katrina first caused fatalities and damage in southern Florida as a category 1 hurricane. After reaching category 5 strength over the central Gulf of Mexico, Katrina weakened to category 3 before making landfall on the northern Gulf Coast.

1) SYNOPTIC HISTORY

The complex genesis of Katrina involved the interaction of a tropical wave, the midtropospheric remnants of Tropical Depression 10, and an upper-tropospheric trough. This trough, located over the western Atlantic and the Bahamas, produced strong westerly shear across Tropical Depression 10, causing it to degenerate on 14 August approximately 825 n mi east of Barbados. The remnant low-level circulation weakened, becoming an open wave on 18 August and dissipating near Cuba on 21 August. Meanwhile, a midtropospheric circulation originating from the depression lagged behind and passed north of the Leeward Islands on 18–19 August. A tropical wave, which departed the west coast of Africa on 11 August, moved through the Leeward Islands and merged with the midtropospheric cyclone on 19 August. The merger produced a large area of showers and thunderstorms north of Puerto Rico. This activity moved slowly northwestward, passing north of Hispaniola and then consolidating just east of the Turks and Caicos on 22 August. Dvorak satellite classifications began at 1800 UTC that day. The upper-tropospheric trough weakened as it moved westward, and the shear relaxed enough to allow the formation of a tropical depression by 1800 UTC 23 August over the southeastern Bahamas about 175 n mi southeast of Nassau (Fig. 1).

The depression became better organized over the central Bahamas that evening, and convective banding increased early on 24 August. The cyclone became a tropical storm at 1200 UTC that day about 65 n mi east-southeast of Nassau. Initially, Katrina moved northwestward within a weakness in the lower-tropospheric subtropical ridge. However, as it developed an inner core and greater vertical depth, a strengthening mid- to upper-tropospheric ridge over the northern Gulf of Mexico and southern United States dominated

the steering and turned Katrina westward on 25 August. An intense burst of deep convection developed over the center that afternoon, which led to Katrina becoming a hurricane near 2100 UTC 25 August.

The strengthening ridge steered the cyclone west-southwestward as it neared southern Florida. Katrina made its first landfall in the United States as a category 1 hurricane with 70-kt winds near the border of Miami-Dade County and Broward County around 2230 UTC 25 August. A well-defined eye became evident on the NWS Miami WSR-88D just prior to landfall. This feature became better defined during landfall and remained intact during its 6-h track across the peninsula. The convective pattern of Katrina over southern Florida was asymmetric because of northerly shear, which placed the strongest winds and heaviest rains south and east of the center in Miami-Dade County. Katrina briefly weakened to a tropical storm over mainland Monroe County, with the center emerging into the southeastern Gulf of Mexico at approximately 0500 UTC 26 August just north of Cape Sable. The cyclone regained hurricane strength an hour later.

A large upper-level anticyclone dominated the Gulf of Mexico, resulting in weak wind shear and increasingly efficient upper-level outflow. This allowed two periods of rapid intensification during 26–28 August. The first period saw maximum sustained winds increase from 65 to 95 kt in the 24-h period ending 0600 UTC 27 August. An eye appeared in infrared satellite imagery early on 27 August, and Katrina became a category 3 hurricane at 1200 UTC that day about 365 n mi southeast of the mouth of the Mississippi River. Intensification then temporarily stopped as the hurricane underwent an eyewall replacement cycle. Accompanying these developments was a significant expansion of the wind field. Based on the radii of tropical-storm-force winds, Katrina nearly doubled in size on 27 August, and by the end of that day those winds extended up to 140 n mi from the center. The mid- to upper-tropospheric ridge shifted eastward toward Florida, while a midlatitude trough amplified over the north-central United States. This evolving pattern resulted in a general westward motion on 27 August and a turn toward the northwest on 28 August when Katrina moved around the western periphery of the ridge. The new eyewall evolved into a sharply defined ring by 0000 UTC 28 August at the start of the second period of rapid intensification. Katrina strengthened from category 3 to category 5 in less than 12 h, reaching an intensity of 145 kt by 1200 UTC 28 August. It reached a peak intensity of 150 kt 6 h later (Fig. 6) while centered about 170 n mi southeast of the mouth of the Mississippi River. The wind field expanded further on 28 August, and by late

that day tropical-storm-force winds extended out about 200 n mi from the center, while hurricane-force winds extended out about 90 n mi. This made Katrina exceptionally large as well as extremely intense.

Katrina turned northward toward the northern Gulf Coast early on 29 August and weakened. The hurricane made landfall at 1110 UTC that day near Buras, Louisiana, with estimated maximum sustained winds of 110 kt (category 3). Katrina continued northward and made its final landfall near the mouth of the Pearl River at the Louisiana–Mississippi border at 1445 UTC with an estimated intensity of 105 kt (category 3).

Katrina's weakening during the last 18 h or so before the first Gulf Coast landfall was primarily due to the deterioration of the inner eyewall and the partial development of a new outer eyewall. Additional possible factors include entrainment of dry air over the western semicircle, gradually increasing wind shear, slightly lower SSTs, and (following the first Gulf landfall) interaction with land. Extensive investigation is required to assess their relative roles. Other major hurricanes approaching the northern Gulf Coast have weakened when one or more of these factors were present. Indeed, since 1980 all 11 hurricanes having a central pressure less than 973 mb 12 h before landfall in the northern Gulf of Mexico weakened during these last 12 h. (Conversely, in that time all 11 hurricanes having a central pressure higher than 973 mb 12 h before landfall in the northern Gulf of Mexico have strengthened.) It should be noted that Katrina remained very large as it weakened, as the extent of tropical-storm-force and hurricane-force winds changed little between late on 28 August and the final landfall.

Katrina continued to weaken over Mississippi, becoming a category 1 hurricane by 1800 UTC 29 August and a tropical storm 6 h later. It accelerated northeastward on 30 August between the ridge over the southeastern United States and the eastward-moving trough over the Great Lakes. Katrina became a tropical depression at 1200 UTC 30 August over the Tennessee Valley, with the depression becoming extratropical by 0000 UTC 31 August. The extratropical low was absorbed by a frontal zone later that day over the eastern Great Lakes.

2) METEOROLOGICAL STATISTICS

Selected surface observations from land stations and from coastal and fixed ocean data buoys are given in Table 7. Data from many Automated Surface Observing System (ASOS) sites, C-MAN stations, and buoys are incomplete because of power outages and other weather-induced failures.

Katrina was almost continuously monitored by air-

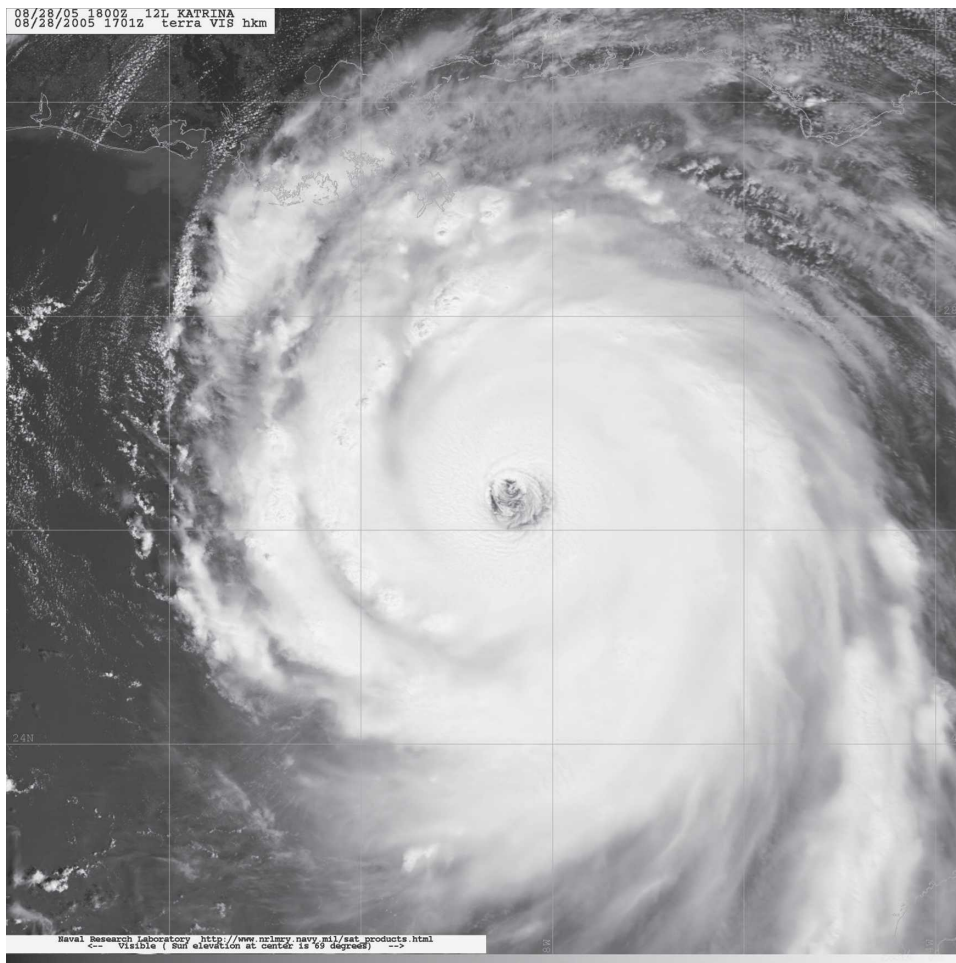


FIG. 6. *Terra* MODIS visible image of Hurricane Katrina near maximum intensity at 1701 UTC 28 Aug 2005. Image courtesy of the NRL, Monterey, CA.

craft from genesis until final landfall. The 53rd WRS flew 12 missions, which produced 46 center fixes. NOAA/AOC WP-3D aircraft flew three missions, producing 19 center fixes, real-time data from the SFMR, and airborne Doppler radar–derived wind analyses provided by the HRD. Additionally, the NOAA G-IV jet conducted six synoptic surveillance missions during 24–29 August. A 53rd WRS aircraft conducted one surveillance mission jointly with the G-IV on 25 August.

Radar velocity data from the Miami WSR-88D, along with 65-kt winds measured by the SFMR, indicated that Katrina became a hurricane at 2100 UTC 25 August. Subsequent radar velocity data were the basis for the Florida landfall intensity. The eye passed over the NWS Miami WFO/NHC, where a pressure of 983 mb was measured at 0105 UTC 26 August. The eastern eyewall then moved over the facility, with sustained winds of 60 kt and a gust to 76 kt measured near 0115 UTC. The strongest sustained wind measured in south-

eastern Florida was 63 kt on Virginia Key. Velocities from the Miami and Key West radars suggest that Katrina weakened to a tropical storm over mainland Monroe County. However, these data and Dvorak intensity estimates showed it regained hurricane strength upon reaching the Gulf of Mexico. The C-MAN station at Dry Tortugas, Florida (6-m elevation), reported hurricane-force winds for 2 h on 26 August, with 2-min average winds of 71 kt and a gust to 91 kt at 2000 UTC that day. The station reported a pressure of 974.4 mb at that time. The remainder of the Florida Keys experienced sustained tropical-storm-force winds with peak gusts of 60–70 kt on 26 August. Katrina also caused tropical storm conditions in portions of western Cuba on 27 August, with gusts as strong as 54 kt and some rainfall totals exceeding 200 mm.

During Katrina's second period of rapid intensification, aircraft observations indicate the central pressure fell 32 mb in 12 h, to 909 mb by 1200 UTC 28 August.

TABLE 7. Selected surface observations for Hurricane Katrina, 23–30 Aug 2005 (est: estimated).

Location	Min sea level pressure		Max surface wind speed			Storm surge (ft) ^c	Storm tide (ft) ^d	Tot rain (mm)
	Date/time (UTC)	Pressure (mb)	Date/time (UTC) ^a	Sustained (kt) ^b	Gust (kt)			
		Florida						
Apalachicola (KAAF)	29/1850	1005.1	29/2055	28	34			6.9
Big Pine Key			26/1340	33	44			
Boca Raton (KBCT)			25/1950		56			
Cache RAWS			26/0715		58			134.9
Chekika RAWS			26/0235		66			206.8
Clearwater Beach						1.13	3.81	
Crestview (KCEW)	29/1523	998.9	29/1855	30	38			
Cutler Ridge SFWMD								282.7
Destin (KDTS)	29/2053	999.3	29/1722	30	44			
Destin (EPSF1)							4.52	
Eglin Air Force Base (KVPS)	29/2023	998.9	29/1958	33	46			
Eglin Air Base 6W of Mary Esther			29/1434	51	60			
Florida City SFWMD								311.2
Florida City SFWMD								160.0
Florida City SFWMD								152.9
Fort Lauderdale (KFLA)	25/2245	988.8	25/2355	52	71			78.0
Fort Lauderdale—Executive Airport (KFXE)			26/0028	41	57			73.7
Fort Myers (KFMV)	26/0950	1004.4	26/1742	26	34			29.7
Fort Myers (KRSW)	26/1008	1004.1	26/1649	27	35			38.9
Fort Myers						0.96	2.34	
Goulds SFWMD								116.1
Homestead ARB (KHST)								356.6
Key West (KEYW)	26/1353	999.3	26/1527	53	64		est 2.5	255.3
Key West NAS (KNQX)			26/1549	48	60			
Leisure City SFWMD								111.8
Marathon (KMTH)	26/0728	1000.7	26/0836	30	44			246.6
Mary Esther (KHRT)	29/1935	998.9	29/1517	38	52			
Miami (KMIA)	26/0020	987.8	26/0124	42	68			129.5
Miami WFO/NHC	26/0105	983.1	26/0115	60	76			149.9
Miami Beach (KMBF)	26/0000	987.8	26/0000	30	47			88.4
Naples (KAPF)	26/1100	1002 ^e	26/1711	24 ^e	36 ^e			16.8
Opa Locka (KOPF)	25/2327	987.5	25/2229	39	57			
Oasis RAWS			26/0430		55			39.4
Ochopee RAWS			26/1135		44			34.5
Panama City (KPFN)	29/1650	1002.4	29/1507	24	34			11.2
Pembroke Pines (KHWO)	25/2156	992.9 ^e	25/2156	39 ^e	56 ^e			
Pensacola (KPNS)	29/1757	995.3	29/1452	49	60			
Pensacola Naval Air Station (KNPA)	29/1756	995.3	29/1811	49	62			
Pensacola (PENF1)							5.37	
Perrine								414.8 ^e
Pompano Beach (KPMP)	25/2213	997.6	25/2213	41	54			41.4
Punta Gorda (KPGD)	26/0956	1006.4	26/1728	29	36			34.8
Raccoon Point RAWS			26/0435		34			100.1
St. Petersburg (KSPG)	27/2053	1006.4	26/1837	34	42			8.4
St. Petersburg						1.07	3.35	
Santa Rosa Sound (FWLF1)							4.10	
Tenraw RAWS			26/0220		63			94.0
Virginia Key AOML	25/2300	988.0	25/2330		66			188.0
Virginia Key RSMAS	25/2254	990.2	25/2355	63	81			
West Kendall Tamiami (KTMB)	26/0109	986.1	26/0137	43	66			195.8 ^e
West Palm Beach (KPBI)	25/2000	1005 ^e	26/0243	28 ^e	35 ^e			30.7
West Perrine SFWMD								297.4
Winter Haven (KGIF)	26/2019	1008.5	26/2038	28	34			5.3

TABLE 7. (Continued)

Location	Min sea level pressure		Max surface wind speed			Storm surge (ft) ^c	Storm tide (ft) ^d	Tot rain (mm)
	Date/time (UTC)	Pressure (mb)	Date/time (UTC) ^a	Sustained (kt) ^b	Gust (kt)			
Cuba								
Bahia Honda	27/0600	1001.2	27/0950	32	40			133.1
Cabo de San Antonio	27/1200	1001.8	27/0930	46	54			24.9
Casa Blanca			27/0505	43	52			
Isabel Rubio	27/0850	1002.3	27/0635	37	46			210.8
La Palma	27/0900	1000.6	27/0930	40	50			148.3
Pinar del Rio	27/1305	1002.3	27/1605	38	48			208.3
San Juan y Martinez	26/2300	1002.6	27/1550	35	45			214.6
Santa Lucia	27/0900	996.4	27/1030	35	44			52.3
Santiago de las Vegas	27/0500	1003.2	27/0600	37	41			176.3
Louisiana								
Algiers COOP								317.2
Angie COOP								304.8
Baton Rouge (KBTR)	29/1553	984.4	29/1710	39	43			60.7
Belle Chase NAS FCMP tower			29/1427	68	89			
Big Branch NWR RAWS			29/1620		50			379.0
Bootheville (KBVE)			28/2137	26 ^e	39 ^e			
Buras ULM 2-m tower	29/1116	920.2	29/1021	73	93			
Covington 4NE COOP								261.9
Eastern New Orleans—Air Products and Chemicals Facility (unofficial)			29/1400		est 104			
Galliano FCMP tower			29/0936	67	83			
Lake Maurepas							3.05 ^e	
Lake Pontchartrain NWS—Mid-Lake			29/1520	68	86		6.8	
Mississippi River Gulf Outlet, eastern New Orleans						15.5		
NASA Michoud Assembly Facility—gauge 2			29/1415		est 107			
New Orleans Int. (KMSY)			29/0305	29 ^e	38 ^e			
New Orleans Int. Airport LLWAS 30-ft tower			29/1405		64			
New Orleans Int. Airport LLWAS 120-ft tower			29/1340		85			
New Orleans Lakefront Airport (KNEW)	29/1300	958.4 ^e	29/1153	60 ^e	75 ^e	11.8		
Paradis 7S COOP								246.4
Ponte a la Hache							14.14 ^e	
SE St. Bernard Parish, near Alluvial City						18.7		
SE St. Tammany Parish, ~10 mi SE of Slidell						16.0		
Slidell (KASD)	29/1400	954.4 ^e	29/1243	32 ^e	44 ^e			
Slidell WFO	29/1438	934.1						295.4
Slidell TTU 10-m tower			29/1500	61	87			
Sun COOP								233.9
Tallulah (KTVR)			29/1834		48 ^e			
Terrytown COOP								246.4
Vacherie TTU 10-m tower			29/1200	48	64			
Mississippi								
Bienville RAWS			29/2105		48			161.3
Biloxi—Keesler AFB (KBIX)			29/1400	52 ^e	85 ^e			
Black Creek RAWS			29/1800	43	69			194.1
Bude RAWS			29/1905		43			94.2
Columbus (KCBM)	30/0355	980.4	30/0100		50			147.1
Copiah RAWS			29/1705		44			
Covington RAWS			29/2005		47			
Green Pass							11.27 ^e	
Greene RAWS			29/1610		57 ^e			
Greenville (KGLH)	30/0156	992.8	29/2223		44			52.8

TABLE 7. (Continued)

Location	Min sea level pressure		Max surface wind speed			Storm surge (ft) ^c	Storm tide (ft) ^d	Tot rain (mm)
	Date/time (UTC)	Pressure (mb)	Date/time (UTC) ^a	Sustained (kt) ^b	Gust (kt)			
Greenwood (KGWO)			29/2153		46			
Gulfport (KGPT)			29/1025	40 ^e	55 ^e			
Hancock RAWS			29/1605	43	74			255.3
Holmes RAWS			30/0105		51			139.2
Jackson (KJAN)	29/2129	973.3	29/2014		56			99.8
Jackson County EOC, Pascagoula (unofficial)					108 ^e			
Long Beach (unofficial—amateur radio operator)			29/1115		106			
Marion RAWS			29/1605		38			208.0
McComb (KMCB)	29/1742	972.2	29/1742	42	56			
Meridian (KNMM)	29/2355	964.4 ^e	29/2051		70 ^e			
Neshoba RAWS			29/2110		52			165.9
Pascagoula (KPQL)			29/0953	38 ^e	44 ^e			
Pascagoula							12.16 ^e	
Pascagoula FCMP tower			29/1549	64				
Pass Christian						27.8		
Pike RAWS			29/1705	34	57			
Pearl River County EOC, Poplarville (unofficial)					117 ^e			
Sharkey Delta Road RAWS			30/0105		44			98.3
Stennis Space Center TTU 10-m tower			29/1500	59	102			
Wausau RAWS			29/1705		57 ^e			151.4
Winborn RAWS			30/0205		35			101.6
Alabama								
Anniston (KANB)	30/0720	997.5	30/0720	29	37			
Birmingham (KBHM)	30/0340	992.9	30/0418	31	45			19.8
Calera (KEET)	30/0349	993	30/0345	28 ^e	39 ^e			21.1 ^e
Dauphin Island							6.63	
Dothan (KDHN)	29/1758	1002.0	29/1848	24	38			54.9
Decatur (KDCU)	30/0522	990.2	30/0952		47			59.2
Evergreen (KGZH)	29/2224	993.9	29/2008	32	42			
Huntsville (KHSV)	30/0934	991.2	30/0427		48			52.1
Mobile (KMOB)	29/1632	983.4	29/1546	57	72			96.5
Mobile Brookley Field (KBFM)	29/1653	985.8	29/1501	58	73			
Mobile State Docks							11.45	
Montgomery (KMGM)	30/0059	995	30/0108	31	39			5.1
Muscle Shoals (KMSL)	30/0721	986.1	30/0101		47			89.4
Oakmulgee RAWS			30/0220		43 ^e			
Open Pond RAWS			29/1620		37			57.7
Perdido Pass							5.81	
Troy (KTOI)	30/0101	999	30/0147	27	36			55.4
Tennessee								
Camden Tower RAWS			30/0505		52			61.5
Coker Creek RAWS			30/1540		49			38.1
Fort Campbell RAWS			30/0915		36			76.5
Meigs EOC RAWS			30/1605		36			11.7
Buoys/C-MAN/NOS sites								
Bayou Gauche, LA, NOS (29.8°N, 90.4°W)	29/1042	975.4 ^e						
Bayou LaBranch, LA, NOS (30.1°N 90.4°W)	29/1130	976.9 ^e	29/1130	43 ^e	61 ^e			
Cedar Key, FL, C-MAN (29.1°N, 83.0°W)	28/0900	1007.8	28/2220	30 ^f	37	2.07	5.1	
Cocodrie, LA, LUMCON (29.3°N, 90.7°W)	29/1100	970.5 ^e	29/0800	43 ^e	54 ^e			
Dauphin Island, AL, C-MAN (30.2°N, 88.1°W)	29/1505	986.1	29/1350	66 ^f	89		6.2	
Dry Tortugas, FL, C-MAN (24.6°N, 82.9°W)	26/2000	974.4	26/2000	71	91			
Fowey Rocks, FL, C-MAN (25.6°N, 80.1°W)	26/0000	997.8	26/2310	57 ^f	69			
Grand Isle, LA, C-MAN (29.3°N, 90.0°W)	29/1100	944.3	29/0820	76 ^{e,f}	99 ^e			
Isle Dernieres, LA, WAVECIS (29.0°N, 90.5°W)	29/1100	968.4 ^e	29/1000	67 ^e	84 ^e			

TABLE 7. (Continued)

Location	Min sea level pressure		Max surface wind speed			Storm surge (ft) ^c	Storm tide (ft) ^d	Tot rain (mm)
	Date/time (UTC)	Pressure (mb)	Date/time (UTC) ^a	Sustained (kt) ^b	Gust (kt)			
Buoys/C-MAN/NOS sites								
Key West, FL, NOS (24.6°N, 81.8°W)	26/1300	999.8	26/1818	40	52		1.4	
Long Key, FL, C-MAN (24.8°N, 80.9°W)	26/0700	1000.2	26/0820	45 ^f	60		2.1	
Marsh Island, LA, WAVECIS (29.4°N, 92.1°W)	29/1100	993.7						
Molasses Reef, FL, C-MAN (25.0°N, 80.4°W)	26/0500	1001.7	26/0600	53	67			
Naples, FL, NOS (26.1°N, 81.8°W)	26/1000	1002.6	26/0700	18	32	2.5	3.0	
NW Florida Bay COMPS (25.1°N, 81.1°W)	26/0554	994.2 ^e	26/0654	51 ^e	60 ^e		2.5	
Panama City Beach, FL, NOS (30.1°N, 85.9°W)	29/2024	1002.3	29/1448	38 ^e	48 ^e		4.2	
Pensacola, FL, NOS (30.4°N, 87.2°W)	29/1300	995.7 ^e	29/1700	37 ^e	49 ^e		3.1	
Salt Point, LA, WAVECIS (29.5°N, 91.6°W)	29/1000	990.3 ^e	29/1000	33 ^e	38 ^e			
Sand Key, FL, C-MAN (24.5°N, 81.9°W)	26/1500	999.7	26/1530	54 ^f	67			
Settlement Point, GBI, C-MAN (26.7°N, 79.0°W)	25/1100	1004.2	25/1050	36 ^f	45			
Sombrero Key, FL, C-MAN (24.6°N, 81.1°W)	26/0900	1000.6	26/0900	58	69			
Southwest Pass, LA, C-MAN (29.0°N, 89.5°W)	29/0500	979.7 ^e	29/0420	72 ^e	88 ^e			
Southwest Pass, LA, NOS (28.9°N, 89.4°W)	29/0948	921.6						
Tambour Bay, LA, LUMCON (29.2°N, 90.7°W)	29/1100	972.9 ^e	29/1000	55 ^e	69 ^e			
Tyndall AFB Tower, FL, C-MAN (29.4°N, 89.9°W)	29/1000	1005.5	29/1000	35	42			
Vaca Key, FL, NOS (24.7°N, 81.1°W)	26/0724	1000.5	25/2200	27	41		2.0	
Virginia Key, FL, NOS (25.7°N, 80.2°W)	25/2254	990.2	25/2330	55	67	1.0	3.2	
Waveland, MS, NOS (30.3°N, 89.4°W)	29/0936	986.5 ^e	29/0936	44 ^e	54 ^e			
Buoy 42001, NOAA (25.8°N, 89.7°W)	28/1950	981.3	28/2030	48 ^f	64			
Buoy 42003, NOAA (26.0°N, 85.9°W)	28/0350	987.8 ^e	28/0230	57 ^{e,f}	78 ^e			
Buoy 42007, NOAA (30.1°N, 88.8°W; went adrift ~29/0500 UTC)	29/1450	927.4	29/1535	56	74			
Buoy 42014, COMPS (25.3°N, 82.2°W)	26/1429	977.9						
Buoy 42036, NOAA (28.5°N, 84.5°W)	28/0950	1003.7	29/1050	29	35			
Buoy 42038, NOAA (27.4°N, 92.6°W)	29/0450	996.6	29/0030	32 ^f	41			
Buoy 42039, NOAA (28.8°N, 86.0°W)	29/0950	1000.2	29/0850	37	47			
Buoy 42040, NOAA (29.2°N, 88.2°W)	29/0950	979.3	29/1010	55 ^f	72			
Buoy 42067, USM (30.0°N, 88.7°W)			29/1130	60 ^e	76 ^e			

^a Date/time is for sustained wind when both sustained and gust are listed.

^b Except as noted, sustained wind-averaging periods for land-based ASOS reports are 2 min.

^c Storm surge is water height above normal astronomical tide level.

^d Storm tide is water height above National Geodetic Vertical Datum (1929 mean sea level).

^e Incomplete record.

^f 10-min average.

The central pressure fell to 902 mb about 6 h later. The strongest 700 mb flight-level wind was 166 kt near 1400 UTC that day, corresponding to about 150 kt at the surface using the standard 90% adjustment. Dropwind-sonde surface wind estimates, derived from the mean wind over the lowest 150 m of the sounding, were 130–135 kt, but a few sondes directly measured 140–143-kt spot winds at the surface (10 m). No sondes were released where the flight-level winds were 166 kt, and it is thus unlikely the sondes measured the maximum surface wind. The SFMR, using a poststorm recalibration to correct a previous low bias at extremely high wind speeds, estimated surface winds as strong as 141 kt on the afternoon of 28 August, when maximum 700-mb flight-level winds were about 160 kt. These data indi-

cate that, on average, the standard 90% adjustment was valid until late on 28 August.

By the time of the initial Louisiana landfall, Katrina's central pressure had risen to 920 mb. Maximum 700-mb flight-level winds were 130–135 kt east of the eye around that time, which agreed well with NWS Slidell radar velocity data. Poststorm analysis of dropwind-sondes, flight-level winds, and SFMR data suggest the flight-level to surface wind adjustment on 29 August was closer to 80% or perhaps even less. Further evidence of this change comes from airborne Doppler radar-derived wind speed cross sections obtained from the NOAA aircraft (Fig. 7). These data reveal an unusual, broad, and elevated wind maximum in the 2–4-km layer (centered near the 700-mb flight level), well above

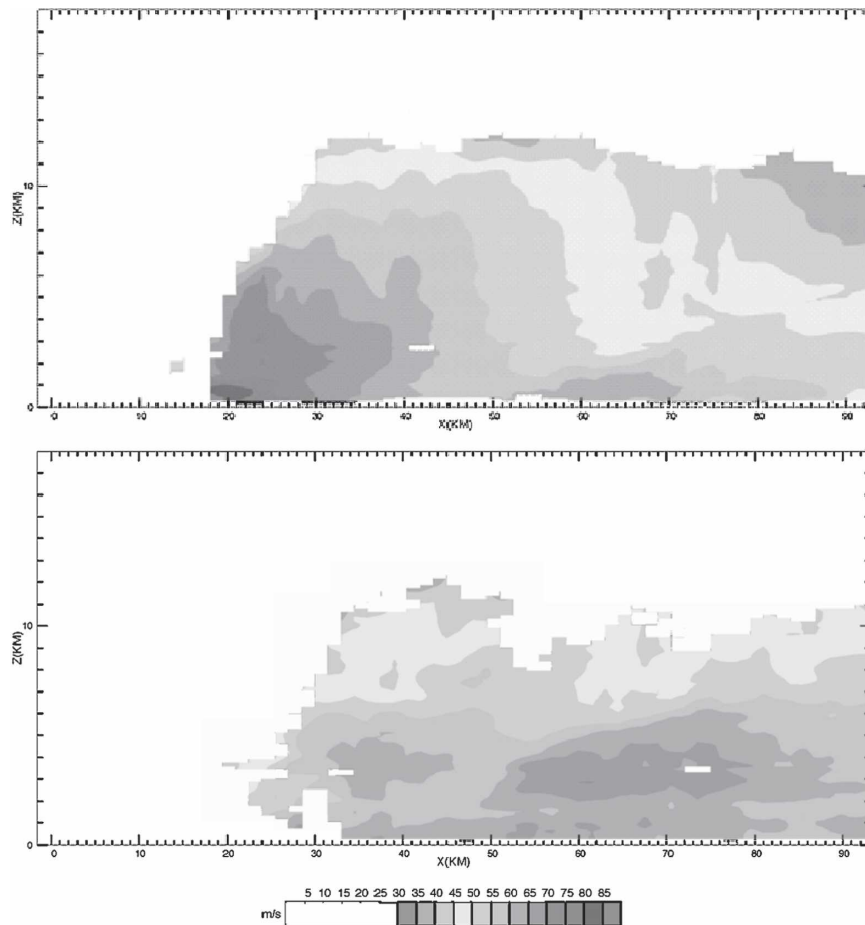


FIG. 7. Airborne Doppler radar cross-section wind speeds (m s^{-1}) for Hurricane Katrina on (top) 28 Aug and (bottom) 29 Aug 2005. Vertical height and distance from the center are in km. For clarity, wind speeds under 30 m s^{-1} have been whited out of the scale, as no such speeds exist in these data.

the more typical location of the maximum wind near the top of the boundary layer ($\sim 500 \text{ m}$) seen on 28 August.

The estimated intensity of 110 kt at the Buras landfall is very low relative to other Atlantic hurricanes with comparable minimum central pressures. In fact, the central pressure of 920 mb is the lowest of record in the basin for that intensity, surpassing Hurricane Floyd (1999; Lawrence et al. 2001), which at one point had a central pressure of 930 mb with an intensity of 110 kt. Application of the Holland (1980) wind model using the central pressure of 920 mb, the concurrently observed outermost pressure of 1006 mb, and the B parameter set to 1 yields an intensity of 102 kt, so the estimated landfall intensity is within Holland's analytical bounds. Katrina's combination of relatively weak winds and low pressure resulted from a broadening of the pressure field on 29 August that decreased the pressure gradient, along with a general weakening of the

convection that likely reduced momentum mixing of winds aloft down to the surface. The 920-mb pressure is the third lowest at U.S. landfall of record, behind only Hurricane Camille in 1969 (909 mb; Simpson et al. 1970) and the 1935 Labor Day hurricane that struck the Florida Keys (892 mb; McDonald 1935).

It should be noted that Katrina was likely at category 4 strength a couple of hours before the first Louisiana landfall. Because of a large radius of maximum winds, it is possible that sustained winds of category 4 strength briefly impacted the extreme southeastern tip of Louisiana before landfall.

The central pressure in Katrina rose to 928 mb before the final landfall near the Louisiana–Mississippi border at about 1445 UTC. However, aircraft data indicated only a slight decrease in the winds between the first and last Gulf Coast landfalls.

The strongest sustained wind measured from a fixed

location at the surface on the morning of 29 August was 76 kt at 0820 UTC by the C-MAN station at Grand Isle (16-m elevation). The anemometer failed near 0900 UTC, about 2 h before closest approach of the eye. The Southwest Pass, Louisiana, C-MAN station (30-m elevation) measured a sustained wind of 71 kt at 0420 UTC, with the station failing because of storm surge about 4 h prior to the closest approach of the eye. The strongest reported wind gust, although unofficial, was 117 kt in Poplarville, Mississippi, at the Pearl River County Emergency Operations Center (EOC). A gust to 108 kt was reported in Pascagoula, Mississippi, at the Jackson County EOC, and a gust to 106 kt was reported by an amateur radio operator at Long Beach, Mississippi. The strongest gust from an official reporting station was 99 kt at the Grand Isle C-MAN station at 0838 UTC 29 August.

When the eye of Katrina passed about 20 n mi east of downtown New Orleans, winds of category 3 intensity were likely present only over water east of the eye. Wind speeds in New Orleans are speculative because of sparse observations and incomplete data records. A few instrumented towers placed in the metropolitan area by the FCMP and by Texas Tech University measured sustained winds in the range of 61–68 kt. The Mid-Lake Pontchartrain NWS site (16-m elevation), located along the Lake Pontchartrain Causeway about 8 n mi north of the south shore of the lake, measured a 1-min average wind of 68 kt. Even though these sites likely did not sample the maximum wind in the area, the Mid-Lake Pontchartrain site had open marine exposure, unlike most locations in the city of New Orleans. The NASA Michoud Facility (about 12-m elevation) measured a peak gust of 107 kt, and a nearby chemical facility (about 9-m elevation) measured a peak gust of 104 kt. Overall, it appears likely that most of the city experienced sustained surface winds of category 1 or category 2 strength.

Precise measurements of Katrina's storm surge along the northern Gulf Coast were complicated by many factors, including the widespread failures of tide gauges and destruction of coastal buildings that could have provided still-water marks. Despite this, high water marks were located and analyzed along the Louisiana, Mississippi, and Alabama coasts under the direction of the Federal Emergency Management Agency (FEMA). These data indicate that the storm surge was about 24–28 ft along the Mississippi coast across a swath about 15–20 n mi wide, centered roughly on St. Louis Bay. The highest observed storm surge was 27.8 ft at Pass Christian, on the immediate Gulf Coast just east of St. Louis Bay. A storm surge of 17–22 ft occurred along the eastern Mississippi coast, roughly from Gulfport to Pascagoula. The surge appears to have penetrated at least

5 n mi inland in many portions of coastal Mississippi and up to 10 n mi inland along bays and rivers. It crossed Interstate 10 in many locations. A lesser, but still significant, storm surge of 10–15 ft occurred along the open coast in Mobile County, Alabama, including Dauphin Island. Surge heights of 8–12 ft were seen in Mobile Bay, particularly along the northern and western shores where flooding occurred several nautical miles inland. Katrina caused a storm surge of up to 10 ft along the coast of Baldwin County, Alabama.

A significant storm surge also occurred west of the path of the eye. The level of Lake Pontchartrain rose, and a 12–16-ft storm surge occurred along its northeastern shore in St. Tammany Parish, including communities from Slidell to Mandeville, Louisiana. A storm surge of 15–19 ft was documented in eastern New Orleans, St. Bernard Parish, and Plaquemines Parish, while a surge of 10–14 ft occurred in western New Orleans along the southern shores of Lake Pontchartrain. Farther west, surge heights reached 5–10 ft along the shores of western Lake Pontchartrain. The surge severely strained the levee system in the New Orleans area, with several levees and floodwalls being overtopped and/or breached. Overtopping occurred along large sections of the levees east of New Orleans, in Orleans Parish and St. Bernard Parish, while a breach occurred along the Industrial Canal east of downtown New Orleans. The Lake Pontchartrain surge caused breaches along the London Avenue Canal north of downtown New Orleans and the 17th Street Canal northwest of downtown. As a result, about 80% of the city of New Orleans flooded, with depths up to about 20 ft, within a day or so after landfall. Following setbacks caused by additional flooding associated with the passage of Hurricane Rita, the Army Corps of Engineers reported on 11 October 2005, 43 days after Katrina's landfall, that all floodwaters had been removed from the city of New Orleans.

The massive water rise produced by Katrina, which was greater than would be expected for a "normal" category 3 hurricane, was due to two factors. The first was Katrina's large size. The radius of maximum winds at the Gulf Coast landfall was about 25–30 n mi, and hurricane-force winds extended at least 75 n mi east of the center. By comparison, Camille, which made landfall in the same area along a similar path, was more intense but far more compact. Camille produced storm surge values comparable to Katrina's along a narrower swath. Second, Katrina had already generated large northward-propagating swells, leading to substantial wave setup along the northern Gulf Coast. NOAA buoy 42040, located 64 n mi south of Dauphin Island, reported a significant wave height (defined as the av-

erage of the one-third highest waves) of 30 ft as early as 0000 UTC 29 August and measured a peak significant wave height of 55 ft at 1100 UTC that day. This matches the largest significant wave height ever measured by a NOAA/National Data Buoy Center buoy.

Katrina also produced storm surge in Florida. Surge heights ranged from up to about 6 ft along the coast of the western Florida panhandle to about 1–2 ft along most of the west-central coast of Florida. A 2–4-ft surge occurred along the extreme southwestern Florida coast. A storm surge of about 2 ft was reported at Key West as Katrina passed to the north on 26 August. Similar surge was reported along portions of the southeastern coast of Florida.

Rainfall distributions associated with Katrina across southern Florida were highly asymmetric about the storm track, with the greatest amounts occurring south of the center. Rainfall totals from Miami-Dade County include 414.8 mm at Perrine, 356.6 mm at Homestead Air Force Base, 311.2 mm at Florida City, and 282.7 mm at Cutler Ridge. Rainfall amounts north of the center over northern Miami-Dade County and Broward County were generally 50–100 mm. Rainfall amounts over interior and western portions of the southern Florida peninsula generally ranged from 25 to 75 mm.

Precipitation amounts during the landfall along the northern Gulf Coast were greatest along and just west of the track of the center. A large swath of 200–250-mm amounts fell across southeastern Louisiana and southwestern Mississippi, with an area of 250–300 mm over eastern Louisiana, including 295.4 mm at the Slidell, Louisiana, WFO. Katrina also produced rainfall amounts of 100–200 mm well inland over Mississippi and portions of the Tennessee Valley.

Katrina produced 43 reported tornadoes. One tornado was reported in the Florida Keys on the morning of 26 August. On 29–30 August, 20 tornadoes were reported in Georgia, 11 in Alabama, and 11 in Mississippi. The Georgia tornadoes were the most in that state for any single day in August.

3) CASUALTY AND DAMAGE STATISTICS

Katrina's size and power, combined with the particular vulnerability of the northern Gulf Coast to storm surge, led to loss of life and property damage of immense proportions. The scope of human suffering inflicted by Hurricane Katrina in the United States has been greater than that of any hurricane to strike this country in several generations.

The total number of known fatalities, either directly or indirectly related to Katrina, is 1833, based on reports from state and local officials: 1577 in Louisiana,

238 in Mississippi, 14 in Florida, 2 in Georgia, and 2 in Alabama. The total number of fatalities directly related to the forces of Katrina is estimated to be about 1500, with about 1300 of these in Louisiana, about 200 in Mississippi, 6 in Florida, and 1 in Georgia. Especially for Louisiana and Mississippi, the number of direct fatalities is highly uncertain and the true number will probably never be known. Several hundred persons are still reported missing in association with Katrina.

Presumably, most fatalities in Louisiana were directly caused by the widespread storm-surge-induced flooding in the New Orleans area. However, several indirect fatalities in Louisiana have been confirmed or are suspected, and some deaths included in the total might not be related to Katrina at all. Persons of more than 60 yr of age constituted the majority of the Katrina-related fatalities in Louisiana. The vast majority of the fatalities in Mississippi probably were directly caused by the storm surge and waves in the three coastal counties. In Florida, three direct fatalities were caused by downed trees in Broward County, with three others due to drowning in Miami-Dade County. A tornado caused one death in Georgia, with a second in a car accident indirectly related to the storm. Alabama reported two indirect fatalities in a car accident during the storm. While inland freshwater floods have produced the majority of fatalities due to tropical cyclones during the past few decades, Katrina provides a grim reminder that storm surge still poses the greatest potential cause for large loss of life in hurricanes.

Where Katrina ranks among the deadliest hurricanes of record in the United States is somewhat uncertain. Katrina is surpassed by the Galveston, Texas, hurricane in 1900 that claimed at least 8000 lives, and by the 1928 Lake Okeechobee, Florida, hurricane with over 2500 fatalities. If the estimated number of directly caused fatalities is correct, then Katrina ranks as the third deadliest hurricane in the United States since 1900, and the deadliest in 77 yr. Two hurricanes in 1893 might each have been directly responsible for more fatalities in the United States than Katrina. One struck the southeastern Louisiana barrier island of Cheniere Caminanda and killed about 2000 people, while the other struck Georgia and South Carolina and claimed between 1000 and 2000 lives. Thus, Katrina ranks fourth or fifth on the list of the deadliest hurricanes of record in the United States.

The extent, magnitude, and impacts of the damage caused by Katrina are staggering beyond the scope of this paper. Thousands of homes and businesses throughout entire neighborhoods in the New Orleans metropolitan area were destroyed by flood. Wind damage also occurred in the New Orleans area, including

downtown where windows in some high-rise buildings were blown out and the roof of the Louisiana Superdome was partially peeled away. The storm surge obliterated entire coastal communities along the Mississippi coast, with little more than the foundations of homes, businesses, government facilities, and historical buildings left in some areas. The surge over Dauphin Island destroyed or damaged dozens of beachfront homes and cut a new inlet through the island's western end. The heavy rains in southern Florida flooded some neighborhoods, primarily in Miami-Dade County. Some structures from Florida and Georgia westward to Louisiana that avoided surge or freshwater floods were damaged by strong winds (Mississippi and Alabama) and tornadoes (Georgia, Mississippi, Alabama, Florida). Katrina left about three million people without electricity, some for several weeks.

The economic and environmental ramifications of Katrina were widespread and could be long-lasting, because of impacts on large population and tourism centers, the oil and gas industry, and transportation. The hurricane severely damaged or destroyed workplaces along the northern Gulf Coast, resulting in thousands of lost jobs and millions of dollars in lost tax revenues for the impacted communities and states. Many severely impacted areas along the northern Gulf Coast could take years to completely rebuild. Large numbers of evacuees have not returned home, producing a shortage of workers for businesses that have reopened. A significant percentage of U.S. oil refining capacity was disrupted due to flooded refineries, crippled pipelines, and rigs or platforms damaged, set adrift, or capsized. Several million gallons of oil spilled from damaged facilities in southeastern Louisiana. Key transportation arteries were disrupted or cut off by the hurricane. Traffic along the Mississippi River was below normal capacity for at least two weeks following the storm. Major highways into and through New Orleans were blocked by floods. Major bridges along the northern Gulf Coast were destroyed, including several in Mississippi and the Interstate 10 Twin Span Bridge connecting New Orleans and Slidell. Major beach erosion occurred along the tourism-dependent coasts of Mississippi and Alabama.

The PCS estimates that Katrina is responsible for \$40.6 billion of insured losses in the United States. The total estimated damage cost of Katrina in the United States is thus about \$81 billion. This figure makes Katrina the costliest hurricane in U.S. history. Even after adjusting for inflation, the estimated total damage of Katrina is roughly double that of Hurricane Andrew (1992; Blake et al. 2005).

Data provided by FEMA indicate that over 1.2 million people along the northern Gulf Coast from southeastern Louisiana to Alabama were under some type of evacuation order, but it is unclear how many people actually evacuated. Media reports indicate that many displaced residents moved either temporarily or permanently to other areas in the United States. It is also reported that many of these people may never return to their pre-Katrina homes or cities. Thousands of people remained displaced from their homes as of this writing.

l. Tropical Storm Lee

A vigorous tropical wave that moved off the west coast of Africa on 24 August spawned a low pressure area while it moved westward across the tropical Atlantic. The associated shower activity became organized and a tropical depression formed at 1200 UTC 28 August about midway between Africa and the Lesser Antilles (Fig. 1). The depression moved toward the west-northwest in an environment of northeasterly shear and degenerated into a broad area of low pressure at 1800 UTC 29 August. The low moved northward and then northeastward around a nontropical low located north of the system. As the former depression moved toward the northeast, convection increased, modest banding features developed, and a ring of deep convection was noted on microwave data. Based on this, it is estimated that a depression regenerated at 0600 UTC 31 August, and became a tropical storm 6 h later. By then, the cyclone was located between Bermuda and the Azores. Thereafter, Lee weakened to a tropical depression as it moved first northeastward and then northwestward around the eastern side of the nontropical low. Lee absorbed the nontropical low and maintained limited convection. The depression weakened to a broad area of low pressure at 0600 UTC 2 September and was absorbed by a cold front at 0000 UTC 4 September.

m. Hurricane Maria

On 27 August, a large and strong tropical wave moved from Africa into the eastern tropical Atlantic. By 28 August two areas of concentrated deep convection, each showing signs of circulation, were evident within the wave. One of these moved northwestward to a location just west of the Cape Verde Islands and subsequently became disorganized. The other area, which was broader, moved westward for a day or so and then turned northwestward. This system developed a well-defined low-level circulation on 31 August. However, an adjacent upper-tropospheric cyclone produced

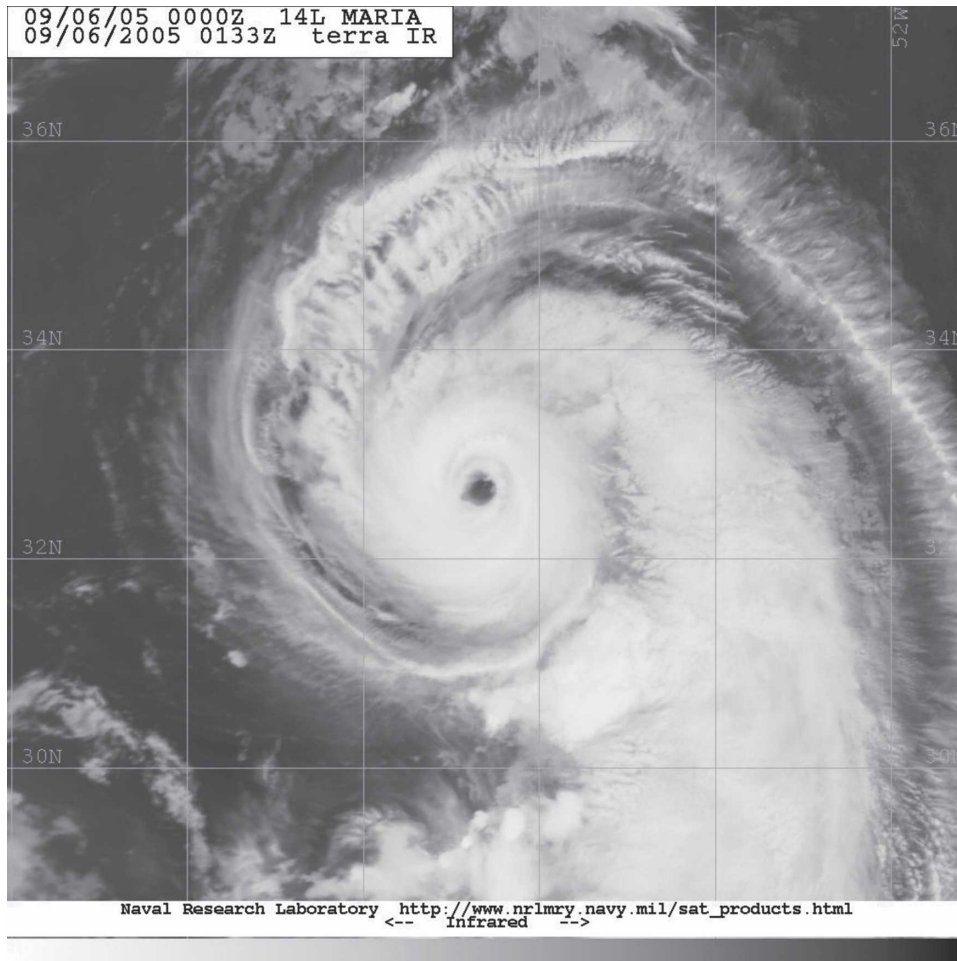


FIG. 8. *Terra* MODIS infrared image of Hurricane Maria near maximum intensity at 0133 UTC 6 Sep 2005. Image courtesy of the NRL, Monterey, CA.

strong south-southwesterly shear that prevented the formation of persistent deep convection near the center. By 1200 UTC 1 September, the central convection became persistent enough to designate that a tropical depression had formed about 910 n mi east of the northernmost Leeward Islands (Fig. 1).

A cell of the subtropical ridge northeast of the tropical cyclone was the primary steering feature, and it drove the system on a west-northwestward to north-westward track for several days. The upper-level low continued to cause shear, which hindered significant intensification for about a day. As the effects of the upper-level low lessened, the depression strengthened into a tropical storm by 1200 UTC 2 September. The environment was still not very conducive for strengthening, however, and further intensification was rather slow. While moving around the western periphery of the subtropical high, Maria eventually became a hurricane at about 0600 UTC 4 September. Upper-level

winds then became more favorable for strengthening, and Maria developed a well-defined eye on 5 September. It reached its estimated peak intensity of 100 kt around 0000 UTC 6 September (Fig. 8). The hurricane was centered about 415 n mi east of Bermuda at this time and had begun to recurve around the subtropical anticyclone.

Maria was a major hurricane very briefly, as a weakening trend was underway by 0600 UTC 6 September. The hurricane turned toward the northeast that day and there was a gradual increase in forward speed over the next couple of days, due to deep-layer southwesterly flow on the northwest side of the subtropical high. The slow weakening trend halted on 7 September, when Maria appeared to combine with an upper-level trough and reintensified slightly. By 8 September, slow weakening was again underway, and the cyclone diminished to tropical storm strength by about 0000 UTC 9 September. Although Maria hung on to tropical character-

istics as it moved into the midlatitudes, it eventually transformed into an extratropical storm around 1200 UTC 10 September while accelerating north-northeastward. Because of strong baroclinic forcing, the storm acquired hurricane-force winds over the North Atlantic on 11 September. It weakened again on 12 September and passed near Iceland on 13 September. Finally, as the system approached Norway, it merged with another strong extratropical cyclone.

Three ships reported tropical-storm-force winds from Maria. The *Faust* (call sign WRYX) reported 37-kt winds at 0500 UTC 10 September, while a ship with the call sign PECS reported 37-kt winds at 1200 UTC 7 September. A ship with the call sign HPII reported 36-kt winds at 0000 UTC 9 September. There were no reports of damages or casualties from Maria as a tropical cyclone. However, the post-Maria merger with another extratropical low produced a powerful cyclone, and it triggered a landslide in Norway that killed one person.

n. Hurricane Nate

Nate resulted from a complex interaction between a tropical wave and a broad upper-level low located northeast of the Bahamas. The wave moved westward from Africa on 30 August accompanied by a vigorous area of convection over the far eastern Atlantic. By 1 September, however, most of the convection had been stripped away by southwesterly shear east of a sharp mid- to upper-level trough extending southward from the central Atlantic Ocean into the deep Tropics. The well-defined wave continued west-northwestward and eventually split, with the northern portion passing between the Leeward Islands and Hurricane Maria on 3 September and the southern portion moving westward into the Caribbean Sea. On 4 September, the northern portion interacted with an upper-level low and elongated surface trough located midway between Bermuda and the northern Leeward Islands. Low-shear conditions northeast of the upper-level low allowed convection to organize along the wave axis. Banding features formed around the periphery of a broad surface low, and it is estimated that a tropical depression formed at 1800 UTC 5 September about 305 n mi south-southwest of Bermuda (Fig. 1).

The cyclone drifted northeastward for the next two days. It strengthened into a tropical storm 6 h after genesis and into a hurricane at 1200 UTC 7 September about 225 n mi south-southwest of Bermuda. The large upper-level low northeast of the Bahamas opened up into a broad trough as a strong short-wave trough approached it from the northwest, then it became elongated northeast to southwest on 7 September as the

short-wave trough dug southward along its west side. After moving at less than 5 kt for nearly 3 days, increasing southwesterly flow southeast of the broad trough caused Nate to move northeastward at 10–15 kt, passing about 110 n mi southeast of Bermuda at 1200 UTC 8 September. Increasing vertical wind shear ahead of the short-wave trough slowed intensification, and Nate struggled to its estimated peak intensity of 80 kt at 0000 UTC 9 September. Later that day, Nate accelerated east-northeastward. Vertical shear and midlevel dry air caused Nate to weaken to a tropical storm by 1800 UTC. Weakening continued as shear increased ahead of the approaching deep-layer trough and associated cold front. Nate became an extratropical low by 1800 UTC 10 September about 700 n mi west of the Azores Islands. Shortly thereafter, the low merged with a weak stationary front extending southwestward from former Hurricane Maria located about 750 n mi northeast of Nate. The remnants of Nate moved northeastward along the front as a gale center for the next 2 days, and were absorbed by a larger extratropical low and frontal zone by 0000 UTC 13 September about 240 n mi north-northeast of the Azores Islands.

Two ships reported tropical-storm-force winds from Nate. The *Maersk New Orleans* (call sign ELZY3) reported an east-northeast wind of 41 kt at 1200 UTC 8 September, and a ship with call sign WCZ858 reported a south-southwest wind of 35 kt at 0600 UTC 10 September. That same day, Bermuda observed a 2-min average easterly wind of 30 kt at 1130 UTC with a gust to 42 kt at 1525 UTC. There are no reports of casualties or damages due to Nate.

o. Hurricane Ophelia

Hurricane Ophelia was a category 1 hurricane that brushed the North Carolina Outer Banks, with its center remaining just offshore from that coast.

1) SYNOPTIC HISTORY

Ophelia formed from a nontropical weather system. A cold front moved off the eastern coast of the United States on 1 September. The front moved southeastward and became part of an elongated trough of low pressure extending from Tropical Depression Lee east of Bermuda to near the Florida peninsula. Two areas of low pressure formed in the trough on 4 September. The eastern low became Hurricane Nate. The western low, near the Bahamas, became Ophelia.

The pre-Ophelia low initially drifted southward. It began a northward drift on 5 September while the associated shower activity became better organized. Based on satellite, surface, and radar observations, it is estimated the low became a tropical depression near

0600 UTC 6 September between Andros and Grand Bahama Islands (Fig. 1). The depression continued generally northward, with the center crossing Grand Bahama about 1600 UTC 6 September. It then moved north-northwestward parallel to the east coast of Florida, reaching a position about 70 n mi east-northeast of Cape Canaveral on 7 September. The cyclone became a tropical storm early on 7 September, and gradual strengthening occurred during the next 24 h as Ophelia made a slow counterclockwise loop off the Florida east coast. Steering currents were weak at this time, as Ophelia remained embedded in a broad trough that extended from Hurricane Maria east of Bermuda through the developing Nate and Ophelia and across Florida.

Ophelia was briefly a hurricane late on 8 September. A similar short-lived hurricane phase occurred late on 9 September while Ophelia moved east-northeastward away from Florida. Ophelia became a hurricane for a third time on 10 September, this time reaching an intensity of 75 kt and maintaining hurricane status for 36 h. The cyclone made a slow clockwise loop on 11–12 September, and it is possible that weakening back to a tropical storm on 12 September was due to Ophelia passing over its wake of upwelled cooler waters. After completing the loop, the storm drifted northwestward on 13 September.

Ophelia moved slowly northward early on 14 September and became a hurricane for the fourth time. A gradual turn toward the north-northeast brought the northern portion of the 50 n mi wide eye over the coast of North Carolina near Cape Fear later that day, although the actual center of circulation stayed offshore. Ophelia moved generally east-northeastward parallel to the North Carolina coast for much of 14–15 September, with the northern eyewall passing over the coastal area from Wilmington to Morehead City. During this time, the hurricane again reached an intensity of 75 kt.

Ophelia turned eastward late on 15 September while its center was south of Cape Hatteras. A combination of increasing vertical shear and dry air intrusion caused weakening, and Ophelia became a tropical storm early on 16 September. As an upper-level trough and associated surface front approached from the west, the storm turned northeastward and accelerated late on 16 September. This motion brought the center about 60 n mi southeast of the Massachusetts coast on 17 September, then over eastern Nova Scotia and Newfoundland, Canada, on 18 September. Ophelia gradually lost organization during this period, and it became extratropical early on 18 September. As an extratropical low, Ophelia moved east-northeastward across the Atlantic on 19–20 September, then northeastward on 21–22 Sep-

tember. The cyclone dissipated over the North Sea on 23 September.

2) METEOROLOGICAL STATISTICS

AFRC and NOAA aircraft made 105 center fixes during Ophelia's lifetime. The maximum flight-level winds observed during the storm were 91 kt from a NOAA aircraft at 700 mb at 2124 UTC 11 September. While this would support surface winds of 80 kt using the normal 90% adjustment, winds from the SFMR, dropsondes, and other flight levels suggest surface winds closer to 65 kt at that time. The peak intensity of 75 kt on 11 September is based on 85-kt winds at 700 mb at 0615 UTC, supported by a dropwindsonde wind of 80 kt at 13 m at 0434 UTC. The second peak intensity of 75 kt on 14–15 September is based on multiple occurrences of 80–85-kt winds at 700 mb and SFMR observations of 75–80-kt winds. A notable aircraft observation was a 74-kt wind at 925 mb on 16 September measured by the first ever successful Aerosonde robotic aircraft mission into the core of a tropical cyclone. The lowest aircraft-observed central pressure was 976 mb at 1218 UTC 10 September.

Ophelia brought hurricane conditions to portions of the North Carolina coast; selected surface observations from land stations and data buoys are given in Table 8. The Cape Lookout C-MAN station (9.8-m elevation) reported 2-min average winds of 65 kt at 2309 UTC 14 September with a gust to 80 kt. The Wrightsville Beach NOS station reported 6-min average winds of 59 kt at 1700 UTC 14 September with a gust of 69 kt. There was an unofficial report of a gust of 90 kt in Davis. Significant ship observations included a report of 64-kt winds from the *Sanmar* (call sign V2EX) at 0000 UTC 15 September, and a report of 62-kt winds from the *Maersk New Orleans* (call sign ELZY3) at 0600 UTC 14 September. Both observations were taken about 85 n mi east-northeast of the center.

Ophelia also brought tropical-storm-force winds to portions of the east-central coast of Florida and the northeastern coast of South Carolina. A NASA station at Cape Canaveral reported sustained winds of 34 kt at 1520 UTC 8 September with a gust of 52 kt. Myrtle Beach, South Carolina, reported a gust of 38 kt.

The lowest pressure observed by a coastal station or buoy was 980.7 mb at the Frying Pan Shoals, North Carolina, C-MAN station at 1300 UTC 14 September. The nearby NOAA buoy 41013 measured a 980.8-mb pressure 3 h earlier as the large eye drifted across both stations.

Ophelia caused storm surges of 4 to 6 ft above normal tide levels in the Pamlico Sound including the lower reaches of the Neuse, Pamlico, and Newport Riv-

ers. Surges of 4 to 6 ft also occurred along the open coasts in Onslow and Cartaret counties. Storm surges of 3 to 4 ft above normal tide levels were common elsewhere along the affected areas of the North Carolina coast. Ophelia also caused tides of 1 to 2 ft above normal along the Florida coast.

Ophelia's slow movement near the North Carolina coast helped produce locally heavy rains. The water treatment plant at Oak Island reported a storm-total rainfall of 444.5 mm, while the Remote Automated Weather Stations (RAWS) station at the Nature Conservancy reported 298.2 mm.

No tornadoes were reported with Ophelia.

3) CASUALTY AND DAMAGE STATISTICS

One death was directly associated with Ophelia—a drowning in high surf in Palm Beach County, Florida. One death was indirectly associated with Ophelia after it became extratropical due to a fall from a roof during rain in Nova Scotia.

The PCS estimates the insured property damage from Ophelia at \$35 million. This yields a property damage estimate for the United States of \$70 million.

p. Hurricane Philippe

Philippe appears to have developed from a tropical wave that moved across the west coast of Africa on 9 September. The wave quickly lost most of its convection as it moved westward and became difficult to track, but on 13 September an area of showers redeveloped about 1200 n mi east of the southern Windward Islands. Maintaining convection over a large area, the sprawling disturbance continued westward without significant development until 16 September, when convection became more concentrated in the southern part of the disturbance about 650 n mi east of Trinidad. QuikSCAT data at 0924 UTC 17 September indicated that the system's circulation was becoming better defined, and it is estimated that a tropical depression formed near 1200 UTC that day about 300 n mi east of Barbados (Fig. 1).

Steering currents were unusually weak for a system so far south in the tropical Atlantic at the height of the hurricane season, and the depression moved slowly northwestward initially as it strengthened, becoming a tropical storm at 1800 UTC 17 September. Philippe moved generally to the north-northwest over the next couple of days toward a weakness in the subtropical ridge, becoming a hurricane at 0000 UTC 19 September about 315 n mi east of the northern Leeward Islands, and reaching its peak intensity of 70 kt about 24 h later.

While Philippe strengthened east of the Lesser An-

tilles, Tropical Storm Rita formed over the Bahamas. Rita generated an impressive outflow pattern on 19 September, which helped the weakness in the subtropical ridge strengthen into a large mid- to upper-level cold low north of the Lesser Antilles the following day. Westerly shear on the south side of the low impacted Philippe, which weakened to a tropical storm by 1200 UTC 20 September. Later that day, Philippe's low-level center became exposed west of the diminishing convection. While Philippe weakened on 21 September, it turned northward and accelerated along the east side of the cold low, which was developing its own surface reflection. For much of 22 September, Philippe was little more than a swirl of low clouds with intermittent convection, and in fact may have temporarily lost its closed surface circulation within the broader cyclonic envelope of the cold low. Late in the day, however, Philippe moved north-northwestward into the large curved band of shallow convection associated with the cold low, and deep convection redeveloped near the center of the tropical cyclone. Looping around the larger low, Philippe turned northwestward and then accelerated westward overnight. Deep convection associated with the tropical cyclone diminished again by 1200 UTC 23 September, and Philippe weakened to a tropical depression. The cyclone degenerated to a remnant low 6 h later. The remnant circulation continued a cyclonic loop, losing its closed circulation after 0600 UTC the following day, although the remnant vorticity center could be followed for another day or so. There were no reports of casualties or damages from Philippe.

q. Hurricane Rita

Rita reached category 5 strength over the central Gulf of Mexico, where it had the fourth-lowest central pressure of record in the Atlantic basin. Although it weakened to category 3 before making landfall near the Texas/Louisiana border, Rita produced significant storm surge that devastated coastal communities in southwestern Louisiana, and its winds, rain, and tornadoes caused fatalities and a wide swath of damage from eastern Texas to Alabama. Rita also caused storm surge flooding in portions of the Florida Keys.

1) SYNOPTIC HISTORY

Rita originated from a complex interaction between a tropical wave and the remnants of a cold front. The tropical wave moved off the west coast of Africa on 7 September, and it produced little deep convection as it traversed the tropical Atlantic, except for one brief period on 13 September. Meanwhile, a cold front pushed southward over the central Atlantic during 11–12 Sep-

TABLE 8. Selected surface observations for Hurricane Ophelia, 6–17 Sep 2005.

Location	Min sea level pressure		Max surface wind speed			Storm surge (ft) ^c	Storm tide (ft) ^d	Tot rain (mm)
	Date/time (UTC)	Pressure (mb)	Date/time (UTC) ^a	Sustained (kt) ^b	Gust (kt)			
Florida								
Bings Landing NOS	09/0900	1009.5				1.55		
Mayport (KNRB)	09/0826	1009.5	08/0412	28	34			
Melbourne WFO								49.8
NASA Cape Canaveral Tower 394			08/1520	34	52			
NASA Shuttle Landing Facility (KTTS)	08/0855	1006.4	08/1855	19	38			70.9
New Smyrna Beach (KEVB)	09/1055	1008.8	08/2250	31	40			
Patrick AFB (KCOF)	08/1955	1006.1	08/1955	25	36			51.6
St. Augustine (KSGJ)	09/0815	1008.8	07/1255	26	34			
Vilano Beach NOS						1.93		
North Carolina								
Back Island RAWs			14/2315		55			178.8
Beaufort (KMRH)	14/2356	991.8	14/2328	37 ^e	55 ^e			121.4
Beaufort RAWs			15/0615		39			99.6
Bogue Field (KNJM)	14/2033	993.2						
Cape Hatteras (KHSE)	15/1256	993.1	15/1256	57 ^e	72 ^e			72.4
Cedar Island	15/0840	988.0	15/0838		78			
Cherry Point (KNKT)	15/0555	994.2	15/0655	37	64			116.1
Croatan RAWs			15/0905		51			137.9
Davis (unofficial)					90			
Elizabeth City (KECG)	15/0854	1008	15/1552	30	39			13.5
Elizabethtown (KEYF)	14/1820	1002.7						47.5
Hoffman Forest RAWs			15/0105		41			108.2
Jacksonville								147.1
Kinston (KISO)			15/0643	23	34			
Kenansville (KDPL)			14/1903	23	35			
Nature Conservancy RAWs			14/1715		53			298.2
New Bern (KEWN)	15/0354	1000.0	15/0241	32	44			87.9
New River (KNCA)	14/2156	994.2	14/2156	38	55			130.0
Newport (KMHX)	15/0420	990.5	15/0534	31	49			238.5
Oak Island Brunswick Co Water Treatment Plant								444.5
Onslow Beach	14/2322	985.0	14/2125	53	68			
Pea Island	15/0850	1003.0	15/1236		57			
Richlands (KOAJ)			15/0015	30	49			
Sandy Run RAWs			15/0015		40			128.5
Southport (KSUT)	14/1504	988.1	14/1824	36	56			187.5
Stumpy Point	15/0750	1004.0	15/0740		37			
Sunny Point RAWs			14/1815		59			272.8
Swan Quarter	15/0730	1000.0	15/0856		49			
Turnbull Creek RAWs			14/1815		42			71.4
Washington (KOCW)			15/0643	20	33			
Whiteville RAWs			14/1815		39			80.8
Wilmington (KILM)	14/1850	989.5	14/1658	42	59			209.0
South Carolina								
Charleston Harbor NOS						1.64		
Fripps Inlet CARO-COOPS						1.78		
Myrtle Beach (KMYR)	14/1050	1000.7	14/0455	25	38			
North Myrtle Beach (KCRE)	14/1336	999.7	14/1253	20	33			160.0
Oyster Landing NOS						2.75		
South Capers Island CARO-COOPS						1.74		
Buoy/C-MAN								
Cape Lookout, NC, C-MAN (34.6°N, 76.5°W)	15/0600	981.9	14/2309	65	80			
Duck, NC, C-MAN (36.2°N, 75.8°W)	15/0930	1008.5	15/1651	34	43			

TABLE 8. (Continued)

Location	Min sea level pressure		Max surface wind speed			Storm surge (ft) ^c	Storm tide (ft) ^d	Tot rain (mm)
	Date/time (UTC)	Pressure (mb)	Date/time (UTC) ^a	Sustained (kt) ^b	Gust (kt)			
Buoy/C-MAN								
Frying Pan Shoals, NC, C-MAN (33.5°N, 77.6°W)	14/1300	980.7						
Mayport, FL, NOS (30.4°N, 81.4°W)	09/0824	1010.1	08/1018		37	3.03		
Slidaway Tower M2R6 C-MAN (31.5°N, 80.2°W)	13/1934	1007.2	13/0234	35	41			
Slidaway Tower R2 C-MAN (31.3°N, 80.6°W)			13/0431	31	35			
Slidaway Tower R8 C-MAN (31.6°N, 79.9°W)	13/2136	1005.4	13/0630	38	44			
St. Augustine, FL, C-MAN (28.9°N, 81.2°W)	09/0905	1008.8	09/0105	34	43			
Settlement Point, GBI C-MAN (26.7°N, 79.0°W)	08/2300	1008.5	07/0630	25	34			
Springmaid Pier, SC, NOS (33.7°N, 78.9°W)	14/0942	1000.5	14/1800	24	37	2.81		
Sunset Beach, NC, CARO-COOPS (33.9°N, 78.5°W)	14/1324	995.6	14/1300	33	47	2.85		
Wrightsville Beach, NC, NOS (34.2°N, 77.8°W)	14/1854	984.8	14/1700	59	69	4.19		
Buoy 41001, NOAA (34.7°N, 72.7°W)	15/2300	1011.5	16/1040	28 ^f	37			
Buoy 41002, NOAA (32.3°N, 75.4°W)	10/2200	998.7	11/2200	49	67			
Buoy 41004, NOAA (32.5°N, 79.1°W)	13/2250	996.4	14/0030	45 ^f	57			
Buoy 41009, NOAA (28.5°N, 80.2°W)	08/1050	1002.3	08/1750	37	47			
Buoy 41010, NOAA (29.0°N, 78.5°W)	09/0820	1000.1	09/1350	37	49			
Buoy 41012, NOAA (30.0°N, 80.6°W)	09/1100	1006.2	08/1300	30	43			
Buoy 41013, NOAA (33.4°N, 77.4°W)	14/1000	980.8	14/1800	54	68			
Buoy 41024, CARO-COOPS (33.8°N, 78.5°W)	14/1300	994.9	14/1500	38	41			
Buoy 41025, NOAA (35.0°N, 75.4°W)	15/1500	988.7	15/1707	55 ^f	73			
Buoy 41030, CARO-COOPS (32.5°N, 79.3°W)			13/2330	38	45			
Buoy 41035, NOAA (34.5°N, 77.3°W)	14/2120	982.0	14/2030	48 ^f	62			
Buoy 41038, CORMP (34.1°N, 77.7°W)			14/2100	50	52			
Buoy 44004, NOAA (38.5°N, 70.6°W)	17/0800	1001.5	17/0730	40 ^f	53			
Buoy 44008, NOAA (40.5°N, 69.4°W)	17/1200	1001.1	17/1100	33	43			
Buoy 44014, NOAA (36.6°N, 74.8°W)			16/1900	27 ^f	35			
Buoy 44024, GOMOOS (42.3°N, 65.9°W)	17/2100	996.9	17/1900	27	35			

^a Date/time is for sustained wind when both sustained and gust are listed.

^b Except as noted, sustained wind-averaging periods for C-MAN and land-based ASOS reports are 2 min; buoy averaging periods are 8 min, while NOS reports are 6 min.

^c Storm surge is water height above normal astronomical tide level.

^d Storm tide is water height above National Geodetic Vertical Datum (1929 mean sea level).

^e Incomplete record.

^f 10-min average.

tember and became stationary a couple hundred nautical miles north of the Leeward Islands on 13 September. The southern portion of the front became a remnant surface trough on 14 September. This trough drifted westward on 15 September as strong high pressure built eastward over the western Atlantic. It passed north of Puerto Rico and the Virgin Islands the next day, producing a large but disorganized area of disturbed weather.

Accompanied by limited convection, the tropical wave moved westward across the Leeward Islands on 16 September and then merged with the surface trough

north of Puerto Rico early on 17 September. Shower and thunderstorm activity became more concentrated later that day north of the Dominican Republic, and the area of disturbed weather was given its first satellite classifications at 1800 UTC. Gradually increasing organization was associated with slight relaxation of vertical shear, as a mid- to upper- tropospheric low previously over the western Atlantic shifted westward over Cuba and the northwestern Caribbean Sea. A tropical depression is estimated to have formed by 0000 UTC 18 September approximately 70 n mi east of Grand Turk in the Turks and Caicos (Fig. 1).

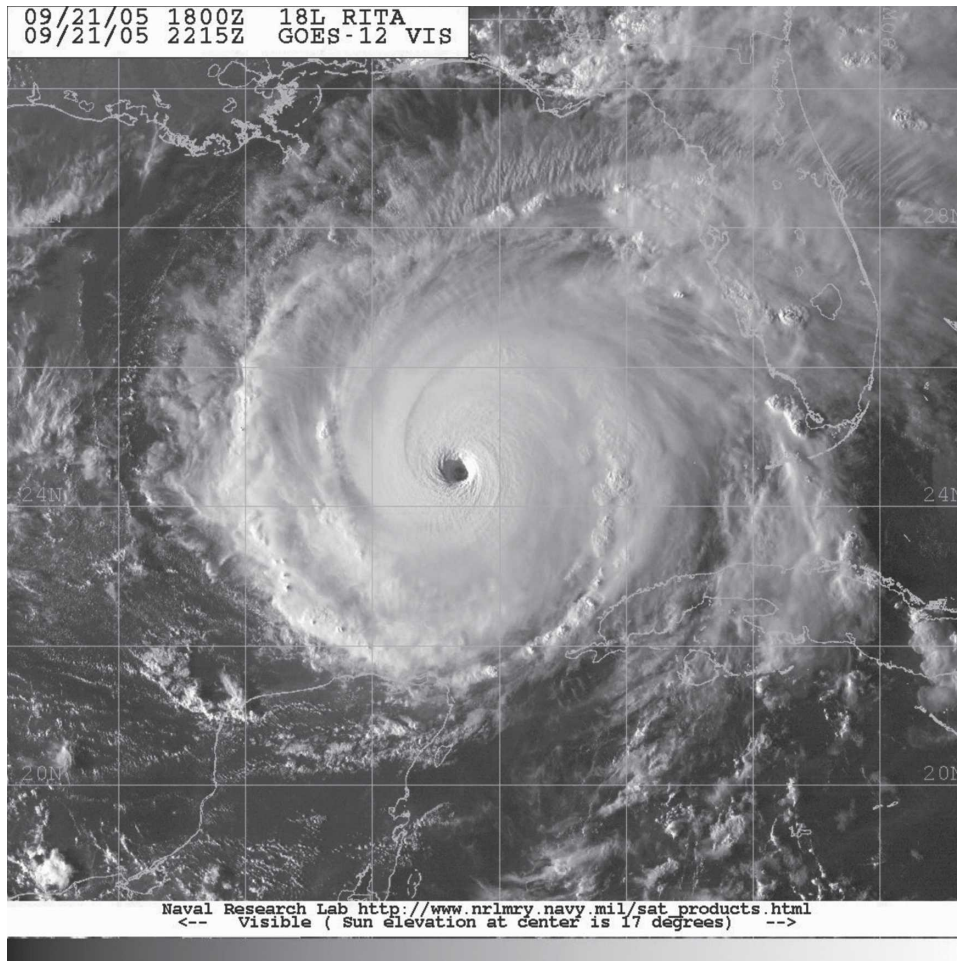


FIG. 9. *GOES-12* visible image of Hurricane Rita at 2215 UTC 21 Sep 2005. Image courtesy of the NRL, Monterey, CA.

On 18–19 September, the cyclone moved toward the west-northwest over the Turks and Caicos and the southeastern Bahamas. Strong convection wrapped around the north side of the center, and the depression became a tropical storm by 1800 UTC 18 September about 25 n mi east-southeast of Mayaguana in the southeastern Bahamas. Moderate southerly vertical shear east of the mid- to upper-level low confined the upper-level outflow and deep convection to the north of the center. Thus, while the steering flow was generally toward the west, the low-level center steadily reformed to the north, resulting in a west-northwestward motion. The upper-level low weakened on 19 September and the shear over Rita relaxed. This allowed Rita to reach an intensity of 60 kt by 1800 UTC that day. The storm turned more westward early on 20 September along the southern periphery of a deep-layer ridge over the western Atlantic and Florida. Rita remained a tropical storm until it reached the Florida Straits. Once

there, however, Rita strengthened to a hurricane by 1200 UTC 20 September about 100 n mi east-southeast of Key West. Rita became a category 2 hurricane by 1800 UTC that day, and its center passed about 40 n mi south of Key West about an hour later.

Rapid to explosive deepening ensued as Rita continued westward over the warm waters of the Loop Current in an environment of weak wind shear. Rita became a major hurricane early on 21 September, then reached an intensity of 145 kt by 1800 UTC that day (Fig. 9). Rita had strengthened from a tropical storm to a category 5 hurricane in less than 36 h. It remained at category 5 strength for about the next 18 h, reaching its estimated peak intensity of 155 kt around 0300 UTC 22 September while located about 270 n mi south-southeast of the mouth of the Mississippi River. During that time it also turned toward the west-northwest around the western extent of the mid- to upper-tropospheric ridge centered over the southeastern United States.

The inner eyewall deteriorated later on 22 September and Rita weakened to a category 4 hurricane by 1800 UTC that day. By early on 23 September a new, outer eyewall had consolidated and the hurricane had grown in size. However, Rita did not reintensify after the eyewall replacement cycle. Increasing southwesterly shear and slightly cooler waters caused steady weakening on 23 September. Rita rounded the western periphery of the ridge and turned northwestward that day. It weakened to a category 3 hurricane by 1800 UTC 23 September about 140 n mi southeast of Sabine Pass at the Texas–Louisiana border. Rita made landfall with an estimated intensity of 100 kt (category 3) at 0740 UTC 24 September in extreme southwestern Louisiana between Johnson’s Bayou and Sabine Pass.

The cyclone weakened after landfall, remaining a hurricane until only about 1200 UTC 24 September when it was centered about 35 n mi north of Beaumont, Texas. As a steadily weakening tropical storm, Rita proceeded northward, with its center moving near the Texas–Louisiana border for the rest of that day. Rita weakened to a tropical depression by 0600 UTC 25 September over southwestern Arkansas and then turned northeastward ahead of an approaching frontal system. The depression degenerated to a remnant low early on 26 September over southeastern Illinois. The low was absorbed into a frontal zone later that morning over the southern Great Lakes.

2) METEOROLOGICAL STATISTICS

Selected surface observations from Rita are included in Table 9. As was the case during Katrina, records from many ASOS sites, C-MAN and NOS stations, and buoys were incomplete because of weather-induced failures.

The 53rd WRS flew 16 operational missions into Rita, producing 63 center fixes. Seven missions flown by the NOAA WP-3D aircraft produced 15 center fixes, surface wind speed data from the SFMR with poststorm calibration conducted by the HRD, and airborne Doppler radar–derived wind analyses also provided by HRD. Additionally, the NOAA G-IV jet conducted eight synoptic surveillance missions around Rita during 19–23 September.

Radar and aircraft data indicate that Rita’s strongest winds stayed just south of the Florida Keys on 20 September, although sustained hurricane-force winds might have briefly impacted portions of the extreme Lower Keys. The Sand Key C-MAN station reported a 10-min average wind of 63 kt at 2110 UTC with an earlier peak gust to 80 kt. Higher winds may have occurred after the instrument was destroyed around 2200 UTC. The Key West International Airport measured a

2-min sustained wind of 54 kt with a gust to 66 kt at 2314 UTC. Most of the remainder of the keys experienced tropical storm conditions. Wind gusts of tropical-storm-force occurred over much of the Florida peninsula south of Lake Okeechobee on 20 September. Tropical storm conditions also occurred in western Cuba on 20–21 September while the center of Rita passed about 40 n mi from the north coast of the island.

Aircraft and satellite data on 21 September indicated that Rita intensified from 95 kt (category 2) to 145 kt (category 5) in just 18 h. The maximum 700-mb flight-level wind during that period was 161 kt at 1935 UTC, which corresponds to about 145 kt at the surface based on the average 90% adjustment. The SFMR estimated 146-kt winds at 1912 UTC 21 September and 144 kt at 1945 UTC. Two dropwindsondes directly measured surface winds of 142 and 149 kt shortly after 1930 UTC that day. A 700-mb flight-level wind of 165 kt was observed at 0538 UTC 22 September, corresponding to about 149 kt at the surface.

The central pressure in Rita fell a remarkable 70 mb in the 24-h period ending 0000 UTC 22 September, reaching an estimated 897 mb with an estimated intensity of 150 kt. This pressure is based upon an 899-mb dropwindsonde observation at 2309 UTC 21 September that had a surface wind of 32 kt. The next central pressure measurements were 898 mb at 0538 UTC 22 September and 899 mb (with a surface wind of 35 kt) at 0715 UTC. Because of the 6-h data gap, the actual lowest pressure and maximum winds are speculative. Since the pressure fell before 0000 UTC and rose after 0600 UTC, and since the aircraft-reported eye diameter contracted during that time, it is estimated that the minimum pressure was 895 mb around 0300 UTC 22 September. At the end of the rapid strengthening, Rita had become a large hurricane, with 34-kt winds extending up to 160 n mi from the center at the time of peak intensity.

The weakening of Rita during the last 48 h before landfall was associated with significant changes in its internal structure. The eyewall replacement cycle on 22–23 September resulted in a 30 n mi wide eye. One consequence of this was additional expansion of Rita’s wind field. By early on 23 September, tropical-storm-force winds extended up to about 180 n mi from the center, and hurricane-force winds extended up to about 75 n mi out. While the central pressure rose slowly, aircraft data indicate the maximum sustained winds decreased fairly quickly, especially in the first 24 h after peak intensity.

During Rita’s passage across the Gulf, it passed directly over NOAA buoy 42001, which reported 10-min average winds of 88 kt with a gust to 119 kt at 0030

TABLE 9. (Continued)

Location	Min sea level pressure		Max surface wind speed			Storm surge (ft) ^c	Storm tide (ft) ^d	Tot rain (mm)
	Date/time (UTC)	Pressure (mb)	Date/time (UTC) ^a	Sustained (kt) ^b	Gust (kt)			
			Louisiana					
Belle Chase (KNBG)	23/2355	1003.7	24/0915		37			
Boyce 7SW COOP								188.0
Brusly COOP								150.1
Bunkie COOP								406.4
Butte La Rose COOP								177.5
Caillou Lake USGS						6.95 ^e		
Cameron RAWS			24/0620	63 ^e	94 ^e			206.5
Carencro COOP							6.29	179.1
Central Plaquemines Parish								
Convent COOP								193.0
Crowley 2SW COOP								211.3
De Ridder Beauregard Regional (KDRI)	24/1101	980.4 ^e	24/0821	31 ^e	54 ^e			
Deridder COOP								355.6
Dove Field RAWS			24/0900	23	46			190.8
Elmer 2SW COOP								195.1
Eunice COOP								221.5
Evangeline/Gardner RAWS			24/2100	23	42			201.4
Fort Polk AAF (KPOE)	24/1200	983.8	24/1400	32	51			156.0
Fort Polk Fullerton (KBKB)	24/1219	992.2	24/1819	26	40			156.0
Grand Coteau COOP								219.7
Greenwell Springs COOP								141.2
Holden								127.5
Houma USGS						4.32		
Jeanerette 5NW COOP								233.9
Jennings COOP								247.7
Johnsons Bayou ULM tower	24/0739	939.1	24/0724	61	79			
Lacassine RAWS			24/0245	38 ^e	62 ^e			
Lafayette (KLFT)	24/0817	992.2	24/1321	44	51			158.5
Lafayette COOP								218.4
Lake Charles (KLCH)	24/0806	968.2	24/0208	50 ^e	64 ^e			195.1
Lake Charles WFO			24/0820		83			
Lake Pontchartrain (NWS)—Mid-Lake						6.5		
Laplace 5NE								315.5
Leesville COOP								124.5
Livingston COOP								176.3
Lutcher COOP								113.8
Marksville COOP								212.6
Moss Bluff COOP								219.5
New Orleans Int. (KMSY)	23/2153	1002.4	24/1840	30	42			52.6
North-central Cameron Parish just east of Calcasieu Lake						8.11		
Oaknolia COOP								133.1
Old Town Bay COOP								213.4
Opelousas COOP								250.2
Plaquemine COOP								134.9
Pontchatoula COOP								143.5
Port Fourchon NOS							5.00	
Ragley COOP								215.9
Red River Lock 2 COOP								205.7
Reserve COOP								118.4
Rigoletes CoE						4.48		
St Martinville 3SW COOP								206.5
Salt Point	23/2153	993.0 ^e	23/2153	19 ^e	38 ^e			
Sam Houston Jones State Park COOP								201.2
Slidell (KASD)	23/2141	1005.1	24/1838	30	38			16.3
Sulphur COOP								241.0
Vernon RAWS			24/1000	22	43			202.2
Western St. Mary Parish near Louisa						11.95		

TABLE 9. (Continued)

Location	Min sea level pressure		Max surface wind speed			Storm surge (ft) ^c	Storm tide (ft) ^d	Tot rain (mm)
	Date/time (UTC)	Pressure (mb)	Date/time (UTC) ^a	Sustained (kt) ^b	Gust (kt)			
Texas								
Angleton (KLBX)	24/0949	992.9	24/0434	28	38			
Battleship Texas St. Park TCOON							3.21	
Beaumont (KBPT)	24/0809	952.3	24/0833	70	91			225.8
Beaumont Research Center COOP								167.1
Clear Creek/Seabrook							3.23	
College Station (KCLL)	24/1420	997.3	24/1914	31	41			
Conroe (KCXO)	24/1540	990.9	24/1619	33	48			
East Matagorda Bay TCOON							4.53	
Galveston (KGLS)	24/0142	994.6 ^e	24/0142	39 ^e	54 ^e			
Galveston Bay Entrance North Jetty NOS/TCOON	24/0800	979.9	24/0300	51	64		3.98	
Galveston Bay Entrance South Jetty TCOON							2.98	
Houston (KIAH)	24/1047	988.1	24/0630	39	53			22.1
Houston Hobby Airport (KHOU)	24/0827	988.8	24/0625	38	48			25.9
Huntsville (KUTS)	24/1420	991.5	24/1644	30	41			
Jasper County Bell Field (KJAS)	24/0525	996.6 ^e	24/0205	24 ^e	37 ^e			
Jasper COOP								194.6
Kirbyville RAWS								206.5
Kountze COOP								226.1
Long King Creek/ Livingston								112.8
Luce Bayou								151.9
Manchester Houston TCOON							3.38	
McFadden RAWS			24/0240	36 ^e	59 ^e			
Nederland FCMP tower	24/0830	942.3	24/0809	57	80			
Onalaska								119.9
Orange FCMP tower	24/0845	941.0	24/0819	65	85			
Orange TTU tower			24/0815	57 ^e	77 ^e			
Orange County Airport (KORG)	24/0428	983.4 ^e	24/0428	31 ^e	47 ^e			
Orange 9N COOP								228.6
Peach Creek								128.0
Pearland (KLVJ)	24/0459	991.9	24/0417	33	41			7.1
Port Arthur FCMP	24/0824	949.7	24/0826	82	101			
Port Arthur TCOON			24/0800	61	82		9.24	
Port Arthur TTU tower				81	101			
Rainbow Bridge TCOON							7.93	
Rollover Pass TCOON							4.58	
Silsbee 4N COOP								317.5
Southern Rough RAWS			24/0940	21 ^e	45 ^e			240.0
Sugarland (KSGR)	24/0934	993.2	24/0750	33	44			11.2
Tomball (KDWH)	24/0938	990.9	24/0145	27	38			
Trinity River (U.S. 90)								116.1
Wildwood COOP								118.6
Woodlake								110.0
Woodville RAWS			24/1200	43 ^e	66 ^e			235.0
Buoys/C-MAN/NOS								
Bayou Gauche, LA, NOS (29.8°N, 90.4°W)	24/0624	1001.6	24/0506	31	42			
Bayou LaBranche, LA, NOS (30.1°N, 90.4°W)	23/2200	1002.9						
Calcasieu Pass, LA, NOS (29.8°N, 93.3°W)	24/0112	983.0 ^e	24/0518	67 ^e	97 ^e		5.50 ^e	
Dauphin Island, AL, C-MAN (30.3°N, 88.1°W)			24/1000	34	47			
Dry Tortugas, FL, C-MAN (24.6°N, 82.9°W)	21/0100	994.0 ^e	21/0120	57 ^{e,f}	76 ^e			
Eagle Point, TX, NOS (29.5°N, 94.9°W)	24/0800	984.3	24/0224	34	48		3.67	
Fowey Rocks, FL, C-MAN (25.6°N, 80.1°W)	20/0900	1007.8	20/1600	48	56			
Galveston Pier 21, TX, NOS (29.3°N, 94.8°W)	24/0818	984.7					3.59	
Galveston Pleasure Pier, TX, NOS (29.3°N, 94.8°W)	24/0700	983.5	24/0600	41	57		4.69	

TABLE 9. (Continued)

Location	Min sea level pressure		Max surface wind speed			Storm surge (ft) ^c	Storm tide (ft) ^d	Tot rain (mm)
	Date/time (UTC)	Pressure (mb)	Date/time (UTC) ^a	Sustained (kt) ^b	Gust (kt)			
Buoys/C-MAN/NOS								
Isle Dernieres, LA, WAVECIS (29.1°N, 90.5°W)			23/1300	50	62			
Key West, FL, NOS (24.6°N, 81.8°W)	20/2100	995.8	20/1600		42		2.5	
Long Key, FL, C-MAN (24.8°N, 80.9°W)	20/1200	1003.3	20/1530	39 ^f	52		1.9	
Naples, FL, NOS (26.1°N, 81.8°W)	20/2000	1009.5				1.5	2.0	
Marsh Island, LA, WAVECIS (29.4°N, 92.1°W)	24/0400	983.6	24/0000	62 ^e	81 ^e			
Molasses Reef, FL, C-MAN (25.0°N, 80.4°W)	20/1200	1003.4	20/1418	36 ^f	45			
Morgans Point, TX, NOS (29.7°N, 95.0°W)	24/0942	982.9	24/0836	43	64		3.04	
Sabine Pass North, TX, NOS (29.7°N, 93.9°W)	24/0542	967.8 ^e	24/0500	55 ^e	70 ^e		8.12 ^e	
Salt Point, LA, WAVECIS (29.5°N, 91.6°W)	23/2300	990.2	23/2300	46 ^e	63 ^e			
Sand Key, FL, C-MAN (24.5°N, 81.9°W)	20/2100	988.5 ^e	20/2110	63 ^{e,f}	80 ^e			
Sea Rim State Park, TX, C-MAN (29.7°N, 94.1°W)	24/0800	951.3	24/0700	71	86		6.37 ^e	
Settlement Point, GBI, C-MAN (26.7°N, 79.0°W)			20/0210	31 ^f	40			
South Timbalier Block, LA, WAVECIS (28.9°N, 90.5°W)	23/1700	995.5						
Sombrero Key, FL, C-MAN (24.6°N, 81.1°W)	20/1600	1001.0	20/1700	61	69			
Vaca Key, FL, NOS (24.7°N, 81.1°W)	20/1500	1001.6	20/1600	33	47		1.5	
Virginia Key, FL, NOS (25.7°N, 80.2°W)	20/0900	1008.7	20/1400	29	44	1.2	2.5	
Buoy 42001, NOAA (25.8°N, 89.7°W)	22/2250	925.7	23/0030	88 ^f	119			
Buoy 42002, NOAA (25.2°N, 94.4°W)	23/2050	1001.3	23/1730	30 ^f	37			
Buoy 42019, NOAA (27.9°N, 95.4°W)	24/0050	995.9	24/0110	34 ^f	49			
Buoy 42035, NOAA (29.3°N, 94.4°W)	24/0650	972.3	24/0450	54	66			
Buoy 42040, NOAA (29.2°N, 88.2°W)	23/0850	1004.5	23/0130	33 ^f	43			
Buoy 42046, TABS (27.9°N, 94.0°W)	23/1330	997.9 ^e	23/1500	31 ^e	45 ^e			

^a Date/time is for sustained wind when both sustained and gust are listed.

^b Except as noted, sustained wind-averaging periods for C-MAN and land-based ASOS reports are 2 min; buoy averaging periods are 8 min, while NOS reports are 6 min.

^c Storm surge is water height above normal astronomical tide level.

^d Storm tide is water height above National Geodetic Vertical Datum (1929 mean sea level).

^e Incomplete record.

^f 10-min average.

UTC 23 September. The buoy also reported a minimum pressure of 925.7 mb at 2300 UTC 22 September.

Near the time of landfall, the strongest 700-mb flight-level winds were 111–115 kt northeast of the eye. WSR-88D velocity data from Lake Charles, Louisiana, showed winds near the top of the boundary layer (about 500 m in altitude) of about 120 kt. Also, a dropwindsonde at 0544 UTC provided an estimated 92-kt surface wind, derived from an average 80% adjustment of the 115-kt mean boundary layer wind speed. Based on these data, and the premise that the maximum surface wind at landfall was likely not sampled, the landfall intensity is set to 100 kt.

The central pressure at landfall measured by dropsondes was 937 mb. The landfall pressure and the 935-mb best-track pressure at 0600 UTC 24 September are the lowest of record in the Atlantic basin for an intensity of 100 kt. Application of the Holland wind model

using the central pressure of 935 mb, the concurrently observed outermost pressure of 1009 mb, and the B parameter set to 1 yields an intensity of 94 kt. Similar to Katrina, Rita’s combination of relatively weak winds and such a low pressure resulted from an observed broadening of the pressure field during its last 48 h over the Gulf of Mexico that weakened the pressure gradient.

The C-MAN station at Sea Rim State Park, Texas (13-m elevation), reported 2-min average winds of 71 kt with a gust to 86 kt at 0700 UTC 24 September (Table 9). Sustained hurricane-force winds were also reported at the Southeast Texas Regional Airport in Beaumont, Texas (70 kt), and at the Calcasieu Pass, Louisiana, NOS station (67 kt), although the latter failed more than 2 h prior to landfall. Several instrumented towers in southeastern Texas also measured sustained hurricane-force winds, as strong as 82 kt, with peak 3-s gusts up to about 100 kt. Many areas in extreme southeastern

Texas and extreme southwestern Louisiana experienced category 1 hurricane conditions, with a few areas experiencing category 2 conditions. Category 3 hurricane conditions were confined to a small area east of the eye along the coast of southwestern Louisiana. Rita produced tropical storm conditions over large portions of southern Louisiana (including cities such as Baton Rouge) and southeastern Texas (including the Houston and Galveston areas).

Rita produced a significant storm surge in vulnerable southwestern Louisiana. Because of the widespread destruction of structures and gauges, only a few high water marks have been collected and analyzed under the direction of FEMA. These data, along with unofficial visual estimates, suggest that the storm surge reached 15 ft in portions of the Cameron, Louisiana, area. Surge heights reached as high as 8 ft in communities along the shore of Calcasieu Lake such as Grand Lake. The surge propagated up the Calcasieu River, flooding portions of the Lake Charles area and reaching Interstate 10 (about 25 n mi inland). Flood waters in downtown Lake Charles were up to 6 ft deep. Farther east, most or all of Vermillion, Iberia, and St. Mary Parishes south of Highway 14 and U.S. 90 (several nautical miles inland) were inundated by the storm surge, visually estimated at 8–12 ft in some of these areas; a high water mark of nearly 12 ft was observed in western St. Mary Parish near the town of Louisa.

Rita also produced a storm surge of 4–7 ft in coastal areas of southeastern Louisiana, flooding some areas that had been impacted by the surge from Hurricane Katrina, including New Orleans, Slidell, and Mandeville. Some levees in southern Jefferson and southern Terrebonne Parishes were overtopped or breached, as were a few repaired levees in the New Orleans area. This surge prolonged the efforts to remove floodwaters from the New Orleans area.

West of the track of the center, incomplete gauge data suggest a storm surge of at least 5 ft occurred at Sabine Pass. Surviving gauges along Sabine Lake measured peak water levels of about 4–5 ft. Storm tides along much of the Texas coast were generally in the 3–5-ft range, and mostly occurred on 23 September. Some flooding occurred along the northern shores of Galveston Island and the Bolivar Peninsula as northerly winds pushed the waters of Galveston Bay southward. Tropical-storm-force winds also resulted in a surge of about 1.5 ft on Lake Livingston, located in southeastern Texas about 50 n mi north of Houston.

Rita also produced storm surge in the Florida Keys during the close pass of the center on 20 September. Visual estimates suggest the maximum storm surge in the keys was about 4–5 ft along the south-facing shores

of Key West and the Lower Keys, and 3–4 ft along portions of the Atlantic shores of the Middle and Upper Keys. The surge flooded the runway at Key West International Airport, and streets up to four blocks inland in Key West were flooded to depths of about three feet.

Rita produced widespread heavy rains across portions of Mississippi, Louisiana, and extreme eastern Texas, with numerous storm totals of 125–225 mm and isolated totals of 250–400 mm. The maximum reported total was 406.4 mm at Bunkie, Louisiana. Flash floods occurred in several areas, including the Big Black River basin of west-central Mississippi, and several cities reported flooded streets. Storm-total rainfall in the Lower and Middle Florida Keys was generally 50–100 mm, with radar estimates of greater than 125 mm across portions of the Upper Keys. A few storm totals exceeding 75 mm were reported over the extreme southern Florida peninsula. Rita caused 75–150 mm of rain in portions of Arkansas.

Rita caused at least 90 tornadoes, mainly north and east of the center in portions of Alabama, Mississippi, Louisiana, and Arkansas. Fifty-six of the tornadoes occurred in central Mississippi, northeastern Louisiana, and southeastern Arkansas. Eleven tornadoes were reported in other portions of Arkansas, and 23 tornadoes were reported in Alabama.

3) CASUALTY AND DAMAGE STATISTICS

The approach of Rita provoked one the largest evacuations in U.S. history. Media reports indicate that the number of evacuees in Texas could have exceeded two million. Additional evacuations involving smaller numbers took place in Louisiana.

Rita directly caused seven fatalities. One person drowned near Lake Charles, Louisiana; two people died in Hardin, Texas, when a tree was blown down onto their home; one person died when a tree fell on her home in Point Blank, Texas; another person was killed by a falling tree in Angelina County, Texas; one person was killed in a tornado near Isola, Mississippi; and one person drowned in a rip current at Miramar Beach in the Florida panhandle on 24 September. At least 55 indirect fatalities have been reported in Texas. A bus accident south of Dallas during the evacuation killed more than 20 persons, mostly elderly evacuees from a nursing home. Six fatalities occurred in Beaumont due to carbon monoxide poisoning. Other persons died during the evacuation due to heat exhaustion.

Rita's storm surge devastated communities in coastal areas of southwestern Louisiana, including Holly Beach, Cameron, Creole, and Grand Cheniere in Cameron Parish. Almost every structure in these areas was

destroyed, and some were completely swept away. Farther inland, numerous homes in Grand Lake were damaged or destroyed. Many portions of the Lake Charles area suffered substantial flood damage, including downtown and some surrounding residential communities. In Vermillion Parish, most structures in the town of Pecan Island were destroyed, and dozens of other homes and businesses were flooded and damaged. Storm-surge damage to homes and businesses in low-lying areas occurred along the entire coast of Louisiana, although the impact in the New Orleans area was not nearly as widespread as during Hurricane Katrina. In Jefferson County, Texas, adjacent to Sabine Lake, the storm surge flooded several homes, and some mobile homes floated away from their original locations. The surge on Lake Livingston caused some damage to the Lake Livingston Dam. Rita also caused surge damage to homes and businesses in portions of the Florida Keys.

Rita's winds, tornadoes, and freshwater floods also damaged homes and businesses in portions of Louisiana, eastern Texas, Mississippi, Alabama, Arkansas, and the Florida Keys. Rita caused wide swaths of downed trees and power lines, leaving well over one million customers in these areas without electrical service. The hurricane disrupted oil and gas production and refining in the northwestern Gulf of Mexico region (largely due to evacuations), but the impacts were not as severe as those due to Katrina. The most recent available estimate by the PCS of the insured property damage in the United States caused by Rita is \$5.63 billion. This produces an estimate for total damage of about \$11.3 billion.

r. Hurricane Stan

Stan was associated with disastrous inland flooding across portions of Central America and Mexico, and some estimates of the death toll are as high as 2000. However, not all of these deaths were directly attributed to Stan.

1) SYNOPTIC HISTORY

A tropical wave that moved across the coast of Africa on 17 September was the likely precursor to Stan. This wave showed little distinction as it moved over the eastern and central tropical Atlantic. The associated cloudiness and showers increased as the wave neared 50°W longitude on 22 September, but north-northeasterly shear created an environment unfavorable for tropical cyclone formation. The wave moved into the eastern Caribbean Sea on 25 September, while shear over the system diminished. By 27 September, associated deep convection became more consolidated over the central

Caribbean Sea. Over the next several days, organization of the system waxed and waned as it moved into the western Caribbean Sea. Development began in earnest on 1 October when the system neared the eastern coast of the Yucatan peninsula. Based on the extent and organization of deep convection as well as surface observations, it is estimated that a tropical depression formed around 1200 UTC 1 October centered about 115 n mi southeast of Cozumel (Fig. 1).

Lower- to midtropospheric ridging north and northeast of the tropical cyclone resulted in a west-northwestward steering current, and an upper-tropospheric anticyclone developed over the area. The depression strengthened into a tropical storm shortly before its center made landfall on the east coast of the Yucatan peninsula, just south of Tulum, around 1000 UTC 2 October. The center of Stan crossed the peninsula in about 18 h while the system weakened back to a depression. It quickly regained tropical storm strength, however, after it moved back over water. Deep-layer high pressure over the western Gulf of Mexico forced the system to turn toward the west-southwest and southwest over the Bay of Campeche. This turn may also have been due to the interaction with a broad, deep-layer cyclonic circulation that covered eastern Mexico and most of Central America. As Stan approached the southern Gulf Coast of Mexico, it became a hurricane around 0600 UTC 4 October. It made its second landfall as a category 1 hurricane around 1200 UTC about 80 n mi east-southeast of Veracruz. Once inland, the cyclone weakened rapidly, and it dissipated over the mountainous terrain of the Mexican state of Oaxaca just after 0600 UTC 5 October.

2) METEOROLOGICAL STATISTICS

An AFRC mission just prior to landfall on 4 October measured a peak 700-mb flight-level wind of 79 kt around 1000 UTC. A little earlier, a dropwindsonde from this mission yielded surface wind estimates of 69–72 kt. These data are the primary bases for setting the peak (and landfall) intensity of Stan at 70 kt.

Three ships reported tropical storm winds during Stan. The *Veendam* (call sign C6NL6) reported 40-kt winds at 0600 UTC 5 October, the *Edyth L* (call sign ZCAM4) reported 37-kt winds at 1200 UTC 2 October, and the *Albert* (call sign DGTX) reported 35-kt winds at 0000 UTC 5 October.

Stan produced widespread heavy rains over portions of southeastern Mexico. There are numerous reports of storm totals of 100–200 mm, with scattered amounts of 200–300 mm. The maximum reported total was 306.8 mm at El Novillero, with 305.1 mm reported at Cuetzalan.

3) CASUALTY AND DAMAGE STATISTICS

It is impossible to determine how many people were killed by Stan. According to the government of Mexico, there were 80 deaths in the Mexican states of Veracruz, Oaxaca, and Chiapas. The actual surface circulation of the tropical cyclone seems to have been confined to Mexico. However, the tropical cyclone appeared to be embedded within the western portion of a broader-scale low-level cyclonic circulation. This larger system produced extensive very heavy rains over portions of extreme eastern Mexico and Central America that resulted in disastrous floods. Estimates of the total number of lives lost, including the 80 direct deaths, in Mexico and Central America are mostly in the range of 1000–2000, with some even higher. Guatemala was particularly hard hit; over 1000 persons may have perished in that country.

s. *Unnamed subtropical storm*

As part of its routine postseason review, the TPC/NHC on rare occasions identifies, from new data or meteorological interpretation, a previously unnoted tropical or subtropical cyclone. The TPC/NHC reanalysis of 2005 has identified a short-lived subtropical storm near the Azores Islands.

An upper-level low formed just west of the Canary Islands on 28 September and moved generally westward for the next two days. A large but transient burst of convection developed near the low on 30 September, accompanied by the formation of a surface trough. The complex system moved generally westward to west-northwestward into a more unstable air mass, which allowed sporadic convection. Surface observations and satellite cloud-motion winds indicate a broad surface low formed within the trough late on 3 October about 400 n mi southwest of São Miguel Island in the Azores. Convection increased in association with the surface low, and it is estimated that the system became a subtropical depression around 0600 UTC 4 October (Fig. 1).

The depression turned northeastward in the warm sector ahead of an approaching cold front associated with a large nontropical low northwest of the Azores. Additional development occurred, and it is estimated that the cyclone became a subtropical storm around 1200 UTC 4 October. The system reached an estimated peak intensity of 45 kt as the center passed through the eastern Azores later that day. The cyclone turned north-northeastward and merged with the approaching cold front early on 5 October. Late that day, the remains of the storm were absorbed by the nontropical low, which would evolve into Hurricane Vince a few days later.

The unnamed subtropical storm brought gale-force winds to the eastern portions of the Azores Islands. Santa Maria Island reported a 10-min average wind of 43 kt at 2100 UTC 4 October with a peak gust of 51 kt. The station reported a minimum pressure of 1006 mb at that time. Ponta Delgada on São Miguel reported 10-min average winds of 33 kt at 2230 UTC 4 October with a gust to 46 kt. The station reported a minimum pressure of 999 mb at 2100 UTC that day. A ship with the call sign VRZN9 reported a pressure of 999 mb and 22-kt winds at 1800 UTC 4 October. There were no reports of damages or casualties from this system.

t. *Tropical Storm Tammy*

A tropical wave crossed the coast of western Africa on 24 September. The wave moved west-northwestward and lost most of its convection over the eastern Atlantic. Convection increased just north of the Leeward Islands on 2 October as the wave interacted with a large mid- to upper-level trough oriented northwest-to-southeast. While convection increased in coverage and intensity through 3 October, moderate shear caused by the trough inhibited development. Late on 4 October, the northern portion of the tropical wave broke off and turned northwestward, moving closer to the upper-level trough axis where the vertical shear was weakest. This motion brought the system into close proximity with an extensive area of surface high pressure situated over the central Atlantic Ocean. The resulting increase in the pressure gradient caused a broad area of gale-force winds just east of the Bahamas.

As the surface trough moved over the Bahamas early on 5 October, a small mass of deep convection developed along the trough axis. By 0600 UTC, surface and radar observations indicated a low pressure center had developed just off the southeastern Florida coast about 20 n mi east of Jupiter. Since 35-kt winds were already present east of the newly formed low, the system skipped the tropical depression phase and became a tropical storm (Fig. 1).

Embedded within southeasterly steering flow east of a deep-layer low pressure system centered over the eastern Gulf of Mexico, Tammy moved northwestward parallel to the Florida east coast. Rotating around the deep-layer low, Tammy turned toward the west-northwest by late on October 5. Strong upper-level diffluence in this area aided the development of persistent deep convection, which allowed Tammy to strengthen to a peak intensity of 45 kt before it made landfall along the northeastern Florida coast near Atlantic Beach at around 2300 UTC.

After landfall, Tammy accelerated westward across southern Georgia early on 6 October. The cyclone

weakened to a depression by 1200 UTC and degenerated into a remnant low 6 h later. The low drifted slowly southwestward across extreme southeastern Alabama and into the western Florida panhandle for the next 12 h. By 0600 UTC 7 October, the remnant low was absorbed by the larger low over the Gulf of Mexico.

Two ships, the *Cordelia* (call sign A8GQ8) and one with the call sign WDC692, located northeast of Tammy's center reported sustained winds of 45 and 44 kt at 0200 UTC and 0300 UTC 6 October, respectively. Also, an automated station run by the Skidaway Institute of Oceanography off the Georgia coast (50-m elevation) reported sustained winds of 45 kt with a gust to 52 kt at 0234 UTC that day (Table 10). The minimum central pressure reported by an AFRC aircraft was 1001 mb at 2005 UTC 5 October. The lowest pressure noted in surface observations was 1002.0 mb at the Mayport, Florida, naval base.

A storm surge of about 2–4 ft caused floods and beach erosion along the coasts and barrier islands of extreme northeastern Florida, Georgia, and South Carolina. Rainfall totals were generally in the 75–125-mm range. However, some isolated rainfall amounts near 250 mm occurred over portions of extreme southeastern Georgia, with a maximum reported total of 367.8 mm at Darien. These rains caused some flood damage. An F0 tornado damaged a hotel roof and snapped trees and power poles near Glynco Airport, Brunswick, Georgia, during the late afternoon of 5 October. The PCS indicates, however, that insured property damage caused by Tammy was less than the catastrophe threshold of \$25 million.

u. Hurricane Vince

Vince originated from the occluded deep-layer frontal low that absorbed the unnamed subtropical storm. This low moved southeastward across the Azores Islands on 6 October. Over the next couple of days, the frontal structure gradually dissipated and banded convection became more concentrated near the circulation center. It is estimated that this convection became sufficiently persistent and organized to designate the cyclone as a subtropical storm near 0600 UTC 8 October, when the system was centered about 500 n mi southeast of Lajes in the Azores (Fig. 1). Although by this time the core convective signature and surface wind field resembled a fully tropical cyclone, the system still had a prominent cold-core cyclonic circulation in the upper-troposphere—hence the subtropical designation.

The subtropical storm initially moved little, but then began to move slowly northeastward on 9 October. AMSU data at 1527 UTC that day showed that a mid-to upper-level warm core was forming, and it is esti-

ated that Vince became a tropical storm near 1200 UTC while over SSTs of 23°–24°C. Later on 9 October a banding eye developed, and Vince became a hurricane near 1800 UTC about 135 n mi northwest of Funchal in the Madeira Islands.

Vince started weakening almost immediately thereafter because of strong westerly shear ahead of an approaching frontal trough. It weakened back to a tropical storm at 0000 UTC 10 October and then accelerated east-northeastward. With convection diminishing and limited to its eastern semicircle, Vince quickly weakened on 10 October as it approached southern Portugal. It weakened to a tropical depression at 0000 UTC 11 October, about 135 n mi west-southwest of Faro, Portugal, although it still maintained some banding structure. The center passed just south of Faro around 0700 UTC that day, and made landfall in Spain near Huelva around 0900 UTC. Vince continued moving rapidly east-northeastward over southern Spain and the circulation dissipated shortly after 1200 UTC 11 October.

Tropical-storm-force gusts were observed at a number of locations in Spain. At the coastline, the Naval Air Station at Rota reported a gust to 42 kt with 10-min average winds of 25 kt at 0930 UTC 11 October. At Moron (87-m elevation), a gust to 40 kt was observed with a sustained wind of 28 kt. Sustained winds of 31 kt were reported at Jerez (27-m elevation) at 1130 UTC, with a gust to 42 kt. It is unclear what effects the local terrain may have had on these observations, as a cluster of ship reports just offshore at 1200 UTC were in the 23–28-kt range. Rainfall totals were mainly less than 50 mm, although 83.9 mm fell at Cordoba. There were no reports of casualties or damages due to Vince, which was the first tropical cyclone of record to make landfall in Spain.

v. Hurricane Wilma

Wilma was an extremely intense hurricane over the northwestern Caribbean Sea. It had the all-time lowest central pressure for an Atlantic basin hurricane, and it devastated the northeastern Yucatan peninsula. Wilma also inflicted extensive damage across southern Florida and Grand Bahama Island.

1) SYNOPTIC HISTORY

Wilma had a complex origin. During the second week of October, an unusually large, monsoon-like lower-tropospheric circulation and a broad area of disturbed weather developed over much of the Caribbean Sea. This system appeared to have been enhanced by an extensive area of diffluent flow south and southwest

TABLE 10. Selected surface observations for Tropical Storm Tammy, 5–6 Oct 2005.

Location	Min sea level pressure		Max surface wind speed			Storm surge (ft) ^c	Storm tide (ft) ^d	Tot rain (mm)
	Date/time (UTC)	Pressure (mb)	Date/time (UTC) ^a	Sustained (kt) ^b	Gust (kt)			
Florida								
Cecil Field Airport (KVQQ)	05/2325	1004.7						
Craig Airport (KCRG)	05/2341	1002.4						
Fernandina Beach								111.8
Gainesville Airport (KGNV)	05/2053	1005.1						
Jacksonville Int. Airport (KJAX)	05/2340	1003.0	05/1020			33		86.6
Jacksonville NAS (KNIP)	05/2242	1002.7						
Mayport Naval Base (KNRB)	05/2253	1002.0	05/1611			36		
St. Augustine Airport (KSGJ)	05/2055 ^e	1002.4	05/1055			34		
St. Johns River I-295 Bridge NOS							2.5	
Vilano Beach NOS							3.0	
Georgia								
Alma Airport (KAMG)	05/0547	1004.7						
Brunswick								210.8
Brunswick/Glynco Airport (KBQK)	06/0020	1005.8	06/0100			38		252.2
Brunswick/McKinnon Airport (KSSI)	06/0050	1004.1	06/0053			40		
Darien								367.8
Nahunta 3E								231.4
Savannah Airport (KSAV)	06/1609	1007.5						112.8
Woodbine								233.9
South Carolina								
Charleston Airport (KCHS)	06/1557	1008.8	05/1619	28	35			92.2
Downtown Charleston (unofficial)			05/1948			43		90.9
Charleston Harbor							2.6	
Fripp Island							3.3	
South Capers Island							2.5	
Buoys/C-MAN/NOS								
Fernandina Beach, FL, NOS (30.7°N, 81.5°W)	06/0000	1002.4					3.2	
Folly Beach, SC, C-MAN (32.7°N, 79.9°W)			05/2030	35 ^f	48			
Fort Pulaski, GA, NOS (32.0°N, 80.9°W)			06/0200	38	45	4.2		
Mayport, FL, NOS (30.4°N, 81.4°W)	05/2242	1002.2	05/1700			34	2.3	
Slidaway Tower M2R6 C-MAN (31.5°N, 80.2°W)	05/2300	1008.0	06/0234	45	52			
Slidaway Tower R2 C-MAN (31.3°N, 80.6°W)			06/0231 ^c	43	47			
Slidaway Tower R8 C-MAN (31.6°N, 79.9°W)	06/0129	1007.9	06/0229 ^e	41	52			
St. Augustine, FL, C-MAN (28.9°N, 81.2°W)	05/2000	1002.9	05/0851			37		
Buoy 41002, NOAA (32.3°N, 75.4°W)			05/1559			36		
Buoy 41004, NOAA (32.5°N, 79.1°W)			06/1113	37 ^f	47			
Buoy 41008, NOAA (31.4°N, 80.9°W)	06/0100	1005.8	06/0054			44		
Buoy 41012, NOAA (31.4°N, 80.9°W)	05/2100	1003.7	05/1000			38		

^a Date/time is for sustained wind when both sustained and gust are listed.

^b Except as noted, sustained wind-averaging periods for land-based ASOS reports are 2 min.

^c Storm surge is water height above normal astronomical tide level.

^d Storm tide is water height above National Geodetic Vertical Datum (1929 mean sea level).

^e Last of several occurrences.

^f 10-min average.

of an upper-level cyclone over the southwestern Atlantic. The easternmost portion of this low pressure area moved northeastward and merged with an extratropical cyclone. However, a more concentrated area of disturbed weather and surface low pressure formed near Jamaica by 14 October, possibly aided by a couple of

tropical waves traversing the Caribbean during this time. By 1800 UTC 15 October, the surface circulation became well defined, with sufficiently organized deep convection, to mark the formation of a tropical depression about 190 n mi east-southeast of Grand Cayman (Fig. 1).

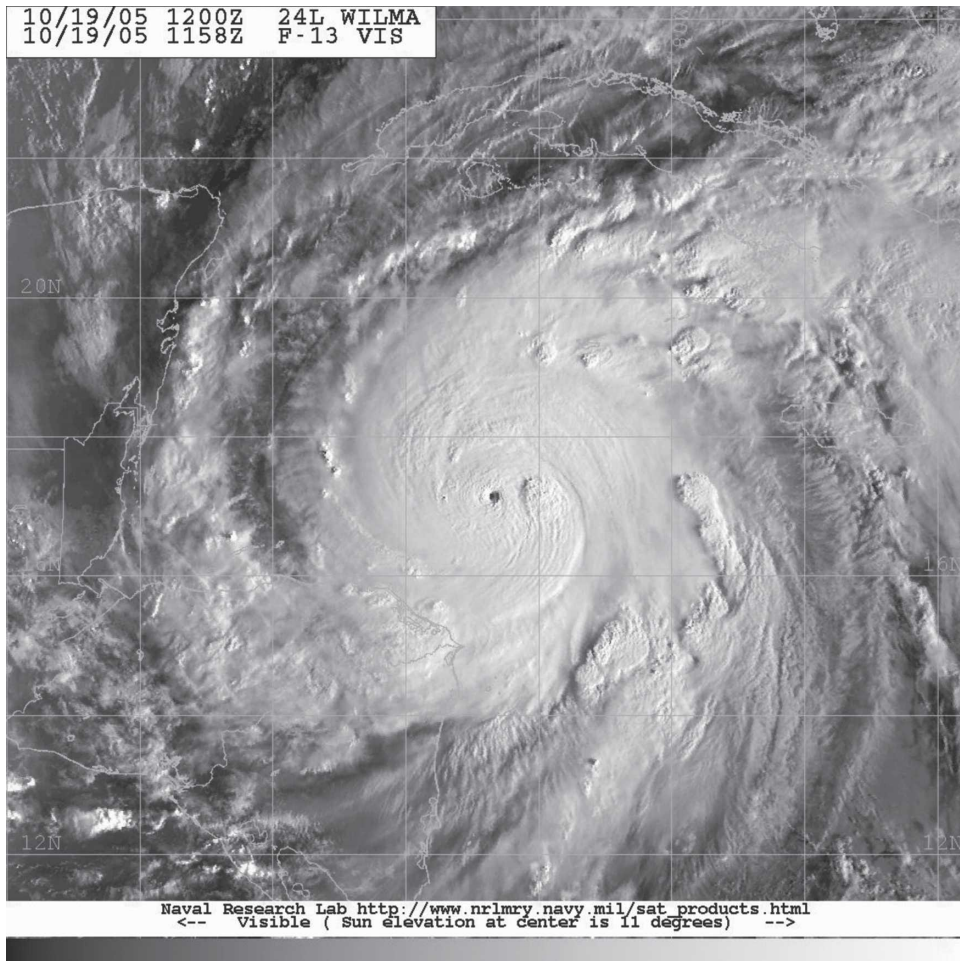


FIG. 10. Defense Meteorological Satellite Program (DMSP) *F-13* visible image of Hurricane Wilma near maximum intensity at 1158 UTC 19 Oct 2005. Image courtesy of the NRL, Monterey, CA.

A weak and ill-defined steering flow prevailed for the first couple of days, with a 500-mb high covering the Gulf of Mexico and another midtropospheric anticyclone located well east-northeast of the tropical cyclone. The depression moved slowly and erratically westward to west-southwestward for a day or so and then drifted south-southwestward to southward for a day or two. There was only slow strengthening during this period, and the system is estimated to have become a tropical storm at 0600 UTC 17 October. On 18 October Wilma turned toward the west-northwest and strengthened into a hurricane. Later that day, a remarkable, explosive strengthening episode began. During the 24 h ending at 0600 UTC 19 October, Wilma intensified from a 60-kt tropical storm to a 150-kt category 5 hurricane, representing an unprecedented intensification for an Atlantic tropical cyclone. Wilma reached its estimated peak sustained wind speed of 160 kt at around 1200 UTC 19 October (Fig. 10). During the

strengthening episode, AFRC aircraft observations indicated that the eye of the hurricane contracted to a diameter of 2 n mi; this is the smallest eye known to NHC staff. The estimated minimum central pressure at the time of peak intensity is 882 mb, which is a new record low value for a hurricane in the Atlantic basin. As discussed below, the actual minimum pressure may have been lower.

Wilma maintained category 5 status until 20 October, when its winds decreased to 130 kt (category 4), and the tiny eye was replaced by one about 40 n mi across. The hurricane would retain an eye of about 40 to 60 n mi in diameter for most of the remainder of its lifetime. By 21 October, as midlevel ridging northeast of Wilma increased somewhat and a series of short-wave troughs in the westerlies began to erode the high over the Gulf of Mexico, the hurricane turned toward the northwest and north-northwest, taking aim at the Yucatan peninsula of Mexico. Wilma's maximum winds remained near 130

kt when its center made landfall on the island of Cozumel around 2145 UTC 21 October, and it was still category 4 when it crossed the coast of the Yucatan peninsula about 6 h later. On 22 October, the midtropospheric high pressure area north of Wilma dissipated, and the hurricane moved slowly northward, crossing the extreme northeastern Yucatan peninsula. Wilma emerged into the southern Gulf of Mexico around 0000 UTC 23 October, with maximum winds of near 85 kt. Although Wilma's intensity had been reduced because of its passage over land, it was still a large and powerful hurricane.

A vigorous midtropospheric trough, moving eastward from the central United States, provided a southwesterly steering current that accelerated Wilma northeastward toward southern Florida. As the upper-level flow over the hurricane increased, so too did the vertical shear, and by early on 24 October the environmental 850–200-mb shear (averaged over an annulus about 100 to 400 n mi from the center) was roughly 25 kt. Despite the strong shear in its surroundings, Wilma strengthened to 110 kt as it approached Florida. Maximum sustained winds were estimated to be near 105 kt (category 3) at landfall in southwestern Florida near Cape Romano around 1030 UTC 24 October. Accelerating further, the hurricane crossed the southern Florida peninsula in 4.5 h, with the center emerging into the Atlantic just southeast of Jupiter around 1500 UTC. Maximum winds decreased to near 95 kt (category 2) during the crossing of Florida. A vigorous cold front associated with the midtropospheric trough swept across the area west of Wilma, yet the cooler and drier air behind the front could not fully penetrate the inner core of the hurricane to weaken it. Upon reaching the Atlantic, the hurricane reintensified one last time, and its winds again reached 110 kt around 0000 UTC 25 October. Thereafter, Wilma weakened because of an unfavorable atmospheric environment while racing northeastward at 40–50 kt. It became extratropical around 0000 UTC 26 October while centered about 200 n mi southeast of Halifax, Nova Scotia. This extratropical low was absorbed by another extratropical cyclone located over eastern Nova Scotia around 0000 UTC 27 October.

2) METEOROLOGICAL STATISTICS

Near the time of peak intensity, the AFRC aircraft measured a 700-mb flight-level wind of 168 kt wind in the southeastern eyewall at 0610 UTC 19 October. Using the standard 90% adjustment yields a surface wind of 151 kt. Since the central pressure was still falling when the aircraft last passed through the eye at 0801 UTC, it is likely that the winds also increased from then

until 1200 UTC. Therefore the peak intensity of Wilma is estimated to be 160 kt at 1200 UTC that day. When Wilma was over the southeastern Gulf of Mexico, the AFRC measured a 700-mb wind of 135 kt at 0646 UTC 24 October, apparently associated with a short-lived mesocyclone in the southeastern eyewall. Because of tilting of the eyewall convection by strong southwesterly shear, the ratio of surface to flight-level winds was probably less than normal. Therefore, the adjustment for 700-mb flight-level winds is reduced from the normal 90%–80%, resulting in an estimated intensity of 110 kt at 0600 UTC 24 October. Later aircraft and radar data in the southeastern eyewall showed that the winds had diminished somewhat, so the intensity of Wilma at landfall in southwestern Florida was assessed at 105 kt.

Wilma deepened at an incredible rate during 18–19 October. Over the period from 1954 to 0801 UTC, the aircraft-measured central pressure fell from 970 to 882 mb (7.3 mb h^{-1}), and over the period from 2310 to 0433 UTC, the aircraft-measured central pressure fell from 954 to 901 mb (9.9 mb h^{-1}). The largest 6-, 12-, and 24-h drops in *best-track* central pressure for Wilma, 54 mb from 0000 to 0600 UTC 19 October, 83 mb from 1800 UTC 18 October to 0600 UTC 19 October, and 97 mb from 1200 UTC 18 October to 1200 UTC 19 October, respectively, are by far the largest in the available records for these periods going back to 1851. The previous record 6-h deepening was 38 mb in Hurricane Beulah, September 1967 (Sugg and Pelissier 1968), the previous record 12-h deepening was 48 mb in Hurricane Allen, August 1980 (Lawrence and Pelissier 1981), and the previous record 24-h deepening was 72 mb in Hurricane Gilbert, September 1988 (Lawrence and Gross 1989).

The minimum central pressure measured by dropsondes was 884 mb at 0801 UTC 19 October. Surface winds from these dropsondes were measured to be 23 kt, so the dropsondes probably did not capture the lowest pressure in Wilma's eye. Therefore the pressure at that time was estimated at a slightly lower 882 mb. Given that the pressure was still falling, it is possible that the pressure then dropped a little below 882 mb.

Selected surface observations from land stations and data buoys are given in Table 11. During Wilma's landfalls in Mexico, Cancun observed a 10-min average wind of 87 kt with a gust to 113 kt, but it is not certain if these were the maximum values at that station. Islas Mujeres, near Cancun, experienced hurricane-force winds in gusts for nearly a 24-h period on 21–22 October.

The highest sustained wind measured at an official surface observing site in Florida was a 15-min average speed of 80 kt from a South Florida Water Manage-

ment District (SFWMD) observation site in Lake Okeechobee. It should be noted that another SFWMD platform located only about 5 n mi to the north recorded a 15-min wind speed of 79 kt at the same time. It is reasonable to assume that these measurements correspond to a peak 1-min average wind speed of at least 90 kt. Several ASOS sites in Miami-Dade and Broward Counties stopped reporting data at their highest noted sustained wind speeds, such as Opa-Locka Airport at 74 kt and Pompano Beach Airport at 72 kt. Stronger winds likely occurred at these sites. Data from the NWS Miami radar indicated a peak velocity of 138 kt at an elevation of about 1500 m over western Broward County. A comparison of Doppler velocities with collocated, official 2- and 1-min surface wind measurements in Miami-Dade and Broward Counties suggests that the ratios of surface to 1500-m sustained wind velocities over southeastern Florida in Wilma were likely in the range of 0.65–0.70. This results in a maximum surface wind speed estimate of 90–95 kt.

Based on the surface and radar data, most of the southeastern Florida peninsula experienced at least category 1 hurricane conditions, and that some parts of northern Miami-Dade County, Broward, and Palm Beach Counties likely had category 2 hurricane conditions, including wind gusts to near 100 kt, at the standard 10-m height above ground.

A storm surge of 4–8 ft was reported from coastal Collier County. It is likely, however, that higher storm surges occurred over uninhabited areas of southwestern Florida south of where Wilma made landfall. Storm surges of 4–5 ft were observed over much of the lower and middle Florida Keys, locally to near 7 ft. However, a storm surge of near 9 ft was estimated visually in the Marathon area. Storm surges were generally in the 4–5-ft range over the upper keys. These resulted in flooding over substantial portions of the keys. Relatively minor storm surge flooding occurred on the Biscayne Bay shoreline of Dade County. Storm surges of 12 ft or more were measured along the southwestern coast of Grand Bahama Island.

Wilma produced torrential rainfall as it moved slowly over portions of the eastern Yucatan peninsula. According to the Meteorological Service of Mexico, a 24-h rainfall total of 1576.1 mm occurred at Islas Mujeres. Because the hurricane moved quickly across the Florida peninsula, however, the rain amounts there were on average not very large. Storm totals ranged generally from 75–175 mm, with a maximum reported total of 336.8 mm at the Kennedy Space Center. Some locations in southeast Florida had totals of not more than 25–50 mm.

Wilma produced 10 tornadoes over the Florida pen-

insula on 23–24 October: one each in Collier, Hardee, Highlands, Indian River, Okeechobee, and Polk Counties, and four in Brevard County.

3) CASUALTY AND DAMAGE STATISTICS

Twenty-three deaths have been directly attributed to Wilma: 12 in Haiti, 1 in Jamaica, 4 in Mexico, 5 in Florida, and 1 in the Bahamas on Grand Bahama Island.

Very severe damage was reported in portions of the northeastern Yucatan peninsula, which dealt a major blow to the tourist industry in that area. Major flooding from storm surge and/or wave action occurred in portions of western Cuba. In southern Florida, damage was unusually widespread, including numerous downed trees, substantial crop losses, downed power lines and poles, broken windows, extensive roof damage, and destruction of mobile homes. Wilma caused the largest disruption to electrical service ever experienced in Florida. Media reports indicate up to 98% of south Florida lost electrical service, and Florida Power and Light reported outages in 42 Florida counties. The total insured damage compiled by the PCS is \$10.3 billion. The total property damage in the United States is thus estimated at \$20.6 billion, making Wilma the third costliest hurricane in United States history, behind only Katrina and Andrew. Significant damage also occurred in the southwestern coastal area of Grand Bahama Island, with widespread destruction of roofs and vehicles along with toppling of poles and trees.

w. Tropical Storm Alpha

Alpha was first Atlantic tropical cyclone ever to be named from the Greek alphabet, as all the names on the standard list had been exhausted. It formed from a tropical wave that reached the Windward Islands on 19 October. Satellite images and surface observations indicated that a low pressure center associated with the wave formed near Barbados and moved toward the west-northwest with increasing convective activity. Under light shear, the shower activity became concentrated, and it is estimated that a tropical depression formed at 1200 UTC 22 October about 180 n mi southwest of San Juan, Puerto Rico (Fig. 1). The depression strengthened while heading toward the south coast of Hispaniola and became a tropical storm 6 h later. Alpha reached its maximum intensity of 45 kt and a minimum pressure of 998 mb at 0600 UTC 23 October.

The cyclone made landfall near the town of Barahona in the Dominican Republic about 1000 UTC 23 October. Thereafter, Alpha weakened to a tropical depression while crossing the high terrain of Hispaniola.

TABLE 11. (Continued)

Location	Min sea level pressure		Max surface wind speed			Storm surge (ft) ^c	Storm tide (ft) ^d	Tot rain (mm)
	Date/time (UTC)	Pressure (mb)	Date/time (UTC) ^a	Sustained (kt) ^b	Gust (kt)			
Florida								
Vandenburg (KVDF)			24/1654	23	36			
Venice								189.2
Vero Beach (KVRB)	24/1531	975.3	24/1353	35 ^f	48 ^f			140.5
Vero Beach COOP								139.7
Vilano Beach NOS			24/1800	27	37	1.77		
West Palm Beach (KPBI)	24/1225	975.0	24/1310	71	88			27.2
West Kendall Tamiami (KTMB)	24/1152	970.5	24/1133	50 ^f	72 ^f			30.0
Winter Haven (KGIF)	24/1236	995.3	24/1630	31	40			121.2
Buoy/C-MAN								
Anclote Key, FL, COMPS (28.2°N, 82.8°W)			24/1054	37	47			
Big Carlos Pass, FL, COMPS (26.4°N, 81.9°W)	24/1054	969.2	24/1054	56	76			
Clearwater Beach, FL, NOS (28.0°N, 82.8°W)			24/1400	41	48			
Cedar Key, FL, C-MAN (29.1°N, 83.0°W)	24/1100	1003.2	24/1650	20 ^e	33			
Duck Pier, NC, C-MAN (36.2°N, 75.7°W)	24/2200	998.4	24/2130	37				
Fowey Rocks, FL, C-MAN (25.6°N, 80.1°W)	24/1243	975.3	24/1159	88	107			
Fort Myers, FL, NOS (26.7°N, 81.9°W)			24/1242	46	62			
Fred Howard Park, FL, COMPS (28.2°N, 82.8°W)			24/1154	39	49			
Homosassa, FL, COMPS (28.8°N, 82.8°W)	24/1754	1001.0	24/1654	31	37			
Key West, FL, NOS (24.6°N, 81.8°W)	24/0818	977.2	24/0836	51	74	2.76		
Isle of Shoals, NH, C-MAN (43.0°N, 70.6°W)	25/1600	995.4	25/1600	46				
Long Key, FL, C-MAN (24.8°N, 80.9°W)	24/1100	982.2	24/0930	57 ^e	76	4.0		
Mt. Desert Rock, ME, C-MAN (44.0°N, 68.1°W)	25/1700	997.1	25/1700	49				
Matinicus Rock, ME, C-MAN (43.8°N, 68.9°W)	25/1700	997.1	25/1400	45				
Molasses Reef, FL, C-MAN (25.0°N, 80.4°W)	24/1200	982.3	24/1220	66 ^e	81			
Naples, FL, NOS (26.1°N, 81.8°W)	24/1024	960.9	24/1200	73	89	2.64		
Port Richey, FL, COMPS (28.3°N, 82.7°W)			24/1654	25	37			
St. Augustine, FL, C-MAN (29.9°N, 81.3°W)	24/2005	999.9	24/1440	35 ^e	44			
Settlement Point, GBI, C-MAN (26.7°N, 79.0°W)	24/1600	969.9	24/1600	83	103			
Sombrero Key, FL, C-MAN (24.6°N, 81.1°W)	24/1000	983.4	24/0920	76 ^e	91	2.1		
Tyndall AFB Tower, FL, C-MAN (29.4°N, 89.9°W)	24/1100	1007.3	24/1400	40				
Slidaway Tower R8 C-MAN (31.6°N, 79.9°W)	24/2128	996.0	24/2128	35				
Vaca Key, FL, NOS (24.7°N, 81.1°W)	24/0924	983.0	24/1412		52	6.43		
Venice, FL, C-MAN (27.1°N, 82.4°W)	24/1100	990.0	24/1500	44	55			
Virginia Key, FL, NOS (25.7°N, 80.2°W)	24/1300	972.4	24/1318	65	87	3.61		
Woods Hole, MA, C-MAN (41.4°N, 71.0°W)	25/1700	989.0	25/1300	48				
Buoy 41009, NOAA (28.5°N, 80.2°W)	24/1720	985.2	24/1720	52	68			
Buoy 41010, NOAA (29.0°N, 78.5°W)	24/1950	969.5	24/2050	62	82			
Buoy 41012, NOAA (30.0°N, 80.6°W)	24/1950	995.3	24/1950	37	45			
Buoy 42003, NOAA (26.1°N, 85.9°W)	23/2050	997.8	24/1020	36 ^e	47			
Buoy 42013, COMPS (27.2°N, 83.0°W)	24/1010	993.1	24/1110	41	49			
Buoy 42023, COMPS (26.1°N, 83.1°W)	24/0759	982.5	24/0959	49				
Buoy 42036, NOAA (28.5°N, 84.5°W)	24/1150	1002.3	24/0850	37	43			
Buoy 42056, NOAA (19.9°N, 85.1°W)	21/0800	986.6	21/0416	67	81			
Buoy 42057, NOAA (17.6°N, 80.7°W)	18/2200	998.1	19/0600	50	59			
Buoy 44004, NOAA (38.5°N, 70.5°W)	25/0050	1002.1	25/0050	37				
Buoy 44005, NOAA (43.2°N, 69.2°W)	25/1750	992.4	25/1650	39				
Buoy 44007, NOAA (43.5°N, 70.1°W)	25/1650	997.6	25/1650	35				
Buoy 44008, NOAA (40.5°N, 69.4°W)	25/1350	984.9	25/1350	39				

TABLE 11. (Continued)

Location	Min sea level pressure		Max surface wind speed			Storm surge (ft) ^c	Storm tide (ft) ^d	Tot rain (mm)
	Date/time (UTC)	Pressure (mb)	Date/time (UTC) ^a	Sustained (kt) ^b	Gust (kt)			
Buoy/C-MAN								
Buoy 44009, NOAA (38.5°N, 74.7°W)	25/0650	989.1	25/0750	37				
Buoy 44013, NOAA (42.4°N, 70.7°W)	25/1650	993.8	25/1550	37				
Buoy 44017, NOAA (40.7°N, 72.0°W)	25/1550	988.1	25/1250	41				
Buoy 44018, NOAA (41.3°N, 69.3°W)	25/1350	987.4	25/1450	37				
Buoy 44025, NOAA (40.3°N, 73.2°W)	25/1450	988.7	25/0950	39				
Buoy 44027, NOAA (44.3°N, 67.3°W)	25/1750	997.5	25/1750	39				
Buoy 44034, GOMOOS (44.1°N, 68.1°W)	25/1704	999.9	25/1704	35				
Buoy 44142, Canadian (42.5°N, 64.0°W)	25/1700	992.4	25/1700	37				

^a Date/time is for sustained wind when both sustained and gust are listed.

^b Except as noted, sustained wind-averaging periods for land-based ASOS reports are 2 min.

^c Storm surge is water height above normal astronomical tide level.

^d Storm tide is water height above National Geodetic Vertical Datum (1929 mean sea level).

^e 10-min average.

^f Instrumentation failed.

The cyclone turned toward the north-northwest and then north over the southeastern Bahamas and the Atlantic, and never regained tropical storm strength. It was absorbed by the much larger circulation of Hurricane Wilma over the western Atlantic at 0000 UTC 25 October.

According to the Meteorological Service of the Dominican Republic, Barahona reported a 1-min average wind of 45 kt as the center of Alpha made landfall. The highest reported rainfall total was 200.7 mm at Las Americas. Media reports indicate that Alpha killed 17 people in Haiti and 9 in the Dominican Republic, primarily from mudslides caused by heavy rains. Floods and mudslides damaged or destroyed at least 400 homes in Haiti.

x. Hurricane Beta

After pounding the island of Providencia, Beta struck a sparsely settled area of Nicaragua with maximum sustained winds near 90 kt.

1) SYNOPTIC HISTORY

Analysis of geostationary satellite imagery indicates Beta formed from the same tropical wave that produced Tropical Storm Alpha. After Alpha formed, the wave continued westward, and by 25 October deep convection consolidated somewhat over the extreme southwestern Caribbean Sea. On 26 October, curved banding features developed, and the system gained sufficient organization by 1800 UTC that day to designate the formation of a tropical depression, centered about 90 n mi north of the northern central coast of Panama (Fig. 1).

Initially the motion was northwestward, but in re-

sponse to a midtropospheric short-wave trough over the southern Gulf of Mexico and a midtropospheric ridge well to the east-northeast, the system gradually turned toward the north. Within an environment of weak vertical wind shear and SSTs of at least 29°C, the cyclone strengthened into a tropical storm around 0600 UTC 27 October. Only slow strengthening occurred over the ensuing 36 h or so, probably due to disruption of the system by weak to moderate northeasterly shear. Beta intensified into a hurricane shortly after 0000 UTC 29 October near Isla de Providencia. As the Gulf of Mexico short-wave trough lifted northeastward and a midtropospheric high built to the north and northwest of the hurricane, Beta turned toward the west and west-southwest and continued to strengthen. The strengthening rate increased around 0000 UTC 30 October, and Beta reached an estimated peak intensity of 100 kt (category 3) about 6 h later (Fig. 11), the seventh and last major hurricane of the season. Moving southwestward, the center of the hurricane made landfall near La Barra del Rio Grande on the central coast of Nicaragua around 1200 UTC 30 October. Shortly before landfall, warming of the central cloud tops suggested weakening, and the landfall intensity is estimated to have been 90 kt (category 2). Beta turned back toward the west and dissipated over west-central Nicaragua by 0600 UTC 31 October.

2) METEOROLOGICAL STATISTICS

The highest 700-mb flight-level winds measured by AFRC aircraft were 77 kt at 2003 UTC 29 October. However, just after the aircraft left the area, microwave imagery showed that the eye contracted, and Dvorak

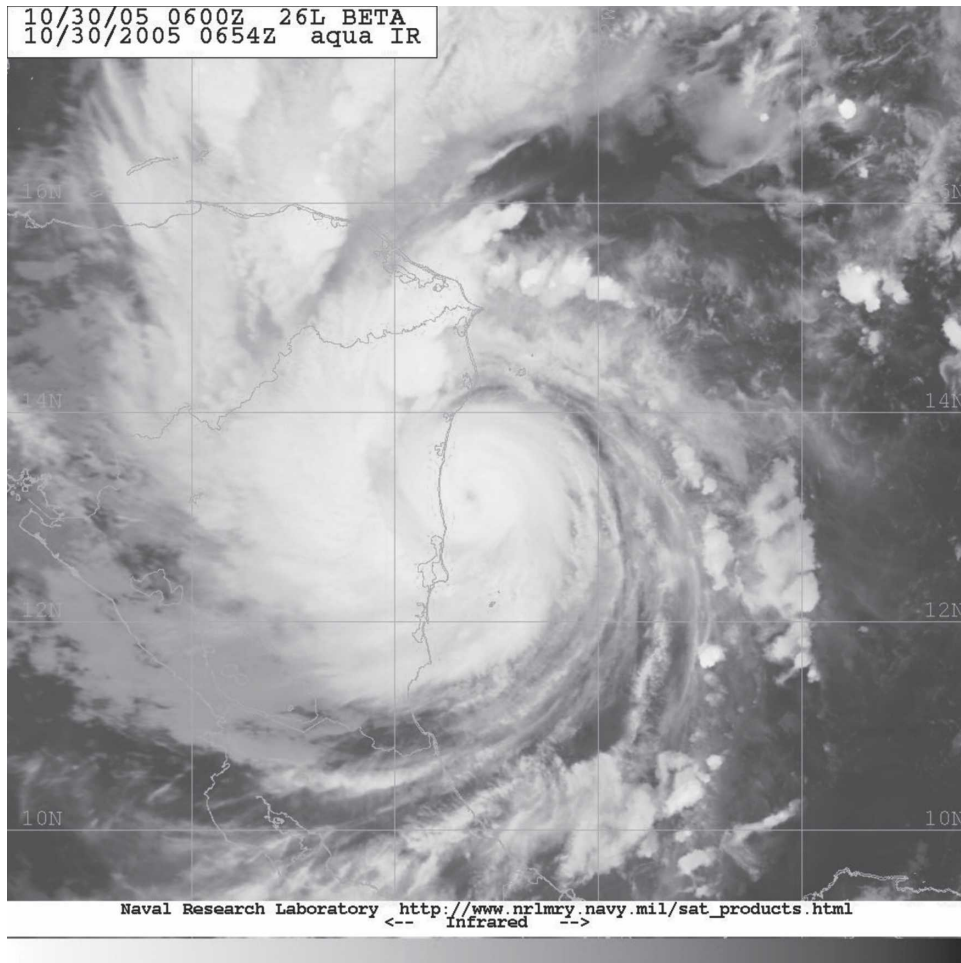


FIG. 11. *Aqua* MODIS infrared image of Hurricane Beta near maximum intensity at 0654 UTC 30 Oct 2005. Image courtesy of the NRL, Monterey, CA.

estimates indicate that Beta strengthened rather rapidly from 0000 to 0600 UTC 30 October.

Aircraft flight-level wind data and satellite images indicate that Beta was a small tropical cyclone; the radius of tropical-storm-force winds was generally 50 n mi or less. Despite the small size, two ships reported tropical-storm-force winds from Beta. The *Edyth L* (call sign ZCAM4) reported 50-kt winds at 0900 UTC 28 October, while the *Dioli* (call sign PJRP) reported 39-kt winds at 0600 UTC 30 October.

Rainfall totals as high as 250–500 mm were observed over portions of Honduras, with a maximum total of 554.2 mm at Trujillo. However, it is not certain whether all of these rains were directly associated with Beta. There are no meteorological reports available near the point of landfall in Nicaragua. Puerto Cabezas, Nicaragua, had a storm-total rainfall of 162.3 mm with 131.1 mm falling in a 6-h period on 29 October.

3) CASUALTY AND DAMAGE STATISTICS

Beta reportedly caused extensive damage on the Colombian island of Providencia; however, details of these impacts are unknown. The government of Nicaragua reported roofs were removed from numerous dwellings as well as moderate storm-surge flooding near the landfall location. Major flooding occurred in Honduras, but it cannot be determined how much of it was directly associated with Beta. There are no reported deaths due to Beta.

y. Tropical Storm Gamma

A vigorous tropical wave moved westward from the coast of Africa on 3 November. For such a late-season system, the wave maintained an unusually large amount of deep convection along and east of the wave axis until reaching the Windward Islands on 13 November. The system produced gusty winds and locally heavy rainfall

as it passed the southern Windward Islands. A broad and poorly defined low developed late that same day over the extreme southeastern Caribbean Sea. Deep convection, previously displaced eastward by moderate shear, now persisted close to the center of the low, and it is estimated that a tropical depression formed at 0000 UTC 14 November about 85 n mi west of St. Vincent (Fig. 1).

The depression continued westward and became better organized despite moderate westerly shear. It is estimated that the cyclone became a tropical storm at 0600 UTC 15 November. Increasing westerly shear caused Gamma to weaken to a depression by 1800 UTC that same day, however, and to degenerate into a tropical wave 24 h later about 265 n mi southeast of Jamaica. A deep-layer subtropical ridge over the southwestern Atlantic Ocean and Gulf of Mexico forced the remnants of Gamma quickly westward across the central Caribbean Sea before the system decelerated over the western Caribbean Sea and eastern Honduras on 17 November.

While the remnants of Gamma crossed the Caribbean, a broad but well-defined low pressure system formed over Panama. This low moved northwestward over the southwestern Caribbean Sea and into northeastern Nicaragua on 16 November. It continued across Nicaragua and merged or interacted with the remnants of Gamma over the mountainous terrain of east-central Honduras early on 18 November. It is estimated that Gamma regenerated into a tropical storm at 1800 UTC that day along the northern coast of Honduras near Limon. While the other low likely aided the regeneration of Gamma, it is difficult to determine which circulation became predominant because of the complex interaction over the elevated terrain of interior Honduras. However, deep convection associated with the remnants of Gamma maintained continuity throughout its lifetime, and it is estimated that the low-level circulation of the other low merged with the remnant low- to midlevel circulation of Gamma.

Gamma drifted northward over the northwestern Caribbean Sea and slowly strengthened, reaching its peak intensity of 45 kt while centered just east of Roatan Island at around 1200 UTC 19 November. Later that day, Gamma drifted eastward, and on 20 November it moved more quickly to the southeast. Moderate southerly shear gradually became northwesterly and displaced most of the convection well southeast of the center. This caused Gamma to weaken to a depression around 1200 UTC that day. The cyclone continued to rapidly weaken and degenerated into a remnant low early on 21 November, and dissipated by 0600 UTC on 22 November just east of Honduras–Nicaragua border.

A private weather station on Roatan Island, Honduras, reported a 1-min wind of 43 kt at 0730 UTC 19 November. There were no ship observations from Gamma while it was a tropical cyclone, although an unidentified ship and NOAA buoy 42057 both reported 35-kt winds associated with the tropical wave.

Reports from the government of Honduras and news media indicate a total of 37 deaths associated with Tropical Storm Gamma: 34 in Honduras and 3 in Belize. The deaths resulted from flash floods and mud slides caused by heavy rain. In addition, 13 people were reported missing in Honduras. News reports from the Associated Press further indicate that “Gamma’s rains and winds affected more than 100, 000 Hondurans, damaging their homes, cutting off their electricity, and leaving them without food and water.” The flooding destroyed 10 bridges and damaged 7 more in Honduras, and decimated more than 5200 acres of banana crops. Reports from private companies indicate banana crop losses were \$13–18 million (U.S. dollars).

z. Tropical Storm Delta

Delta had a nontropical origin. A broad area of low pressure formed on 19 November about 1200 n mi southwest of the Azores. The system moved generally east-northeastward through 20 November while in the vicinity of a cold front trailing from another low to the north. The pre-Delta low then turned northeastward on 21 November while it started developing central convection. By 0900 UTC 22 November, QuikSCAT data indicated the formation of an inner wind maximum, while AMSU data indicated the formation of an upper-level warm core. These data indicated the low was acquiring some tropical cyclone characteristics. By 1800 UTC that day, satellite imagery indicated the low had become more isolated from the frontal cloud bands, and it is estimated that a subtropical storm formed about that time when centered about 755 n mi southwest of the Azores (Fig. 1).

The storm moved little early on 22 November, but began a south-southwestward motion late that day. The convection consolidated, and it is estimated that Delta became a tropical storm near 1200 UTC 23 November. Delta turned southeastward late on 23 November and then stalled on 24 November about 1150 n mi west-southwest of the Canary Islands. The cyclone reached a first estimated peak intensity of 60 kt by 1200 UTC that day. Delta moved southwestward on 25 November, followed by turns toward the southeast and east-northeast on 26 November. Increasing vertical wind shear caused weakening during this time, with the maximum winds decreasing to an estimated 35 kt.

Delta accelerated east-northeastward on 27 November in response to an intensifying deep-layer trough over western Europe. This was accompanied by reintensification, with the short-lived formation of a ragged eye near 1200 UTC. It is estimated that the maximum winds again reached 60 kt at that time. The cyclone turned east-northeastward on 28 November while it moved into the surface baroclinic zone associated with the European trough. A combination of increasing vertical shear and cold air entrainment caused Delta to lose tropical characteristics, and it is estimated it became extratropical about 1200 UTC 28 November about 215 n mi west-northwest of the western Canary Islands. The extratropical storm continued eastward, with the center passing about 90 n mi north of the Canary Islands later that day. It moved eastward into Morocco early on 29 November and then accelerated east-northeastward across Morocco and rapidly weakened. The cyclone dissipated late on 29 November over northwestern Algeria.

Several ships encountered Delta, particularly during its early life when it had a large cyclonic envelope. The strongest winds were from the *British Merchant* (call sign VQIB9), which reported 60-kt winds and a 990.8-mb pressure at 1800 UTC 27 November. Additionally, a drifting buoy reported a pressure of 984.4 mb at 0200 UTC 23 November. Delta did not affect land as a tropical or subtropical storm. However, as an extratropical low, it hit the Canary Islands hard. A station on Tenerife reported sustained winds of 63 kt with a gust of 79 kt at 2130 UTC 28 November, while a station on La Palma reported a gust to 82 kt at 2000 UTC. The Izaña Observatory (2367-m elevation) reported sustained winds of 98 kt with a gust to 134 kt at 2031 UTC.

Based on the ragged eye, and on the 60-kt ship report in what would normally be the weaker side of an east-northeastward-moving tropical cyclone, it is possible that Delta briefly reached hurricane strength on 27 November. However, the data were not conclusive enough to justify an after-the-fact upgrade.

There were no reports of damage or casualties associated with Delta as a tropical or subtropical storm. However, as an extratropical low, the former Delta was responsible for seven deaths in and near the Canary Islands. This included 6 people who drowned when their boat overturned, with 12 people from the boat reported missing. The winds caused widespread power outages in the Canary Islands.

aa. Hurricane Epsilon

Late on 27 November a surface gale center developed beneath a nontropical upper-level low about 1000 n mi east of Bermuda. At this time a stationary front

extended from just north of the surface low eastward to near Tropical Storm Delta, which was then beginning to lose tropical characteristics. The surface low began to separate from the frontal zone the following day, but as it did so the associated nonfrontal convection was limited and poorly organized. Early on 29 November, however, deep convection developed just north of the surface low center, and by 1500 UTC had wrapped completely around the center into a ring not more than 40 n mi across. Based on this organized core convection, and a presumed collocated radius of maximum wind, it is assessed that the low became a tropical storm near 0600 UTC 29 November (Fig. 1).

After becoming a tropical storm, Epsilon moved west-southwestward along the southern periphery of a high-latitude ridge. Initially, Epsilon was embedded within the upper low from which it formed, and this provided a weak shear and unstable environment conducive to modest strengthening. Epsilon developed a ragged eye and its winds reached 55 kt on 30 November. Still embedded within the upper low, Epsilon then executed a cyclonic loop on 1 December with little change in strength as a deep-layer trough approached from the western Atlantic. The upper low then weakened, leaving Epsilon in a light west-southwesterly flow ahead of the approaching trough. Moving northeastward, Epsilon strengthened over 22°C waters and became a hurricane at 1800 UTC 2 December, about 850 n mi east-northeast of Bermuda. This made Epsilon only the sixth hurricane of record in the month of December.

Epsilon turned eastward on 3 December, remaining south of the main belt of strong westerlies. Anticyclonic outflow developed in the northern semicircle and the hurricane took on an annular appearance with a 30–35 n mi diameter eye. Little change in structure or strength occurred over the next two days as Epsilon moved slowly eastward over cool waters, with an estimated peak intensity of 75 kt occurring early on 5 December. Late that day, the frontal zone associated with the deep-layer trough passed just north of Epsilon, and with high pressure building behind this trough, Epsilon's eastward motion slowed. Epsilon turned southwestward to the south of the building ridge on 6 December, while maintaining its strength and eye structure. The next day, strong upper-level northwesterly flow disrupted the eye and displaced the deep convection southeast of the center. After spending five days as a hurricane—a record for December—Epsilon weakened to a tropical storm at 1800 UTC 7 December about 800 n mi southwest of the Azores. Strong shear continued and stripped Epsilon of its deep convection early on 8 December. Epsilon weakened to a tropical

depression at 1200 UTC that day and degenerated to a remnant low by 1800 UTC. On 9 December, the remnant circulation became elongated in advance of an approaching frontal zone and the circulation dissipated later that day.

The development of Epsilon into a hurricane over sea surface temperatures of 22°C is unusual, but not unprecedented. In 1980, Hurricane Ivan formed over 23°C sea surface temperatures, while Hurricane Karl formed over 20°C sea surface temperatures (Lawrence and Pelissier 1981).

bb. Tropical Storm Zeta

Zeta resulted from the interaction between a weakening frontal boundary and an upper-tropospheric trough. By 28 December, the trough had cut off and evolved into an upper-level low centered about 650 n mi west-northwest of the Cape Verde Islands. A weakening front extended from northeast to southwest beneath the upper-level low. A surface low formed on 29 December about 675 n mi northwest of the Cape Verde Islands, aided by diffluence just northwest of the center of the upper-level low. Late that day, thunderstorm activity increased near the center of the surface low, and it is estimated that the system gained sufficient organization to be designated a tropical depression at 0000 UTC 30 December (Fig. 1). Convective banding wrapped around the low-level center, and the cyclone became a tropical storm 6 h later.

Initially, Zeta moved slowly northwestward around a midlevel low to its southwest. A weak low- to midlevel ridge to its north forced Zeta to turn westward on 31 December, but upper-level westerlies slowed its forward motion. This westerly shear stripped Zeta of nearly all its deep convection by the end of the day. Convection soon returned, however, as Zeta was located beneath an upper-level diffluent region, albeit one with some persistent westerly shear. Zeta drifted southwestward on 1 January and first reached its estimated peak intensity of 55 kt at 1800 UTC that day about 900 n mi northwest of the Cape Verde Islands.

Zeta moved southwestward early on 2 January, with the low-level center becoming mostly exposed by 1200 UTC. A burst of deep convection over the center later that day caused reintensification. Zeta again reached an estimated peak intensity of 55 kt at 0000 UTC 3 January while centered about 1000 n mi west-northwest of the Cape Verde Islands. On 4 January, the tropical storm turned westward to the south of a deep-layer ridge over the central Atlantic, and increasing westerly shear triggered a prolonged and final weakening phase. Zeta turned west-northwestward on 5 January and accelerated between the western extent of the ridge and

an approaching cold front. It weakened to a tropical depression by 0600 UTC 6 January and degenerated to a remnant low 12 h later. The low moved northwestward until it dissipated late on 7 January about 575 n mi southeast of Bermuda.

The *Liberty Star* (call sign WCBP) reported 34-kt winds about 40 n mi north of the circulation center at 0800 UTC 31 December. QuikSCAT data at 0752 UTC 30 December estimated surface winds as strong as about 45 kt. Based on this, it is estimated the depression became a tropical storm with winds of 40 kt by 0600 UTC 30 December. Additionally, drifting buoy 62557 reported a pressure fall of 11.9 to 1006.7 mb near the center during the 20-h period ending 0800 UTC 30 December.

Zeta formed 6 h earlier than Hurricane Alice (1954–1955; Dunn et al. 1955), making it the second latest tropical storm of record in the Atlantic basin.

3. Nondeveloping depressions

Two tropical and one subtropical depressions that did not reach tropical storm strength occurred during the 2005 season. Tropical Depression 10 formed from a tropical wave that emerged from the coast of Africa on 8 August. The wave moved westward and showed signs of convective organization starting on 11 August. Development continued, and it is estimated that a tropical depression formed around 1200 UTC 13 August about 925 n mi east of Barbados. The depression moved erratically westward and, due to strong southwesterly shear, weakened to a remnant low the next day. The low moved generally west-northwestward and occasionally produced convection until it degenerated to a tropical wave on 18 August just northeast of the Leeward Islands. The midlevel remnants of this system played a part in the genesis of Hurricane Katrina.

Tropical Depression 19 formed from a tropical wave southwest of the Cape Verde Islands at 1200 UTC 30 September. The depression rapidly weakened as it moved northward and encountered strong southwesterly wind shear produced by a large upper-level low. The shear removed most of the thunderstorm activity, and the system dissipated on 2 October.

Subtropical Depression 22 formed from a large mid-/upper-level trough that persisted over the central North Atlantic Ocean during the first week of October, aided to some extent by the outflow from Tropical Storm Tammy. A mid- to upper-level low formed in the trough around 5 October, and an associated surface trough developed east of the low on 6 October. The surface trough moved northwestward on 7–8 October on the northeast side of the upper low. The surface

system developed a closed circulation and organized convection on 8 October, and it is estimated that it became a subtropical depression around 0600 UTC about 535 n mi southeast of Bermuda. The depression turned westward on 9 October on the north side of the upper low. Strong easterly shear caused the convection to diminish, and the depression became a remnant low on 10 October about 150 n mi west-southwest of Bermuda. The low turned northwestward later that day and merged with a cold front on 11 October east of Cape Hatteras, North Carolina. The low then intensified as an extratropical system, causing gale-force winds northeast of the center as it meandered off the mid-Atlantic states from 12 to 14 October. The system was absorbed by a larger extratropical low late on 14 October.

4. Forecast verification and warnings

For all operationally designated tropical cyclones in the Atlantic and eastern North Pacific basins, the NHC issues an “official” forecast of the cyclone’s center position and maximum 1-min surface wind speed. These forecasts are issued every 6 h, and each contains projections valid 12, 24, 36, 48, 72, 96, and 120 h after the forecast’s nominal initial time (0000, 0600, 1200, or 1800 UTC). At the conclusion of the season, the forecasts are evaluated by comparing the forecast positions and intensities to the corresponding poststorm-derived best track positions and intensities for each cyclone. Forecasts are included only if the system was a tropical or subtropical cyclone at both the forecast and the verifying time; all other stages of development (e.g., extratropical, tropical wave, remnant low) are excluded. The verifications reported here include the depression stage. For verification purposes, forecasts associated with special advisories² no longer supersede the original forecast issued for that synoptic time; rather, the original forecast is verified. This is a change in procedure from 2004.

It is important to distinguish between *forecast error* and *forecast skill*. Track forecast error is defined as the great-circle distance between a cyclone’s forecast position and the best-track position at the forecast verification time. Skill, on the other hand, represents a normalization of forecast error against some standard. Particularly useful standards are those that are independent of operations and can be applied retrospectively to his-

torical data. To assess the degree of skill in a set of track forecasts, the track forecast error can be compared with the error from CLIPER5,³ a climatology and persistence model that contains no information about the current state of the atmosphere (Neumann 1972; Aberson 1998). Errors from the CLIPER5 model are taken to represent a “no skill”⁴ level of accuracy for evaluating other forecasts. If CLIPER5 errors are unusually low during a given season, for example, it indicates that the year’s storms were inherently “easier” to forecast than normal or otherwise unusually well behaved.

Forecast intensity error is defined as the absolute value of the difference between the forecast and best-track intensity at the forecast verifying time. Skill in a set of intensity forecasts can be assessed using a model such as the five-day Statistical Hurricane Intensity Forecast (SHIFOR5) (Jarvinen and Neumann 1979; Knaff et al. 2003), the climatology and persistence model for intensity that is analogous to the CLIPER5 model for track. While the SHIFOR5 model can be a useful benchmark, it will overestimate skill in cases where a storm interacts with (or is forecast to interact with) land because of a lack of predictors involving land. A more appropriate intensity skill benchmark would be a SHIFOR-like model that also included a decay component. Such a model is presently under development.

Table 12 shows the results of the NHC official track forecast verification for 2005, along with results averaged for the previous 10-yr period 1995–2004. Because of the extremely active season, the NHC issued a record number of Atlantic basin tropical cyclone forecasts in 2005. Mean track errors ranged from 35 n mi at 12 h to 286 n mi at 120 h (Franklin 2006). The mean official track forecast errors were smaller in 2005 than for the previous 10-yr period (by roughly 15%–25% out to 72 h), and in fact, at forecast projections through 72 h the errors were close to the all-time lows set in 2004 (Franklin 2005). Fairly substantial vector biases were noted in 2005, with the official forecast tending to fall to the northwest of the verifying position through 72 h, and to the north and northeast of the verifying position at 4 and 5 days, respectively. These biases were about 10%–35% of the mean error magnitude, somewhat larger than the long-term generally westward biases, and similar in magnitude to the biases noted in 2004. They also imply a general tendency to forecast too rapid a recur-

² Special advisories are issued whenever an unexpected significant change has occurred or when watches or warnings are to be issued between regularly scheduled advisories.

³ CLIPER5 and SHIFOR5 are 5-day versions of the original 3-day CLIPER and SHIFOR models.

⁴ To be sure, some “skill,” or expertise, is required to provide proper initialization data for the CLIPER model.

TABLE 12. Homogenous comparison of official and CLIPER5 track forecast errors in the Atlantic basin for the 2005 season for all tropical and subtropical cyclones. Long-term averages are shown for comparison.

	Forecast period (h)						
	12	24	36	48	72	96	120
2005 mean OFCL error (n mi)	35.1	59.7	84.2	106.4	156.2	219.8	285.6
2005 mean CLIPER5 error (n mi)	49.0	101.6	159.8	209.9	284.5	367.6	453.2
2005 mean OFCL error relative to CLIPER5 (%)	-29	-41	-47	-49	-45	-40	-37
2005 mean OFCL bias vector [$^{\circ}$ (n mi) $^{-1}$]	313/6	314/15	318/28	319/38	312/35	353/25	043/78
2005 number of cases	591	534	478	429	338	264	207
1995–2004 mean OFCL error (n mi)*	42.2	75.3	106.9	137.8	202.4	235.7	310.2
1995–2004 mean CLIPER5 error (n mi)*	51.0	104.1	162.7	220.2	323.9	472.1	584.9
1995–2004 mean OFCL error relative to CLIPER5 (%)*	-17	-28	-34	-37	-38	-50	-47
1995–2004 mean OFCL bias [$^{\circ}$ (n mi) $^{-1}$]	271/7	279/13	288/18	302/23	290/29	338/17	021/20
1995–2004 number of cases	3400	3116	2848	2575	2117	649	535
2005 OFCL error relative to 1995–2004 mean (%)*	-17	-21	-21	-23	-23	-7	-8
2005 CLIPER5 error relative to 1995–2004 mean (%)*	-4	-2	-2	-5	-12	-22	-23

* Averages for 96 and 120 h are for the period 2001–04.

vature into the midlatitude westerlies. An example of this tendency can be seen in forecasts for Wilma, several of which called for the hurricane to move northeastward across Florida two days before it actually did.

Not only were the 12–72-h forecasts more accurate in 2005 than during the previous decade, but the forecasts were also more skillful. This was despite the fact that CLIPER5 errors during 2005 were slightly below normal from 12–72 h, indicating below-normal forecast difficulty. However, an examination of annual skill trends (not shown) suggests that, following a sharp increase in the late 1990s, forecast skill has changed little over the past four seasons.

The NHC began making 96- and 120-h forecasts in 2001 (although they were not released publicly until 2003), so the “long term” record for these forecast pe-

riods is limited. Official track errors in 2005 for 96 and 120 h were somewhat smaller than the 2001–04 period means, although unusually low CLIPER5 errors in 2005 at these forecast periods mean that these longer-range forecasts were less skillful in 2005 than in any previous year.

Table 13 shows the results of the NHC official intensity forecast verification for 2005, along with results averaged for the preceding 10-yr period. Mean forecast errors ranged from about 7 kt at 12 h to 22 kt at 120 h. Given the record number of category 5 hurricanes and the large number of rapidly intensifying storms, it is perhaps not surprising that the mean intensity errors in 2005 were mostly larger than the previous 10-yr means. As an extreme example, the 72-, 48-, and 24-h intensity forecasts for Wilma verifying at 1200 UTC 19 October

TABLE 13. Homogenous comparison of official and SHIFOR5 intensity forecast errors in the Atlantic basin for the 2005 season for all tropical and subtropical cyclones. Long-term averages are shown for comparison.

	Forecast period (h)						
	12	24	36	48	72	96	120
2005 mean OFCL error (kt)	6.9	10.9	13.4	15.6	20.2	20.1	21.9
2005 mean SHIFOR5 error (kt)	10.4	16.6	19.6	21.0	25.0	26.0	24.0
2005 mean OFCL error relative to SHIFOR5 (%)	-34	-34	-32	-26	-20	-23	-9
2005 OFCL bias (kt)	-0.3	-0.5	-1.6	-3.4	-5.0	-8.0	-6.9
2005 number of cases	591	534	478	429	338	264	207
1995–2004 mean OFCL error (kt)*	6.3	9.8	12.4	14.7	18.3	19.7	21.7
1995–2004 mean SHIFOR5 error (kt)*	8.0	12.4	15.7	18.2	21.3	24.6	24.4
1995–2004 mean OFCL error relative to SHIFOR5 (%)*	-22	-21	-21	-20	-14	-20	-11
1995–2004 OFCL bias (kt)	0.0	0.1	0.0	-0.2	0.1	0.7	0.4
1995–2004 number of cases	3392	3109	2841	2566	2115	649	535
2005 OFCL error relative to 1995–2004 mean (%)*	10	11	8	6	10	2	1
2005 SHIFOR5 error relative to 1995–2004 mean (%)*	30	34	25	15	17	6	2

* Averages for 96 and 120 h are for the period 2001–04.

TABLE 14. Watch and warning lead times for hurricanes (H) and tropical storms (TS) affecting the United States in 2005. If multiple watch/warning types were issued, the type corresponding to the most severe conditions experienced over land is given.

Storm	Landfall or closest approach point	Watch/warning type	Watch lead time (h)	Warning lead time (h)
Arlene	Pensacola, FL	H*	28	16
Cindy	Grand Isle, LA	TS**	30	18
Cindy	Ansley, MS	TS	None issued	24
Dennis	Santo Rosa Island, FL	H	46	34
Katrina	Broward/Miami-Dade county line, FL	H	32	20
Katrina	Buras, LA	H	44	32
Ophelia	Cape Fear, NC	H	96	36
Rita	Johnson's Bayou, LA	H	59	41
Tammy	Atlantic Beach, FL	TS	None issued	12
Wilma	Cape Romano, FL	H	37	31

* Arlene never reached hurricane strength and made landfall as a tropical storm.

** Cindy was upgraded to a hurricane in postanalysis. Operationally, it was called a tropical storm at landfall.

had errors of 80, 80, and 70 kt, respectively. The intensity forecasts also featured pronounced biases, with an official intensity bias of -5.0 kt at 72 h and -8.0 kt at 96 h. In contrast, long-term intensity biases are near zero. Through 72 h, SHIFOR5 forecast errors in 2005 were significantly above their previous 10-yr means, indicating that this year's storms were more difficult than normal to forecast (the increased number of landfalls notwithstanding). A review of annual errors and skill trends (not shown) suggests that intensity forecast skill has improved slightly in recent seasons, even though raw errors have remained nearly constant.

The NHC defines a hurricane (or tropical storm) warning as a notice that 1-min average winds of hurricane (or tropical storm) force are *expected* in a specified coastal area within the next 24 h. A watch is defined as a notice that those conditions are *possible* during the next 36 h. Table 14 list lead times associated with those tropical cyclones that affected the United States in 2005. Because observations are usually inadequate to determine when hurricane or tropical storm conditions reach a coastline, for this discussion the lead time is defined as the time elapsed between the issuance of a watch or warning for the landfall area or closest point of approach and the time of landfall or closest approach. Such a definition will usually overstate the actual lead time, especially for tropical storm conditions. This is particularly noticeable in the watch time for Dennis, Katrina, and Rita, which all had large radii of tropical-storm-force winds. Issuance of warnings for non-U.S. territories is the responsibility of the governments affected and is not included here.

The warnings for three cyclones require additional comment. A hurricane warning was issued for the Gulf Coast during Arlene in anticipation that the storm would become a hurricane after reaching an intensity of 60 kt. This did not occur. A tropical storm warning was

issued for the Gulf Coast during Cindy, in anticipation that the system would not reach hurricane strength. It was assessed not to have done so operationally. However, poststorm analysis indicated it was 5 kt stronger than assessed operationally, which made it a hurricane at landfall. Both cyclones were in environments that were only marginally favorable for strengthening, and they highlight the difficulty in forecasting (and occasionally analyzing) which side of the tropical storm–hurricane threshold a tropical cyclone will wind up on.

The third case was Ophelia, which featured a 96-h lead time for the hurricane watch on the North Carolina coast. This long lead time was because of the slow and erratic motion of the hurricane, which approached the coast later than originally forecast.

Acknowledgments. The authors thank Jeff Hawkins and his colleagues at the Naval Research Laboratory in Monterey, California, for the satellite imagery presented here. Ethan Gibney of the TPC created the track chart. Much of the data on local impact were provided by the local NWS WFOs in the affected areas, the NWS National Data Buoy Center, and the meteorological services of the other countries affected. Additional data on local impact were provided courtesy of several federal, state, and university meso-networks. Peter Black and Eric Uhlhorn of the HRD in Miami, Florida, provided the recalibrated SFMR data. Timothy Garner of NASA provided observations and helpful descriptions of the local topography for Hurricane Vince. Derrick Herndon and Chris Velden of the Cooperative Institute of Meteorological Satellite Studies at the University of Wisconsin (Madison, Wisconsin) provided poststorm analysis satellite data for the unnamed subtropical storm. David Roth of the Hydrometeorological Prediction Center in Washington, D.C., provided helpful rain-

fall data. Three anonymous reviewers provided useful input to the manuscript.

REFERENCES

- Aberson, S. D., 1998: Five-day tropical cyclone track forecasts in the North Atlantic basin. *Wea. Forecasting*, **13**, 1005–1015.
- , and J. L. Franklin, 1999: Impact on hurricane track and intensity forecasts of GPS dropwindsonde observations from the first season flights of the NOAA Gulfstream-IV jet aircraft. *Bull. Amer. Meteor. Soc.*, **80**, 421–427.
- Bell, G. D., and Coauthors, 2000: Climate assessment for 1999. *Bull. Amer. Meteor. Soc.*, **81**, S1–S50.
- Blake, E. S., E. N. Rappaport, J. D. Jarrell, and C. W. Landsea, 2005: The deadliest, costliest and most intense United States tropical cyclones from 1851 to 2004 (and other frequently requested hurricane facts). NOAA Tech. Memo. NWS TPC-4, U.S. Department of Commerce, National Weather Service, Washington, DC, 48 pp.
- Dunn, G. E., W. R. Davis, and P. L. Moore, 1955: Hurricanes of 1955. *Mon. Wea. Rev.*, **83**, 315–326.
- Dvorak, V. E., 1984: Tropical cyclone intensity analysis using satellite data. NOAA Tech. Rep. NESDIS 11, National Oceanic and Atmospheric Administration, Washington, DC, 47 pp.
- Franklin, J. L., cited 2005: 2004 National Hurricane Center Forecast Verification Report. [Available online at http://www.nhc.noaa.gov/verification/pdfs/Verification_2004.pdf.]
- , cited 2006: 2005 National Hurricane Center Forecast Verification Report. [Available online at http://www.nhc.noaa.gov/verification/pdfs/Verification_2005.pdf.]
- , M. L. Black, and K. Valde, 2003: GPS dropwindsonde wind profiles in hurricanes and their operational implications. *Wea. Forecasting*, **18**, 32–44.
- , R. J. Pasch, L. A. Avila, J. L. Beven II, M. B. Lawrence, S. R. Stewart, and E. S. Blake, 2006: Atlantic hurricane season of 2004. *Mon. Wea. Rev.*, **134**, 981–1025.
- Hawkins, J. D., T. F. Lee, J. Turk, C. Sampson, F. J. Kent, and K. Richardson, 2001: Real-time Internet distribution of satellite products for tropical cyclone reconnaissance. *Bull. Amer. Meteor. Soc.*, **82**, 567–578.
- Hebert, P. J., and K. O. Poteat, 1975: A satellite classification technique for subtropical cyclones. NOAA Tech. Memo. NWS SR-83, U.S. Department of Commerce, National Weather Service, Fort Worth, TX, 25 pp.
- Herndon, D. C., and C. Velden, 2004: Upgrades to the UW-CIMSS AMSU-based tropical cyclone intensity estimation algorithm. Preprints, *26th Conf. on Hurricanes and Tropical Meteorology*, Miami, FL, Amer. Meteor. Soc., 118–119.
- Hock, T. F., and J. L. Franklin, 1999: The NCAR GPS dropwindsonde. *Bull. Amer. Meteor. Soc.*, **80**, 407–420.
- Holland, G. J., 1980: An analytical model of the wind and pressure profiles in hurricanes. *Mon. Wea. Rev.*, **108**, 1212–1218.
- Holliday, C. R., and A. H. Thompson, 1979: Climatological characteristics of rapidly intensifying typhoons. *Mon. Wea. Rev.*, **107**, 1022–1034.
- Jarvinen, B. R., and C. J. Neumann, 1979: Statistical forecasts of tropical cyclone intensity for the North Atlantic basin. NOAA Tech. Memo. NWS NHC-10, 22 pp.
- Knaff, J. A., M. DeMaria, B. Sampson, and J. M. Gross, 2003: Statistical, five-day tropical cyclone intensity forecasts derived from climatology and persistence. *Wea. Forecasting*, **18**, 80–92.
- Lawrence, M. B., and J. M. Pelissier, 1981: Atlantic hurricane season of 1980. *Mon. Wea. Rev.*, **109**, 1567–1582.
- , and J. M. Gross, 1989: Atlantic hurricane season of 1988. *Mon. Wea. Rev.*, **117**, 2248–2259.
- , L. A. Avila, J. L. Beven, J. L. Franklin, J. L. Guiney, and R. J. Pasch, 2001: Atlantic hurricane season of 1999. *Mon. Wea. Rev.*, **129**, 3057–3084.
- McDonald, W. F., 1935: The hurricane of August 31 to September 6, 1935. *Mon. Wea. Rev.*, **63**, 269–271.
- Morey, S. L., S. Baig, M. A. Bourassa, D. S. Dukhovskoy, and J. J. O'Brien, 2006: Remote forcing contribution to storm-induced sea level rise during Hurricane Dennis. *Geophys. Res. Lett.*, **33**, L19603, doi:10.1029/2006GL027021.
- Neumann, C. B., 1972: An alternate to the HURRAN (hurricane analog) tropical cyclone forecast system. NOAA Tech. Memo. NWS SR-62, 24 pp.
- Norton, G., 1951: Hurricanes of the 1950 season. *Mon. Wea. Rev.*, **79**, 8–15.
- Riehl, H., 1979: *Climate and Weather in the Tropics*. Academic Press, 611 pp.
- Simpson, R. H., 1974: The hurricane disaster potential scale. *Weatherwise*, **27**, 169, 186.
- , A. L. Sugg, and Staff of National Hurricane Center, 1970: The Atlantic hurricane season of 1969. *Mon. Wea. Rev.*, **98**, 293–306.
- Sugg, A. L., and J. M. Pelissier, 1968: The hurricane season of 1967. *Mon. Wea. Rev.*, **96**, 242–250.
- Tsai, W.-Y., M. Spender, C. Wu, C. Winn, and K. Kellogg, 2000: SeaWinds of QuikSCAT: Sensor description and mission overview. *Proc. Geoscience and Remote Sensing Symposium 2000*, Vol. 3, IEEE, Honolulu, HI, 1021–1023.
- Uhlhorn, E. W., and P. G. Black, 2003: Verification of remotely sensed sea surface winds in hurricanes. *J. Atmos. Oceanic Technol.*, **20**, 99–116.
- Velden, C. S., and K. F. Brueske, 1999: Tropical cyclone warm cores as observed from the NOAA polar orbiting satellite's new Advanced Microwave Sounder Unit. Preprints, *23rd Conf. on Hurricanes and Tropical Meteorology*, Dallas, TX, Amer. Meteor. Soc., 182–185.